Tumor infiltrating lymphocyte therapy for renal cell carcinoma: methods for *ex vivo* expansion and T-cell memory induction

By

Mitchell W. Braun
B.S., Kansas State University, 2014

Submitted to the graduate degree program in Pathology and the Graduate Faculty of the University of Kansas in partial fulfillment of the requirements for the degree of Doctor of Philosophy.

_____
Committee Chair: Andrew K. Godwin, PhD

_____
Timothy Fields, MD, PhD

_____
Mary A. Markiewicz, PhD

_____
Brandon DeKosky, PhD

_____
Fariba Behbod, PhD

_____
Jay L. Vivian, PhD

Date Defended: April 27th, 2021.

The dissertation committee for Mitchell W. Braun certifies that this is the approved version of the following dissertation:

Tumor infiltrating lymphocyte therapy for renal cell carcinoma: methods for *ex vivo* expansion and T-cell memory induction

_____

Chair: Andrew K. Godwin, PhD

_____

Graduate Director: Soumen Paul, PhD

Date Approved: May 10th, 2021.

Abstract

Tumor infiltrating lymphocyte (TIL) therapy is a personalized treatment for locally advanced or metastatic cancer. TIL therapy requires the surgical excision of a portion of the malignant tissue and subsequent *ex vivo* expansion of tumor reactive immune cells, primarily T-lymphocytes (T-cells), prior to reinfusion into the patient. TIL therapy has been shown to be efficacious in numerous forms of cancer; however, a lack of consistent *in vitro* TIL production has hindered the development of this potentially curative cell therapy for renal cell carcinoma (RCC). I (Mitchell W. Braun) report my work, in the Godwin research laboratory, which has aimed to advance the prospect of TIL therapy for RCC. A novel method for TIL expansion has been developed that has shown a 94% success rate for creating TIL cultures from clear cell RCC. This method generates a TIL product with an optimal phenotype relative to other established TIL production protocols, namely the pre-rapid expansion protocol (PreREP)/REP and FTD + beads method. PreREP involves IL-2 supplementation alone as the source of exogenous stimulation during the first phase of expansion. The fresh tumor digests (FTD) + beads method involves supplementation of IL-2, as well as anti-CD3/CD28 beads to initiate TIL cultures. Relative to the PreREP and FTD + beads protocols, our method involves adherent cell depletion (ACD), referred to as panning, and generates significantly fewer regulatory ($CD4^+/CD25^+/FOXP3^+$) ($p=0.049$, $p=0.005$), tissue-resident memory ($CD8^+/CD103^+$) ($p=0.027$, $p=0.009$), PD-1^+/TIM-3^+ double-positive ($p=0.009$, $p=0.011$) and $TIGIT^+$ T-cells ($p=0.049$, $p=0.026$), respectively. These phenotypic changes were achieved while increasing the average tumor reactive T-cell yield in the final TIL product. However, using this method a majority of the $CD8^+$ expanded TILs bear an effector-memory or effector phenotype, which is sub-

optimal for adoptive transfer and similar to the other protocols. Therefore, various methods to induce a less differentiated phenotype during *in vitro* TIL expansion were. AKT inhibition (AKTi) during TIL expansion was shown to increase expression of the memory-associated/lymph-node homing selectin, CD62L ($p<0.0001$), which would be expected to increase TIL effectiveness and the durability of responses. However, AKTi decreased TIL yield after two weeks of expansion ($p=0.047$). To identify a pathway that might mimic the advantageous effects of AKTi but avoid the loss of TILs, a reverse phase protein array (RPPA) was used to identify downstream targets of AKTi. This analysis identified the kinase GSK3β as a major down-regulated target of AKTi. Inhibition of GSK3β is known to upregulate the pioneer transcription factor TCF1, which is associated with T-cell memory development. Subsequent investigation demonstrated that treatment with a GSK3β inhibitor (GSK3βi) during TIL expansion did indeed recapitulate the positive effect of increasing expression of CD62L ($p=0.029$). Importantly, though, GSK3βi did not affect TIL yield ($p=0.76$). This approach has the potential to increase the persistence of the TIL product after infusion leading to increased durable response rates in RCC and potentially other tumors. I submit these findings, as well as additional data, as part of my application for the degree of Doctor of Philosophy in Pathology and Laboratory Medicine from the University of Kansas Medical Center.

Acknowledgements

First and foremost, I would like to thank the patients who agreed to donate their tissues to this research project, without these contributions none of this work would have been possible. I acknowledge the University of Kansas Cancer Center's Biospecimen Repository Core Facility and staff, in particular Mr. Alex Webster, who are sponsored, in part, by the NIH/NCI Cancer Center Support Grant P30 CA168524 for their assistance with obtaining the tissues, under informed consent, which made this work possible. We acknowledge the Flow Cytometry Core Laboratory, which is sponsored, in part, by the NIH/NIGMS COBRE grant P30 GM103326 and the NIH/NCI Cancer Center grant P30 CA168524. The IL-2 used in these studies was obtained through the National Cancer Institute (NCI) Biological Resources Branch (BRB) Preclinical Biologics Repository under HHSN 75N91019D00024. The muse cell counter used in these studies was acquired with an equipment grant from a NIH Clinical and Translational Science Award grant (UL1 TR002366). Funding for this work was provided by the Department of Pathology and Laboratory Medicine under a Graduate Research Assistant (GRA) appointment (KUID: 2517941) and the Kansas Bioscience Authority (KBA) Eminent Scholar grant, the Kansas Institute for Precision Medicine COBRE (P20 GM130423), and the Chancellors Distinguished Chair in Biomedical Sciences endowed Professor awarded to Dr. Andrew K. Godwin.

I would like to thank all members of the Godwin research program for their advice and support. Particularly, I would like to thank Harsh Pathak who has been invaluable when troubleshooting the countless problems which I have encountered over the last four years;

Neil Dunavin who has been both a clinical and research mentor and aided in the early development of this project; Haitham Abdelhakim who is has continually aided in keeping this project clinically relevant ensuring future translation is possible; Meizhang Li who helped overcome early problems from a basic science standpoint; and Andrew Godwin for his willingness to allow me to pursue the exact field of research that I was and remain most interested in, his vital mentorship which has allowed me to be successful in my research training and the friendship that has grown from our shared failures and successes in research as well as our numerous common interests outside of the laboratory.

To my loving wife Allyson, thank you for supporting me during these past four years of research and six years a KUMC, there have been times of stress, sorrow, and failure as well as relief, success and celebration and you've stuck by me through it all which has made this possible. To my one-year old son Henry, I love you so much and am confident that this hard work has set me on a path to provide you with the life you deserve. And to my mother, father, sister and brother, I'm forever grateful for your support and willingness to let me rant about T-cells and cancer even when you didn't care and/or didn't know what I was talking about.

Table of Contents

List of Figures

List of Tables

Chapter 1: Introduction

Immunotherapy for the treatment of cancer has revolutionized the field of oncology over the last decade. Previously there were only few indications for this form of therapy; however, now approximately half of all cancer patients in the United States are eligible for an immune modulating agent and these therapies are a cornerstone of oncology alongside surgery, radiation, targeted therapies and chemotherapy. This decade long boom of improved patient outcomes due to the advent of novel immunotherapeutics started in March of 2011 with the FDA approval of the first immune checkpoint inhibitor, ipilimumab, which targets the CTLA-4 receptor. However, harnessing the immune system in an attempt to treat cancer has been continually explored since William Coley (recognized as the *Father of Cancer Immunotherapy*) first began inoculating sarcoma patients with erysipelas in the 1890s (1). At that time, Coley did not fully appreciate the mechanism of tumor regression due to immune activation as a result of pathogen associated molecular patterns (PAMPs), streptococcal superantigens or lipopolysaccharide (LPS); however, his reports sowed the seeds from which modern cancer immunotherapy has grown.

Over the next several decades, debates regarding the origins of cancer led to the first well-formed hypotheses, largely accredited to Thomas and Burnet, describing somatic mutations giving rise to neoantigens which were capable of being recognized by the immune system (2-4). The resulting theory of immunosurveillance arose as the first descriptions of T-cells mediating graft rejection were reported; the connection was made that the same immune effector cells could be responsible for the rare reports of spontaneous tumor regression. As the understanding of the innate and adaptive immune

systems grew over the remainder of the 20th century it became clear that T-cells and NK cells possessed an extraordinary ability to recognize and eliminate neoplastic cells. However, developing therapeutics that could leverage this potential and be safely translated into broad patient populations would prove to be a difficult endeavor.

There are several different approaches to enhance the immune system's ability to eliminate cancer and a comprehensive review of these therapies will be covered in **Chapter 2**; however, this report is focused on an individualized form of adoptive cell transfer (ACT) known as tumor infiltrating lymphocyte (TIL) therapy. Clear cell renal cell carcinoma (ccRCC) has many of the hallmarks of tumor types that would respond well to TIL therapy: it is a highly immunogenic neoplasm with a consistent reactive T-cell infiltrate and is known to respond to other immunotherapies including aldesleukin (IL-2), interferon-α, and checkpoint inhibitors (5-11). However, RCC has been labeled a difficult target for TIL-based therapies because the only randomized, phase III trial exploring TIL treatment for RCC was terminated early in 1997 due to lack of efficacy. Notably, 41% of patients randomized to the experimental group did not receive a TIL infusion due to a failure of *in vitro* TIL manufacturing (12). Since the termination of this trial, little work has been done to explore why *in vitro* culture failed for such a large proportion of RCC patients. This clinical void leaves an unmet need to develop novel methods for TIL expansion from RCC.

Although RCC is an immunogenic tumor with a consistent T-cell infiltrate, the conundrum remained regarding why it is so challenging to clinically generate TIL cultures. TIL expansion in the phase III trial was attempted using a two-stage protocol. IL-2 (1,200

IU/mL) alone was used to establish TIL cultures followed by an early version of a rapid expansion protocol (REP) involving phytohemagglutinin stimulation after CD8 selection. TIL expansion protocols have changed considerably since this trial and Andersen and colleagues have shown that with an improved pre-rapid expansion protocol (PreREP) protocol and pooling of the bulk “young TIL”, a TIL generation success rate of 92% can be achieved from RCC. However, it required up to 2 months of culture for this first phase of the TIL expansion protocol to be complete (13). This prolonged duration required to establish TIL cultures from RCC will likely hinder the application of this therapy for patients with aggressive disease. This limitation was partially addressed by Baldan *et al.*, who showed that optimized tumor dissociation and immediate addition of mitogenic stimulation via anti-CD3/anti-CD28 paramagnetic beads to the fresh tumor digest (FTD) increased successful TIL generation rates from RCC in a 15-day time frame (14). It is important to note that the criteria for considering a TIL culture successful is not standardized and therefore, the prospective head-to-head comparison of these expansion methods with our novel technique, which is reported in **Chapter 3** is a valuable data set which helps unveil the differences in TIL yields, phenotype and function that are a result of the methods used.

We hypothesized that TIL generation from RCC could be further improved by using an additional technique: removal of the immunosuppressive tumor and stromal cells that are present in the surgical specimen by adherence-based separation. Investigation of this hypothesis is documented in detail in **Chapter 3** of this dissertation. During efforts to optimize TIL generation from RCC, we first experimented with ways to enrich TILs from

FTDs including fluorescence-activated cell sorting (FACS) and magnetic bead-based sorting to remove TILs from their immunosuppressive environment prior to expansion. These methods added an additional time and resource requirement to the already labor and resource intensive TIL production process. Labeling and additional manipulation were also required which subjected the limited tumor digests to cell loss and stress and proved to have a negative impact on expansion and successful culture rates. However, the immunosuppressive cell types within the tumor microenvironment that we aimed to exclude, including tumor cells, cancer associated fibroblasts, and some myeloid derived suppressor cells, all share the *in vitro* characteristic of adherence. Therefore, we developed and evaluated a technique to promote the expansion of RCC TILs (referred to as “panning”), which involves an overnight adherent cell depletion (ACD) step following tumor dissociation and prior to TIL stimulation. We report that this strategy, which requires minimal time, resources, and manipulation, increases average TIL yield in a 14-day time frame and creates fewer regulatory T-cells, fewer tissue resident memory T-cells, and fewer dysfunctional T-cells expressing multiple inhibitory immune checkpoints. These differences are expected to contribute to the robustness of TIL function for use in anti-tumor clinical applications.

In addition to developing an effective, rapid protocol for TIL production, we also sought to make a “better,” more effective TIL that could produce durable responses. These efforts are documented in **Chapter 4** of this dissertation. The ability for *in vitro* expanded tumor reactive T-cells to produce durable responses after re-infusion is partially dependent upon their differentiation/memory state (15, 16). Although more terminally differentiated

effector-memory (T_{em}) and effector (T_{eff}) T-cells possess the ability to directly lyse tumor cells, their less differentiated central-memory (T_{cm}) and stem-cell like memory (T_{scm}) counterparts have greater anti-tumor efficacy *in vivo* (17-21). This is because less differentiated T-cell populations have a greater ability to engraft and persist and subsequently produce a pool of effectors upon antigen re-encounter. A weakness of most TIL production protocols, including our newly developed ACD method, is that before and after TIL expansion a vast majority of $CD8^+$ T-cells bear a T_{em}/T_{eff} phenotype. To address this drawback, we aimed to modulate intracellular signaling pathways during TIL expansion to promote a desirable memory phenotype without impacting the magnitude of TIL expansion. We report that a desirable phenotype is achieved by small molecule inhibition of either AKT (protein kinase B) or glycogen synthase kinase 3β (GSK3β). However, only GSK3β inhibition (GSK3βi) was able to achieve this without impacting TIL proliferation.

The following work shows that consistent *in vitro* production of TILs with a phenotype that is hypothesized to produce durable responses is possible from ccRCC. The stigma from the 1990's that TIL therapy is not feasible for RCC should be disregarded and renewed efforts at translating this promising therapy into the clinics for patients with advanced ccRCC is warranted.

Chapter 2: The Past, Present, and Future of Cancer Immunotherapy and Renal Cell Carcinoma: A Literature Review

2.1 Cancer Immunotherapy

Enhancing the body's natural ability to eliminate malignant cells is an intuitive treatment strategy. A majority of approaches to achieve this aim revolve around modulating one or more aspects of T-cell activation including stimulation through the T-cell receptor/CD3 complex (or mimicking this signal using an engineered receptor), signaling through co-receptors (such as stimulatory CD28 or inhibitory PD-1), and signaling through cytokine receptors. There are several different approaches that are being widely explored to unleash the immune system to eliminate cancer and these can be broadly characterized as: 1) The supplementation of recombinant forms of naturally occurring, or synthetically modified cytokines; 2) vaccination using common tumor specific/associated antigens or personalized vaccination strategies involving the identification of patient specific neoantigens; 3) blockade of inhibitory co-receptors or the augmentation of stimulatory co-receptor signaling; and 4) adoptive cell therapies involving *in vitro* growth and reinfusion of naturally occurring or genetically modified tumor reactive T-cells. All of these approaches show promise and have at least one FDA approved indication; the following will review the basic science and clinical data regarding these treatment strategies.

2.1.1 Cytokines

Cytokine therapy was one of the first widely used immuno-modulatory treatments for cancer, with interferon-α (IFNα) receiving FDA approval for the treatment of leukemia in 1986. IFNα is most widely known to be a primary mediator of the innate immune response to viral pathogens. Receptors are ubiquitously expressed and ligand interaction results in JAK-STAT signaling and activation of a family of transcription factors known as

interferon regulatory factors (IRFs). This signaling cascade primes cells to an anti-viral state. In the setting of malignant transformation, these signaling cascades have beneficial effects on both the neoplastic cells as well as the innate and adaptive immune system. This observation led to therapeutic supplementation of recombinant IFNα being explored for renal cell carcinoma, melanoma, AIDS-related Kaposi's sarcoma, follicular non-Hodgkin's lymphoma, hairy cell leukemia, chronic myelogenous leukemia, multiple myeloma cutaneous T-cell lymphoma, neuroendocrine tumors, and several other forms of cancer. IFNα can limit proliferation and induce apoptosis of tumor cells by increasing expression and enhancing the function of the tumor suppressor p53, although IFNα signaling alone does not activate p53 (22). Another critical effect of IFNα on tumor cells is its ability to influence antigen presentation by upregulating transporters associated with antigen processing on the endoplasmic reticulum as well as class I major histocompatibility complexes (23, 24). These effects make the tumor cells more susceptible to antigen recognition by $CD8^+$ T-cells and subsequent killing. There are also several indirect effects of supplemental IFNα which enhance tumor control and elimination by influencing immune cell populations. For instance, IFNα aids in the development of dendritic cells (DCs) from monocyte precursors (25). As a result, these professional antigen presenting cells (APCs) are ready to phagocytose tumor specific/associated antigens, migrate to lymph nodes and cross-present these peptide fragments to naïve or memory $CD8^+$ T-cells resulting in a more robust adaptive immune response against the tumor. IFNα also has direct effects of T-cells, neutrophils, NK cells and many if not all tissues in the body (26-29) making it a relatively non-specific form of immune modulation.

Recombinant interleukin-2 (IL-2) is another cytokine therapy which received FDA approval in 1992 for the treatment of metastatic renal cancer. The discovery of IL-2 was first reported in 1976 and 1977 and was aptly named T-cell growth factor for its ability to support *in vitro* growth of human T-cells for over 13 months (30, 31). IL-2 has since been solidified as the prototypical cytokine to support T-cell activation and growth. The IL-2 receptor (IL-2R) has two separate forms that can transduce an intracellular signal, and the differences have significant clinical implications. The first is a heterotrimer composed of the IL-2R α-chain (CD25), IL-2R β chain (CD122) and the common ɣ chain (CD132) which binds IL-2 with high affinity (K_d ~ 10^{-11} M). This complex is found primarily on regulatory T-cells (Tregs) and recently activated conventional T-cells. The second is a heterodimer consisting of the IL-2R β-chain and the common ɣ chain which binds with intermediate affinity (K_d ~ 10^{-9} M) and is primarily expressed by memory T-cells and NK cells. The IL-2R α-chain alone binds with low affinity but does not transduce a signal without the other subunits present (32). As a result of the different receptor affinities and the T-cell subsets that express them, the dosing regimen of IL-2 has a drastic impact on the observed outcome. High-dose IL-2 administration induces an immunostimulatory state in which the differentiation of effector T-cells from memory and naïve precursors predominates which is beneficial for the treatment of renal cell carcinoma and metastatic melanoma (7). However, with low-dose IL-2 administration the higher affinity receptors sequester most of the cytokine resulting in preferential regulatory T cell (Treg) activation and expansion. This results in an immunosuppressive state that can be leveraged for the treatment of autoimmunity, graft-versus-host disease, and to prevent the rejection of a

transplanted organ (33-35). High-dose IL-2 alone has fallen out of favor in oncology clinics due to the emergence of newer targeted therapies and immune checkpoint inhibitors; however, this cytokine still has a critical role for *in vitro* T-cell production for adoptive cell therapies and is also used as an adjuvant infusion or bolus injection in this setting to help promote *in vivo* proliferation and engraftment of infused T-cell products.

There are several other cytokine-based therapies that have been and are actively being explored. Three of the most prominent that have been studied in clinical trial settings for numerous indications, including cancer, are interleukin-7 (IL-7), interleukin-12 (IL-12) and interleukin-15 (IL-15). IL-7 and IL-15 are in the same class as IL-2, referred to as common ɣ chain cytokines, because their receptors all utilize the CD132 subunit. However, IL-12 is in a separate class of cytokines and largely functions by inducing a type 1 T-cell phenotype upon the activation of naïve T-cells. Signaling through the common gamma chain cytokine receptors has shown to have both overlapping and differential effects on T-cell activation, proliferation, and differentiation (36). IL-7 is known to be critical for T-cell development in the thymus and plays a homeostatic role within naïve and memory T-cells, while IL-15 has been implicated in $CD8^+$ T-cell memory induction and survival, but also the generation of $CD4^+$ T-cells with a regulatory-like phenotype, although “Tregs” induced by IL-15 alone may have less suppressive activity than conventional Tregs (37-41). Determining the optimal balance of supplemental cytokines to bolster anti-tumor immune responses is an active area of research which has promise when combined with other forms of immunotherapy, notably – adoptive cell therapies.

2.1.2 Cancer Vaccines

Vaccines are typically thought be administered to healthy individuals to prime a cellular and humoral immune response and prevent future pathogenesis. With respect to cancer, this form of vaccination has been highly effective at preventing cancers associated with viral infection, such as human papillomavirus which is associated with cervical, anal, throat, vaginal, vulvar, and penile cancers, as well as the hepatitis B virus which has been linked to hepatocellular carcinoma. Attempts at preventively vaccinating individuals against tumor specific antigens associated with cancers that arise due to somatic mutation have been far less successful. However, a separate form of vaccination aimed at treating patients who have already developed cancer has proven to be efficacious in certain settings.

Treatment-based cancer vaccines have been developed in several different forms including autologous or allogeneic tumor cell lysates, common or patient specific purified tumor antigens, and dendritic cell vaccines which bridge the gap between adoptive cell therapy and vaccination (42-44). The latter is the only form of treatment-based cancer vaccination which has received FDA approval and this therapy is indicated for metastatic castrate-resistant prostate cancer (44).

This autologous dendritic cell vaccine involves removing peripheral blood mononuclear cells from the patient through an apheresis process, activating and differentiating dendritic cells from this population in the presence of a prostate acid phosphatase (PAP)/granulocyte-macrophage-colony-stimulating-factor (GMCSF) fusion protein and

then reinfusing PAP primed DCs at three separate time points. The mechanism of therapeutic efficacy is through the robust anti-PAP T-cell response that results after the DCs present the PAP antigen to T-cells both *in vitro* (i.e., the T-cells within the infusion product) as well as *in vivo* after cell infusion. Response rates and increased overall survival due to this therapy have been very encouraging, particularly considering the advantageous safety profile, and as a result similar approaches are being explored for melanoma, renal cell carcinoma, glioblastoma, breast cancer and several other forms of neoplasia (45-49).

An emerging personalized form of cancer vaccination that involves the i) rapid identification of patient specific neoantigens via whole exome sequencing, ii) *in vitro* validation for a stimulatory T-cell response and iii) administration of up to 20 synthetic long peptides with a poly-ICLC adjuvant to the patient. This approach is showing promise in early phase clinical trials (NCT03633110) (50). It is likely that highly personalized approaches involving multiple target antigens, as highlighted in this study, are going to be necessary if significant responses within diverse patient populations with various tumor types are going to be achieved. This approach will be essential because even within a tumor subset, it is not common to have a single antigen unique to the tumor, which is expressed by all tumors or even all tumor cells within an individual patient.

2.1.3 Immune Checkpoint Modulators

The discovery of the inhibitory immune checkpoints known as cytotoxic T-lymphocyte associated protein 4 (CTLA-4) and programmed cell death 1 (PD-1) where two of the most transformative events in oncologic history. James Allison and Tasuku

Honjo were awarded the 2018 Nobel Prize in Physiology or Medicine for these discoveries and subsequent work showing that blocking these receptors “released the brakes” on the immune system to fight cancer. As of March 2021, the FDA has approved seven immune checkpoint inhibitors (ICIs) for at least 15 indications, one of which is a broad indication for any form of cancer with high microsatellite instability or defective mismatch repair (51, 52). ICIs have increased response rates relative to previous standard of care therapies and the most transformative aspect of these treatments is the highly durable response which is often obtained and was previously unprecedented in patients with metastatic cancer (53). However, the path to broad clinical implementation of this novel class of therapeutics had several setbacks and although improved responses are worthy of praise there is still a large cohort of patients which do not benefit from ICI alone.

There are two general approaches when it comes to modulating “signal 2” of the T-cell activation paradigm to increase T-cell function: blocking co-inhibitory signals or augmenting co-stimulatory signals. The former has proven to be highly efficacious with a tolerable safety profile; however, the latter was also explored and resulted in a catastrophe which shocked the field of immunotherapy, medicine in general and regulatory agencies alike. CD28 is the prototypical co-stimulatory molecule for T-cells. Academic researchers in Germany, in collaboration with the biotech company TeGenero, aimed to augment signaling through this receptor by developing a superagonist antibody (TGN1412) which bound to this receptor outside of the typical ligand binding cleft. At the time, their pre-clinical data indicated this monoclonal antibody may preferentially activate Tregs and be a potential therapeutic for autoimmune disease, but that it also had the

potential to activate T_{em} cells and could potentially be leveraged for the treatment of cancer as well - depending on the state of the patient's immune system. A first in human Phase 1 clinical trial was approved by the European Medical Agency in 2006 and six healthy male participants were enrolled and given a dose thought to be 500 times lower than what would be tolerable. Rapidly after infusion all six participants developed life threatening cytokine release syndrome (CRS) and were barely kept alive in the intensive care unit (54). This trial created a fear of manipulating the immune system and resulted in broad changes to clinical trials in general. There has not been an approved therapy that augments co-stimulatory T-cell signals for the treatment of cancer; however, there are ongoing trials exploring 4-1BB (CD137), OX40 and GITR augmentation, all of which are additional T-cell co-stimulatory receptors, and no such life-threatening reactions have been reported when administered under newly established regulatory guidelines (55-57).

Blocking co-inhibitory T-cell signals has proven to be highly effective at augmenting anti-tumor T-cell responses but the mechanisms behind each class of ICI are not redundant and as a result they have different effects on T-cells and produce different clinical outcomes. Anti-CTLA-4, Anti-PD-1, anti-PD-L1 are the three classes of immune checkpoint inhibitors which have approvals. Although targeting PD-1 and PD-L1 do have differential effects, first the differences between targeting the CTLA-4 pathway and the general PD-1 pathway will be explored. CTLA-4 inhibits T-cell activation by outcompeting CD28 for its ligands CD80 and CD86. It achieves this because it has a higher affinity for these molecules than CD28. As a result, CTLA-4 inhibition largely functions during T-cell priming by professional APCs in secondary lymphoid tissues. Since it functions at this

early stage of T-cell activation is to increase the clonal diversity of a T-cell response and in theory lead to new T-cells entering an otherwise “cold” tumor. However, because it is working early in the T-cell response pathway, clinical improvement is slow relative to the other ICIs due to the time it takes for expansion of the new T-cell populations. In contrast, targeting the PD-1 pathway results in relatively rapid clinical responses. These rapid responses occur because PD-1 pathway inhibition works primarily on T-cells already in the tumor microenvironment, which are considered exhausted. PD-1 signaling interferes with the intracellular cascade downstream of the TCR, preventing effectors from utilizing their cytotoxic potential after antigen recognition. For these reasons, inhibiting the PD-1 pathway does not tend to increase the clonal diversity of the T-cell infiltrate, in contrast to CTLA-4 inhibition. Anti-PD-1 and anti-PD-L1 do have a few important differences. First, the PD-1 receptor has two known ligands. By targeting this receptor, PD-1 signaling is inhibited regardless of the ligand. In contrast, anti-PD-L1 therapy only blocks PD-1/PD-L1 interaction and not PD-1/PD-L2 interaction (58). Next, the *in vitro* EC_{50} values are lower for the anti-PD-L1 antibodies (e.g., atezolizumab, avelumab and durvalumab) relative to the anti-PD-1 antibodies (e.g., nivolumab and pembrolizumab) indicating that they are more effective at inhibiting the PD-1/PD-L1 interaction specifically (59). The best translation of these differences is exemplified with clinical data from a metanalysis of ICI use across cancer types in which overall response rates were greater when using anti-PD-1 monotherapy (27.5%) relative to anti-PD-L1 monotherapy (17.6%) (60). However, the trend in any grade immune-related adverse events (irAE) was also the same with 26% of anti-PD-1 patients and 13.7% of anti-PD-L1 patients experiencing an adverse event (60).

ICIs have changed the treatment of cancer. Over 43% of all U.S. cancer patients are now eligible for this form of therapy (61); however, there is still a clear need for improved outcomes. To address this need, there are ongoing investigations focused on blocking additional inhibitory immune checkpoints including LAG-3, TIM-3, VISTA, and BTLA; currently there are more than 1,500 clinical trials exploring the safety and efficacy ICIs as monotherapy or as a combination therapy, some of the most intriguing being the combination of ICIs and adoptive cell therapy (clinicaltrials.gov).

2.1.4 Adoptive Cell Therapy (ACT)

ACT is process of harvesting, manufacturing, and administering either autologous or allogeneic T-cells for the treatment of cancer. There are three primary forms of ACT being explored including tumor infiltrating lymphocyte (TIL) therapy, engineered T-cell receptor (TCR) therapy and chimeric antigen receptor (CAR) T-cell therapy. Although the definition of ACT could logically include hematopoietic stem cell transplantation (HSCT), NK cell therapy and similar therapies for the treatment of various other disease states, this focused definition will be utilized and an overview each form will be provided in the following.

Tumor Infiltrating Lymphocyte (TIL) Therapy

TIL therapy involves creating an autologous tumor reactive T-cell product from a patient's own surgically resected tumor tissue. The T-cells present within the tumor are enriched with TCRs that are tumor reactive relative to peripheral blood T-cells, however,

they are failing to control or eliminate the cancer at the time of surgery. By virtue of numerically expanding these cells *ex vivo* in conditions optimized to reinvigorate the lymphocytes the balance can be shifted in favor of tumor elimination once the cells are reinfused into the patient.

Protocols for TIL therapy have varied widely over the decades and they continue to change to allow for consistent *in vitro* TIL growth while maintaining tumor reactivity and optimal response to therapy after infusion. Most protocols begin with the surgical excision of a portion of the tumor burden at either the primary site or a metastatic lesion; however, there is rationale for ipilimumab treatment prior to surgery, since CTLA-4 blockade has shown to induce new T-cell infiltrates into the tumor, as described above. In this setting, the resulting TIL product may have a broader range of tumor reactivity leading to increased responses and it could also increase the successful TIL culture rate if the absolute number of TIL in the resected tissue is a limiting factor when neoadjuvant ipilimumab is not used. Finally, neoadjuvant ipilimumab may prevent disease progression during the TIL manufacturing timeframe leading to an increased percentage of patients who ultimately receive the cell infusion. For these reasons, this approach is being actively investigated in the clinic (NCT01701674) (62, 63).

After the surgical removal of tumor tissue, the TIL manufacturing process begins. There are two approaches for the first step of *in vitro* TIL growth: expansion from intact tumor fragments or expansion from a single cell suspension by creating a fresh tumor digest (FTD) (64). The traditional approach is to culture TILs from fragments approximately 3-5

mm^3 in size within individual wells of a 24-well plate. This approach requires less manipulation potentially resulting in fewer incidences of technical error. However, TILs are required to migrate out of the tumor tissue for robust expansion and the extracellular matrix (ECM) can be immunosuppressive as well as a physical barrier to T-cell growth. Therefore, it is now common practice to expand TILs after the combination of physical and enzymatic dissociation commonly using type IV collagenase, DNase and sometimes hyaluronidase.

Currently, the most widely used method for TIL expansion is a two-phase protocol known as the “young TIL” method which is an adaptation of the protocol now known as “standard TIL” (65, 66). The first phase is known as pre-rapid expansion (PreREP). During this time fragments or FTDs are cultured in media containing 6,000 IU/mL of IL-2. Supplementing IL-2 alone is thought to induce selective proliferation of tumor reactive clones since the only source of TCR stimulation is presumptive tumor antigens. This first phase of IL-2 alone mediated TIL expansion is continued until a dense carpet of T-cells is visible in each well and generally takes between 10 and 18 days (66); however, it can take up to 60 days depending on the type of tumor and criteria for considering the culture “established” (13). The “standard TIL” protocol has an extended PreREP phase in which microcultures are split and maintained in IL-2 only until a pre-determined cell number is reached. After the PreREP phase, the “standard TIL” protocol requires the identification of individual TIL cultures that display tumor reactivity by using an *in vitro* screening technique such as a cytokine release assay in response to autologous or HLA-matched tumor cell lines. Individual tumor-reactive TIL microcultures are subsequently rapidly

expanded to clinical scale. This complex technique has been largely abandoned because it has been shown that *in vitro* screening does not always correlate with the actual *in vivo* anti-tumor function of the T-cells (66). Therefore, a simple technique is now commonly used in which all of the “young TIL” microcultures established from an individual patient are grown only to confluency in their initial well, then pooled and subjected to the rapid expansion protocol (REP) in order to create the final cell product. This process is faster and results in a T-cell product with longer average telomeres and higher expression of CD27 and CD28 all of which are correlated to higher overall response rates (ORRs) and/or the durability of response (65-67).

The REP is the final stage of this common expansion method and involves stimulating the PreREP cultures with irradiated (40 Gy) allogeneic PBMCs at a 200:1 feeder cell to TIL ratio along with 30 ng/mL OKT3 and 6,000 IU/mL of IL-2 for 11 to 14 days. Typically a 500- to 2,000-fold expansion can be achieved when using specialized T-cell culture vessels with a gas permeable silicon base allowing for excess media to be stacked in the flask so nutrient availability does not become a limiting factor (64).

Prior to infusing the expanded T-cell product it is common practice to utilize a non-myeloablative lymphodepleting (NMA-LD) chemotherapy regimen (68). NMA-LD chemotherapy creates a niche for the TIL product to engraft. It also acts by depleting the host of non-desirable T-cell populations, critically the regulatory T-cells which are commonly elevated in cancer patients and produce a suppressive environment which can counteract the expanded TIL function (69). Depleting the host of pre-existing T-cells

before TIL infusion also may prevent these populations from acting like a “cytokine sink” and sequestering the adjuvant IL-2 as well as naturally occurring homeostatic cytokines such as IL-7 and IL-15 (70). The most common NMA-LD regime begins 7 days prior to TIL infusion and involves two days of 60 mg/kg of cyclophosphamide followed by 25 mg/m^2 of fludarabine for five days (known as Cy/Flu) (71). Following TIL administration, typically between 10^{10} and 10^{11} total T-cells, adjuvant IL-2 is given, commonly an intravenous dose of 720,000 IU/kg every 8 hours up to a maximum of 15 doses or until dose limiting toxicities are experienced (71). However, decrescendo IL-2 regimens as well as subcutaneous IL-2 injection have also been explored (72, 73). Typically, this is the entire TIL therapy process; however, TIL infusion at multiple time points (73) as well as adjuvant ICI administration for up to 2 years after cell infusion is also being explored (NCT03645928).

Melanoma is one of the most widely studied forms of cancer with regards to immunotherapy. Prior to this new era in oncology, the average life expectancy for a patient with metastatic disease was approximately six months. The combination of nivolumab and ipilimumab is now the preferred and FDA approved treatment option providing an objective response rate (ORR) of 58% and a complete response (CR) rate of 22% (74). However, TIL-based therapy has provided more impressive responses in subsets of melanoma patients on clinical trials even before the beginning of the checkpoint inhibitor revolution. At the National Cancer Institute (NCI), Steven Rosenberg’s group has pioneered TIL therapy and has reported ORRs of up to 72% (18/25) and CR rates up to 40% (10/25) for metastatic melanoma patients depending upon the treatment protocol

(preparative Cy/Flu + 12 Gy total body irradiation) (75). These outcomes make TIL therapy the most efficacious treatment ever explored for this patient cohort; yet no form of TIL therapy has ever been approved for any type of cancer. This is largely due to the logistical, technical and regulatory complications associated with standardizing the creation of a cell product from a patients' own tissue. However, this may soon change with the advent of Lifileucel (LN-144), which is a TIL product developed by Iovance Biotherapeutics in pivotal/Phase 3 trials for melanoma and cervical cancer. Similar products are being explored in Phase 1/2 trials for head and neck cancer, non-small cell lung cancer, ovarian cancer and sarcomas.

TIL-based therapies have produced durable responses in numerous forms of cancer with recent clinical trials exploring efficacy for the treatment of melanoma, cervical cancer, ovarian cancer, breast cancer, non-small cell lung cancer, hepatocellular carcinoma, head and neck squamous cell carcinoma, glioblastoma, gastric cancer, colorectal cancer, neuroendocrine tumors, osteosarcoma, soft-tissue sarcomas, pancreatic ductal adenocarcinoma, and cholangiocarcinoma (clinicaltrials.gov) (75-80). However, there is only a single ongoing phase 1 trial exploring the safety and efficacy of TIL therapy for RCC (NCT02926053) (13). It has been known since the 1980s that TIL therapy was feasible for RCC (81) and an early clinical trial showed limited promise in a small cohort (82). However, the last phase III trial was terminated in the 1990s because of a failure of the cell manufacturing process, and thus there has been a reluctance to revisit TIL therapy for RCC. This is unfounded because modern TIL manufacturing processes are drastically different and have much higher successful culture rates - including the adherent cell

depletion (ACD) method described in **Chapter 4** (83). As a result, not only will more patients who are randomized to the treatment group receive a cell infusion, but the absolute number of tumor reactive TIL will be much higher in the final product. As few as 5×10^7 total T-cells were infused in the RCC TIL trial in the 1990s and it took up to 7 weeks to obtain those cell counts beginning with a minimum of 10 grams of tumor tissue. This is a remarkably low number of cells for a TIL product and exemplifies how poor the manufacturing protocol from the 1990s truly was. The trial in the 90s was also performed at a time when NMA-LD chemotherapy was not standard in ACT protocols and so there was no neoadjuvant Cy/Flu to promote engraftment and to deplete the non-desirable effects of the pre-existing T-cell populations. For this reason, the calls for revisiting TIL therapy for RCC with improved approaches are justified (14, 83, 84).

Chimeric *Antigen Receptor (CAR) T-cell Therapy*

CAR T-cell therapy involves the *in vitro* genetic modification T-cells to promote the expression of a fusion protein which has the extracellular antigen binding domain of a single chain of an antibody, a transmembrane domain, the intracellular signaling domain of CD3 zeta chain and commonly one or more co-stimulatory signaling domains, such as CD28, 4-1BB, or OX-40 (85). This expression construct creates a new receptor which gives the specificity of an antibody to the T-cell. Upon antigen binding, this chimeric receptor transduces a signal that mimics the TCR and co-receptor activation, leading to the cytotoxicity of cells expressing the target antigen. CAR T-cell therapy was the first FDA approved form of gene therapy for any indication and has revolutionized the treatment of B-cell derived hematologic malignancies. Tisagenlecleucel (KYMRIAH®,

Novartis) was approved in 2017 and since that time three additional CAR-T cell therapies have been FDA approved, with the most recent coming in February of 2021 (86). All four FDA approved CAR constructs target CD19 which is a molecule that is almost exclusively expressed by B-cells. As a result, T-cells that are transduced with the CAR construct effectively eliminate CD19 expressing tumors. However, they also eliminate normal CD19 expressing B-cells as well, known as the on-target-off-tumor effect, and in this scenario the result is hypogammaglobulinemia. B-cell malignancies are unique in this manner because most uniformly express the CD19 molecule (prior to treatment), making it a perfect therapeutic target when one considers that a patient can live a relatively regular life without their normal B-cells by treating the hypogammaglobulinemia with prophylactic intravenous immunoglobulin (IVIg) therapy (87, 88).

CAR T-cell therapy has improved outcomes for patients with various forms of B-cell malignancies (89-93); however, there have been several hurdles that have arisen which limit its efficacy and hamper the ability to translate this therapy to other forms of cancer.

One of the biggest drawbacks to CAR T-cell therapy is that it is largely limited to targeting a single, cell surface antigen. In the setting of B-cell malignancies, the on-target-off-tumor effect is manageable and nearly all the tumor cells express CD19. However, it has been reported that relapse after CAR-T is often due to the occurrence of CD19-negative B-cell malignancy, which was essentially unheard of before CD19 targeted therapies arose (94, 95). This tumor recurrence is the inevitable result of cancer immunoediting which happens when only a single antigen that is not essential for tumor survival is targeted. As a result,

newer CAR-T cell constructs are being designed to target multiple tumor-associated antigens (e.g., bispecific CAR-T cells) to make immune escape less likely (96-99). However, CAR-T is still largely limited by the targeting of cell surface molecules which are associated with the tumor and overexpressed, not specific for the tumor. One alternative approach that could be more specific and promising is targeting oncofetal surface molecules (100). In any event, there is a continual balance of managing on-target-off-tumor toxicities, which can be treatment-limiting when trying to target the most abundant form of cancer, epithelium-derived sold tumors.

Carcinomas are the “elephant in the room” for CAR-T cell therapy. Unlike B-cell malignancies, where one can target the prototypical B-cell marker, CD19, and manage the toxicity of the on-target-off-tumor effect, targeting common epithelial markers is far more problematic because of the life-threatening systemic reactions that could result if the CAR-T cells activate in response to every epithelial cell in the body. There are unique approaches being explored to prevent adverse reactions to common antigens that are overexpressed by epithelial tumor cells. This includes modifying the antigen density requirement for CAR-T activation which sets a threshold that is only reached in the setting of target antigen overexpression on tumor cells, but not low-level expression in normal tissues (101-103). There is a potential therapeutic window using this approach; however, it is likely that this will simply lead to immune editing and eventual escape of a tumor with lower levels of target antigen expression.

“The single greatest challenge in targeting solid tumors [with CAR-T cells] is the identification of suitable target antigens” says Marcela Maus and Carl June (104). As opposed to limiting target antigens to cell surface molecules expressed by the tumor, an alternative approach is to exploit the cellular machinery that has evolved to bring peptide fragments from foreign or mutated-self, tumor-specific intracellular proteins to the cell surface and present them to immune cells. This antigen processing pathway is present in all nucleated cells of the human body and is how the natural T-cell receptor (TCR) recognizes target cells. Leveraging natural antigen presentation is the mechanism behind TIL therapy and engineered TCR therapy and this may be a more efficacious approach for targeting many solid tumors.

Engineered T-cell Receptor (TCR) Therapy

Engineered TCR therapy is a form of ACT that uses the genetic modification of T-cells, similar to CAR-T; however, instead of inducing the expression of a chimeric receptor, this form of therapy promotes the expression of natural (or affinity tuned) TCR(s) which are known to target tumor antigen(s) presented on a given MHC/HLA molecule. Engineered TCR therapy can be broadly split into two classes: those that target known cancer antigens such as NY-ESO-1 and those that identify patient-specific neoantigens and corresponding TCRs using methods such as the tandem minigene (TMG) approach.

NY-ESO-1 is the most common target in the field of engineered TCR therapy with at least 31 clinical trials utilizing TCRs specific for this antigen (105). NY-ESO-1 is a cancer/testis antigen (CTA), meaning the only adult tissue in which it is expressed is the testis as well

as many forms of solid tumors, making it a potential immunotherapeutic target. However, NY-ESO-1 is an intracellular protein making it infeasible to target with CAR-T technology, but an ideal target for engineered TCR therapy (106). Retroviral transduction of a TCR specific for a NY-ESO-1 epitope has produced objective responses in patients with melanoma, non-small cell lung cancer, multiple myeloma and synovial cell sarcoma and is being explored in several other CTA expressing solid tumor types (107-109). However, not every patient, who has a given form of cancer, expresses NY-ESO-1 in their tumor. Also, the TCRs designed to target this antigen are HLA-A*0201 restricted. While this is a relatively frequent HLA-A allele in the general population, specifically among people of European descent (110), for both of these reasons not all patients' are eligible for this form of engineered TCR therapy.

One of the most intriguing forms of cancer immunotherapy currently being explored is engineered TCR therapy targeting patient specific neoantigens using patient specific TCRs. This approach is still in its infancy and appears to have suffered a setback, with several of the first clinical trials being withdrawn or suspended. It was reported by an NIH task force that the U.S. FDA shut down cell manufacturing facilities run by Dr. Steven Rosenberg at the NIH due to the "discovery of widespread contamination" and failure to adhere to a set of standard safety and compliance principles. However, there is a single ongoing trial utilizing neoantigen targeted engineered TCR therapy at the City of Hope Cancer Center (NCT03970382).

Nevertheless, this therapeutic approach has proven to be feasible preclinically and has been repeatedly utilized in the basic science laboratory to identify the neoantigen specific TCRs within the T-cell products of patients undergoing TIL therapy (80, 111-115). The most prevalent method to achieve the identity of an individual patients' neoantigen specific TCRs is known as the tandem minigene (TMG) approach. The TMG approach is a spin-off of TIL therapy in which exact TCR/neoantigen matches are identified by an *in vitro* assay. Numerous co-cultures of TILs and autologous DCs transfected with various minigenes containing multiple patient-specific neoantigens are conducted. Co-cultures that show TIL activation are then further investigated to identify the exact neoantigen/TCR match. The neoantigens within the original TMG that produced a TIL response are teased out and loaded individually into autologous DCs for a second round of co-culture. The T-cells that respond in co-culture can be sorted, based on an activation marker such as 4-1BB, and subjected to single cell paired alpha/beta TCR sequencing. This approach identifies the exact TCR responding to a given neoantigen and this TCR can then be transduced into autologous peripheral blood lymphocytes to make a potent, individualized cell therapy.

In general, the TMG method is laborious and time consuming which may hinder its clinical utility when used as a monotherapy unless it becomes highly standardized. However, it could be implemented in a multi-tiered adoptive cell therapy approach in which bulk TILs are i) rapidly expanded after surgery, ii) infused into the patient and iii) if a complete durable response is not achieved with TIL, then a booster of neoantigen specific TCR transduced peripheral blood lymphocytes (PBLs) could be administered.

2.2 Renal Cell Carcinoma (RCC)

Renal cell carcinoma (RCC) accounts for approximately 85% of all primary neoplasms in the kidney and originates from the tubular epithelium. There are approximately 14,000 deaths and 76,000 new cases of RCC annually in the U.S. and 175,000 deaths and 403,000 new cases worldwide (116). Incidence rates are increasing worldwide and RCC is approximately two times more common in men relative to women (117). The average age of diagnosis is 64 and the overall 5-year survival rate is 75%; however, there is a large disparity between early and late stage disease. Partial or radical nephrectomy is potentially curative early in the disease course, but there is only a 12% 5-year survival rate for metastatic disease (118).

2.2.1 Histological and Molecular Subtypes of RCC

Traditional classification of RCC relies upon histology and separates RCC into three common subtypes: Clear cell, papillary and chromophobe (and other rare subtypes such as medullary, collecting duct, and translocation). However, molecular profiling is revealing additional subtypes which have clinical significance.

Clear cell accounts for approximately 75% of all RCCs and originates from the proximal tubular epithelium (119, 120). Upon gross pathology, clear cell RCC (ccRCC) appears orange or yellow and is a soft tumor type with variable necrotic, hemorrhagic, and fibrotic portions. Microscopically, the cytoplasm is largely filled with lipids and glycogen, which is washed out by alcohol during tissue processing and not stained by hematoxylin and eosin

(H&E), thus giving these tumor cells the “clear cell” morphology. The clear cells typically form clusters or nests with “chicken wire” vasculature separating them. ccRCC is the most common subset to display sarcomatoid features, although it is a rare occurrence. Sarcomatoid dedifferentiation consist of atypical spindle-shaped cells and giant cells with high density and is indicative of aggressive disease and a poor prognosis due to common metastasis and resistance to therapy (121, 122). Immunohistochemical staining can aid in the diagnosis and ccRCC will typically stain positive for carbonic anhydrase IX (CAIX) and paired box 8 (PAX8).

Papillary RCC (PRCC) is the second most common subset accounting for approximately 16% of RCC diagnoses and is thought to arise from the distal tubular epithelium (119, 120). At gross examination, the papillary subtype appears tan to reddish-brown and this tumor is typically friable. Microscopically, the tumor cells form papillae or finger-like projections with fibrosis and vasculature at the core. PRCC has been divided into two types which vary with regards to tumor cell size, pale/eosinophilic cytoplasmic staining, nucleus/nucleolar prominence, the presence of foamy macrophages in papillae core and cytokeratin 7 staining (123). Overall, PRCC has a better prognosis than clear cell with a 5-year survival rate of ~86% (124).

Chromophobe RCC (ChRCC) is the third most common subset accounting for approximately 7% of RCC diagnoses and arises from the intercalated cells of the distal convoluted tubules (120). ChRCC is usually well circumscribed, encapsulated and appears tan. Microscopically, the cells have a pale cytoplasm with prominent cell

boarders and grow in sheets, nests, or alveoli-like structures. The chromophobe subset rarely develops metastases nor involves the lymph nodes and therefore has a near 100% five year survival rate (125).

The molecular characterization of RCC has revealed unique differences in the epigenetics, genomics, and gene expression signatures that are associated with each histological subtype and also reveal new subtypes and mechanisms of pathogenesis with clinical implications. The most prominent molecular association in RCC is the link between loss of von Hippel-Lindau (VHL) protein expression and ccRCC pathogenesis. VHL inactivation occurs in at least 86% of histologically confirmed ccRCC cases and is considered pathognomonic for the clear cell subtype by many (126). Inactivation can occur through various mechanisms, including loss of the short arm of chromosome 3 (3p) on which the *VHL* gene resides, DNA sequence alteration or epigenetic alterations such as *VHL* promoter methylation. Over 80% of ccRCC has a loss of at least one copy of chromosome 3p and subsequent loss of expression from the second copy results in a sequela that leads to tumor formation, although VHL protein loss alone appears to be insufficient for tumorigenicity (127, 128). The VHL protein acts as a tumor suppressor and is part of a ubiquitin ligase complex that leads to the degradation of hypoxia inducible factor-1 (HIF-1) (129). In the absence of VHL, HIF-1 is constitutively expressed and promotes the aberrant expression of numerous genes, notably vascular endothelial growth factor (*VEGF*) resulting in tumor angiogenesis and the multidrug resistance (MDR1) gene which makes ccRCC a difficult therapeutic target (130, 131). This clinical manifestation was the initial rationale for exploring VEGF inhibition as a treatment option

and the results have been encouraging, especially in combination with immune checkpoint inhibition, although complete response remain rare even with this combination therapy (132).

Another significantly mutated gene in ccRCC is Polybromo 1 (*PBRM1*), which also resides on 3p and codes for a protein involved in chromatin remodeling. The *PBRM1* mutation status has been implicated in response to antiangiogenic therapy and immune checkpoint blockade. There is increased progression-free and overall survival for patients' with *PBRM1* mutations who receive these therapies relative to patients with wild-type *PBRM1* (133-135). However, the effects were modest and some patients with wild-type *PBRM1* showed clinical benefit, so the mutational status of this gene alone is not a clinical indication for a given therapy.

BAP1 is another significantly mutated gene in ccRCC and has been proposed to define a new subset kidney cancer. *BAP1* also resides on 3p, like *VHL* and *PBRM1*; however, *BAP1* and *PBRM1* mutation are inversely correlated. Approximately, 70% of ccRCC have one of these genes mutated, while *BAP1* mutations are found in approximately 15% of these tumors (136). This molecular characterization begins to help explain the pathogenesis of ccRCC. Specifically, the loss of 3p and mutation or silencing of the second copy of *VHL* sets the stage for tumorigenesis, while the subsequent complete loss of PBRM1 or BAP1 function helps drive the separate forms ccRCC. This paradigm has potential clinical implication. Although, ccRCC is considered to be radioresistant,

BAP1 deficient tumors may be uniquely sensitive to radiation therapy as well as poly (ADP-ribose) polymerase (PARP) inhibition (136).

2.2.2 clear cell RCC: Presentation, Management, and an Unmet Medical Need

The classic presentation of a patient with RCC is the triad of flank pain, hematuria, and a palpable abdominal mass; however, this clinical presentation occurs in less than 10% of RCC patients and indicates advanced disease. Due to increased usage of abdominal imaging studies for unrelated chief complaints, many early stage cases of RCC are diagnosed incidentally, and this has contributed to the increased survival rates in recent years (137). However, approximately 25% of patients have locally advanced or metastatic disease at the time of diagnosis, and this is the patient cohort for which novel therapeutics are needed.

For the 75% of patients who present with localized disease, most of them can be cured with nephrectomy and nephron sparing surgery is appropriate in select patients. In the setting of metastatic disease, surgery also plays a prominent role in the treatment plan of many patients, which is an important aspect with regards to clinical trials for TIL therapy – patients do not have to be subjected to a surgery that would otherwise not be indicated. RCC is a relatively radioresistant tumor type (see section **2.2.1**); however, radiation therapy may be used to treat limited metastases, and chemotherapy has essentially no role in the treatment of RCC (not including the role of NMA-LD chemotherapy as a neoadjuvant to TIL) (138). Systemic therapy with immune checkpoint inhibitors (ICIs) and molecularly targeted therapies inhibiting the vascular endothelial growth factor (VEGF)

pathway play an important role in the first-line management of advanced disease (132, 139). However, the best approved combination therapy for advanced RCC provides a disappointing ~9% complete response rate and thus this leaves most patients and clinicians seek more efficacious options (139).

Chapter 3: Adherent Cell Depletion Promotes the Expansion of Renal Cell Carcinoma Infiltrating T-cells with Optimal Characteristics for Adoptive Transfer

This work was previously published as open access articles (CC-BY) and reprinted here with additional, never-before published text:
Braun, M.W., Abdelhakim, H., Li, M., et al. Adherent cell depletion promotes the expansion of renal cell carcinoma infiltrating T-cells with optimal characteristics for adoptive transfer. *Journal for ImmunoThearpy of Cancer*. 2020;**8:**e000706.doi:10.1136/jitc-2020-000706. PMID: 33037114.

Braun M.W., Godwin A.K. (2021) An *in vitro* Model for Evaluating Autologous T-cell and Tumor Cell Interactions in Renal Cell Carcinoma. J Clin Cell Immunol. 12:609.

There is a clear need for novel therapeutics to treat metastatic ccRCC. A promising approach to address this need is the development of new T-cell based therapies which can overcome the historical problems of inconsistent and time-consuming TIL generation from this form of cancer. The following exemplifies that the rapid and consistent generation of TILs from clinical ccRCC tissue samples is feasible and therefore warrants re-visiting TIL-based therapy with a modern approach to *in vitro* manufacturing and clinical administration of the cell product.

3.1 Consistent liberation of viable CD8⁺ effector memory T cells from ccRCC

Using our RCC tumor digestion protocol involving gross tumor dissection, mechanical and enzymatic digestion, and ammonium-chloride-potassium (ACK) mediated RBC lysis we observe both viable presumptive lymphocytes (green arrows) and tumor cells (red arrows) in the preparation using trypan blue exclusion (**Figure 1A**). We confirmed that there was both a viable $CD4^+$ and $CD8^+$ T-cell infiltrate liberated within tumor digests of the 10 ccRCC samples from which pre-expansion phenotypes were analyzed and found the average CD4/CD8 ratio to be approximately 5:4 (**Figure 1B, C)**. We also found that 50% of the samples had greater than 10% of double-positive T-cells ($CD3^+/CD4^+/CD8^+$) prior to expansion (**Figure 1B, C**). Double-positive T-cells within the tumor microenvironment have been proposed to be a clonal/oligoclonal population of dysfunctional, tumor-specific T-cells capable of being reactivated by checkpoint inhibitors; however, the significance of these double positive T-cells outside of the thymus is largely unknown (140, 141). We next characterized the differentiation state of pre-expansion TILs

and showed that an average of 62% of ccRCC infiltrating $CD8^+$ T-cells have an effector-memory (T_{em} = $CD45RA^-/CD62L^-$) phenotype prior to expansion, a subset which is known to have proliferative potential, in contrast to the average 29% with an effector phenotype (T_{eff} = $CD45RA^+/CD62L^-$, AKA T_{emra}) which have a minimal ability to divide and are prone to apoptosis (**Figure 1D, E**). In summary, we consistently liberated viable $CD8^+$ effector-memory T-cells from freshly collected RCC tumor tissue specimens which should have the capacity for *in vitro* expansion. Therefore, in subsequent experiments we directly compared PreREP to other methods of TIL expansion in order to determine if the reported

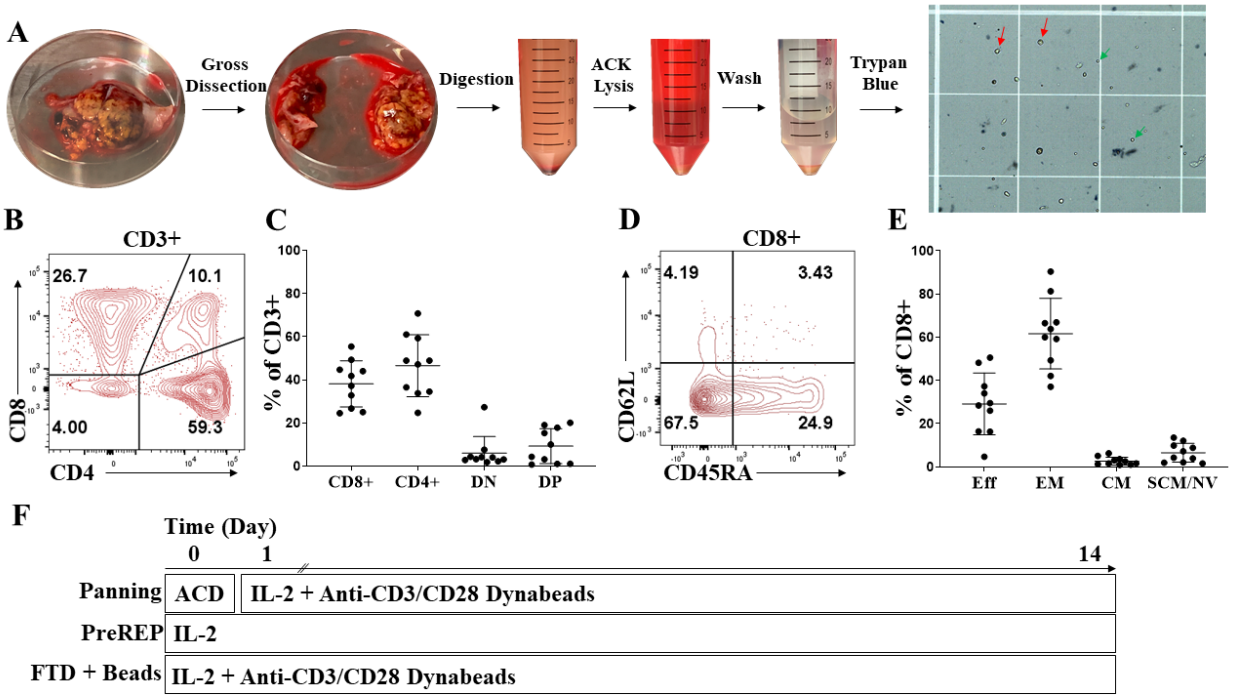

Figure 1. Consistent liberation of viable $CD8^+$ effector-memory T-cells from ccRCC. (**A**) Creation of a fresh tumor digest from clear cell renal cell carcinoma. Green arrows indicate viable presumptive lymphocytes and red arrows indicate viable presumptive tumor cells after trypan blue exclusion (**B**) Representative $CD4^+$ and $CD8^+$ staining of pre-expansion $CD3^+$ RCC TILs. (**C**) Frequencies of pre-expansion $CD8^+$, $CD4^+$, Double-Negative (DN), and Double-Positive (DP) T-cells from 10 clear cell RCC samples. (**D**) Representative effector (eff), effector-memory (em), central-memory (cm), and stem-cell like memory/naïve (scm/nv) staining of pre-expansion $CD3^+/CD8^+$ RCC TILs. (**E**) Frequencies of pre-expansion $CD3^+/CD8^+$ with a eff, em, cm, and scm/nv phenotype from 10 clear cell RCC samples. (**F**) Outline of the three TIL expansion methods utilized. ACD = Adherent Cell Depletion.

high failure rates for expanding TILs from whole RCC FTDs with IL-2 alone could be overcome with alternative protocols. **Figure 1F** depicts the schema for the three TIL expansion protocols which were explored.

3.2 Tumor cells predominate in the adherent cell population within ccRCC and express immunosuppressive ligands

We hypothesized that inhibitory signals from tumor and/or stromal cell populations within the FTD could be suppressing mitogenic stimulation from tumor antigens and exogenous IL-2 and that this could be responsible for the reported failures for generating TIL cultures from whole RCC FTDs with IL-2 supplementation alone. First, we observed that the adherent cultured cells from the ccRCC samples have a striking morphology which differs from adjacent normal renal cortical tissue (**Figure 2A**). There are prominent vacuoles within the cytoplasm of the adherent cells, likely filled with lipids and glycogen, which give the parent tissue its characteristic “clear cell” morphology. This was our first clue that tumor cell growth dominated the adherent population as opposed to other stromal populations. Also, primary adherent cell cultures from ccRCC uniformly express cytokeratin reflecting the epithelial origin of these tumors as well as the transcription factor PAX-8 which is expressed in the proximal tubules of the kidney that is thought to be the cell of origin of ccRCC (**Figure 2B**). Next, to further characterize the adherent cells, we evaluated gene mutations using a next generation sequencing gene panel (275 genes, covering primarily the coding regions) on DNA isolated from 3 consecutive adherent ccRCC cultures. We detected pathogenic *VHL* mutations, the most commonly mutated gene in ccRCC (128), in all three of the adherent primary cultures. Mutant *PBRM1* (2 of

3), *SETD2* (1 of 3), and *TP53* (1 of 3) were also detected in the adherent cell cultures, all with greater than 98% mutant allele frequency, confirming a near pure population of clonal tumor cells grows out after five or more passages (**Table 1**). This genomic analysis confirmed that primary tumor cells were enriched in the adherent cell cultures and this is critical because it allows for subsequent T-cell functional assays to be performed using a near pure population of autologous tumor cells.

Gene	RCC11	RCC12	RCC13
VHL	Val155Met	Ser72fs	His115Asn
PBRM1	WT	Ile97fs	Asp419Gly
SETD2	WT	WT	Lys1712_Ser1714del
TP53	WT	WT	Leu330His

Table 1. Mutation profile of adherent RCC TCLs. Pathogenic, likely pathogenic, and selected mutations of uncertain significance detected in primary adherent cell lines established from clear cell RCC using a 275 oncology NGS gene panel. WT = wild-type.

Next, we asked if these adherent tumor cells expressed immunosuppressive ligands *in vitro,* which could be responsible for failed TIL generation from whole FTDs. We found that adherent cells in culture are able to express programmed death ligand 1 (PD-L1), a well characterized inhibitory immune checkpoint lingand. Two of three samples displayed at least a 10-fold increase in MFI relative to the isotype when cultured in fresh media (FM – blue historgram); however, in response to autologous stimulated TIL conditioned media (TIL CM – red histogram) for 24 hours all three samples massively upregulated PD-L1 with an average 80-fold increase in MFI relative to the isotype contorl (**Figure 2C**). This

is likely due to interferon-γ (IFNɣ) present in the TIL CM because PD-L1 has been shown to be an interferon inducible ligand in many cell types (**Figure 2D**) (142, 143). Galectin-9 (Gal-9) is a ligand for the T-cell immunoglobulin and mucin-domain containing-3 (TIM-3) receptor and it has been shown to be a negative prognostic factor in ccRCC likely due to suppression of type 1 T-cell responses by teathering the inhibitory TIM-3 receptor to the supramolecular activation cluster on the surface of T-cells (144-146). We found that adherent RCC cells during *in vitro* culture express galectin-9 (Gal-9), as shown by the average 5-fold increase (n=3) in mean fluorescence intensity (MFI) relative to the isotype control (**Figure 2E**). IFNɣ is known to upregulate Gal-9 in certain cell types (147); however, we observed a slight decrease in MFI when RCC cells were cultured in TIL CM. This could be due to complex interplay of Gal-9 expression and secretion because Gal-9 is known to be secreted by non-classical pathways involving multivesicular bodies (MVB) which mediates exosomes biogenesis, however, little is known about the regulation of this secretion (148).

Together, these data suggest that the adherent cells left in culture are primarily tumor cells and during TIL expansion will they express multiple inhibitory ligands that have the potential to counteract the stimulatory signals from exogenous IL-2. This phenomenon can be visualized by comparing cultures of autologous TILs expanded by panning, PreREP, and FTD + beads over the first 6 days of culture, in which TILs expanded after adherent cell depletion rapidly form proliferating clusters of T-cells requiring splitting at

day 4 and again at day 6, relative to both other protocols in which adherent cells are left in culture and splitting was not indicated in the first 6 days (**Figure 2F**).

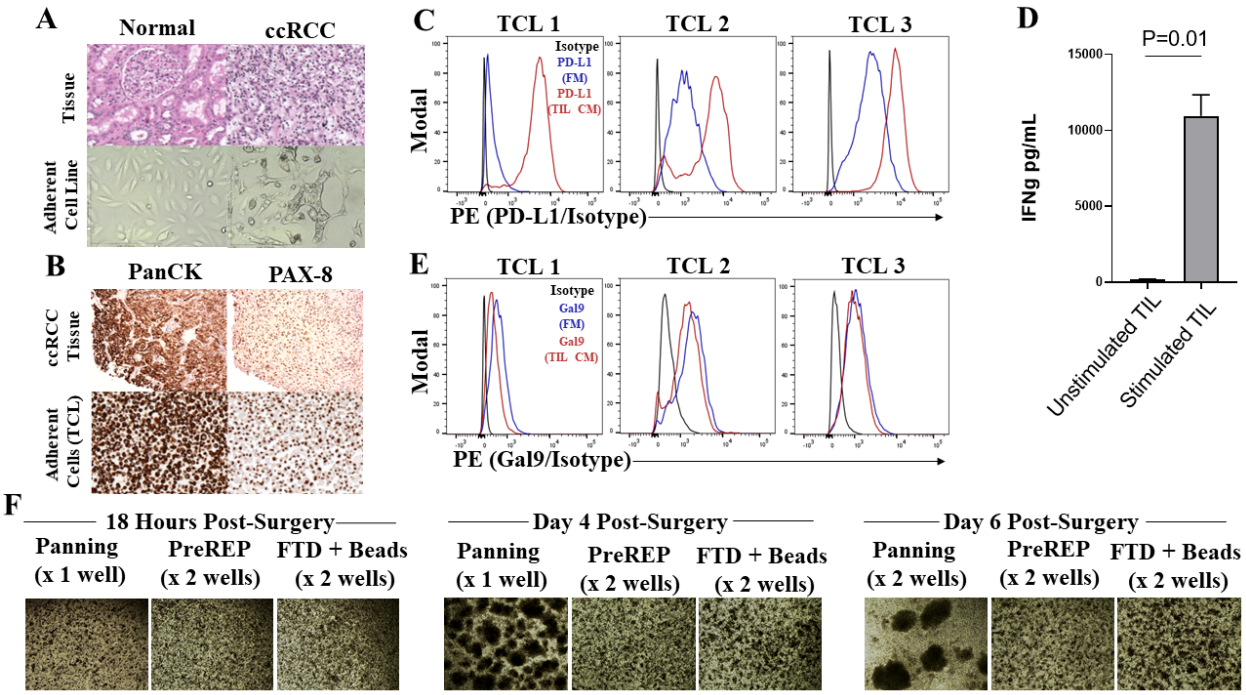

Figure 2. Tumor cells predominate in the adherent cell population within ccRCC and express immunosuppressive ligands. (**A**) Hematoxylin and eosin (H&E) staining of adjacent normal renal cortex and autologous clear cell RCC (top panel) and corresponding passage 0 adherent cell lines established from those tissues (bottom panel). (**B**) Pan-cytokeratin (PanCK) and PAX-8 staining of RCC tissue (top panel) and the autologous, adherent cells at passage 0 derived from the same sample (bottom panel). (**C**) PD-L1 expression on the surface of adherent primary RCC cells cultured in fresh media or conditioned media from autologous TILs (TIL CM). (**D**) Interferon gamma (IFNγ) enzyme-linked immunosorbent assay (ELISA) results from RCC TIL conditioned media (CM) of autologous TILs left unstimulated or stimulated with IL-2 and anti-CD3/CD28 Dynabeads. (**E**) Galectin-9 (Gal-9) expression within adherent primary RCC cells. (**F**) 40X photomicrographs of TILs expanding in 24 well plates using the Panning, PreREP, and FTD + beads protocols at 18 hours, Day 4, and Day 6 post-surgery.

In addition to the immunosuppressive properties of the adherent RCC cells themselves, myeloid derived suppressor cells (MDSCs: CD33+ /HLA-DR-) are known to impact T-cell expansion and function. Therefore, we examined if monocytic-MDSCs (mMDSCs: CD33+/HLA-DR-/CD14+), granulocytic-MDSCs (pmnMDSCs: CD33+/HLA-DR-/CD15+),

and/or early-MDSCs (eMDSC: CD33+/HLA-DR-/CD14-/CD15-) were depeleted by removing adherent cells prior to expansion. We found that MDSCs were a rare subset within three RCC FTDs and that a portion of CD33+ myeloid cells in general were depleted during the ACD step involving overnight culture in T-cell media (*i.e.,* rare in both the adherent and non-adherent population relative to day 0); however, some of the persisting pmnMDSCs and eMDSCs seem to have been preferentially depleted by adherence based selection indicating that panning does reduce T-cell exposure to these non-desirable cell types during TIL expansion (**Figure 3**).

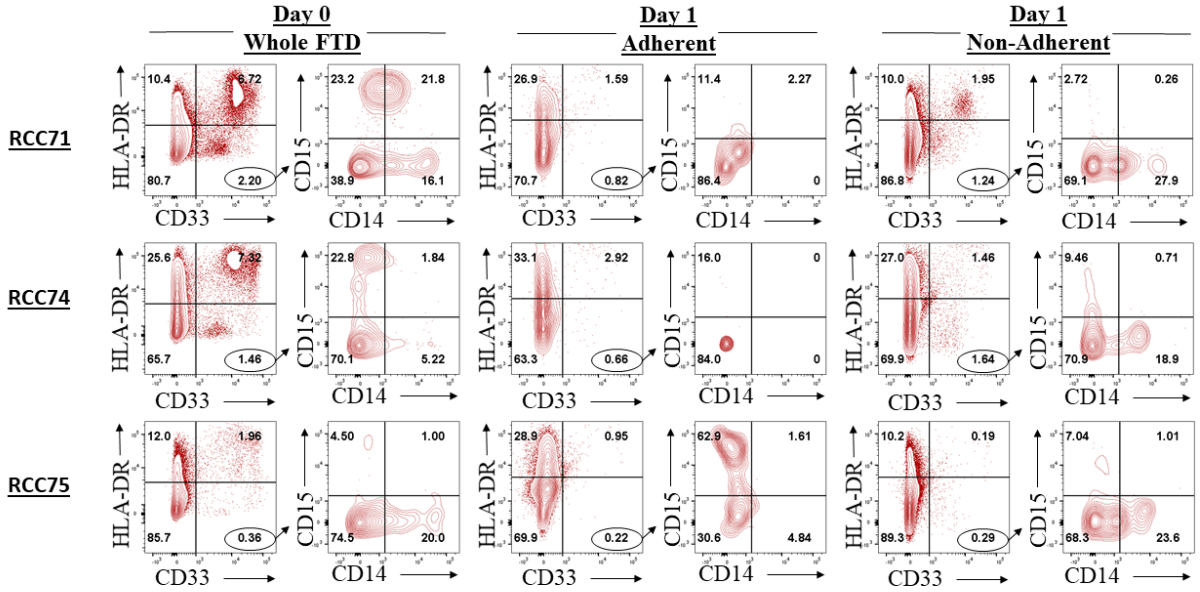

Figure 3. A subset of pmnMDSCs and eMDSCs are depleted by adherence-based selection. MDSCs characterization in whole FTDs and the corresponding adherent and non-adherent populations after overnight selection.

3.3 TILs generated by panning have an optimal phenotype for adoptive transfer

For this study, tissue specimens from 76 patients undergoing radical or partial nephrectomy were used; 55 of the samples were used for establishing a tumor digestion protocol, optimizing adherent tumor cell culture, characterization of pre-expansion TIL and MDSC phenotypes and exploring *ex vivo* TIL expansion methods. A validation cohort

of 19 consecutive samples were then used to confirm consistent TIL expansion using the ACD method which was developed. Within the validation cohort, we observed a 94% success rate (15/16 consecutive samples) for establishing TIL cultures from histologically confirmed ccRCC using our panning protocol and a 0% success rate for establishing TIL cultures from papillary (0/2) and chromophobe RCC (0/1). Digests of 6 of the ccRCC samples in the validation cohort contained at least 1.2 x 10^7 total viable cells (samples designated by "*" in **Table 2)**, which was the minimum number of total cells within the FTD needed to compare autologous TIL expansion using all three protocols (4 x 10^6 cells/protocol). No more than 6 x 10^6 total viable cells were used to initiate TIL cultures using each protocol in order to improve comparability between samples. Importantly, 5 of the 6 samples used to compare protocols were from TNM stage 3 ccRCC, one of which had confirmed metastatic disease, making this cohort clinically relevant because early stage RCC is often cured by nephrectomy (149), whereas later stage disease has a poor prognosis and is the main focus of efforts to improve outcomes using immunotherapies.

BSR ID	RCC #	Age at Date of Surgery	Gender	Race/Ethnicity	Histologic Classification	Grade	TNM Stage
29299	1	66	Male	White/Not Hispanic or Latino	clear cell RCC	G4	pT1bNxM(N/A)
29321	2	61	Male	White/Not Hispanic or Latino	clear cell RCC	G4	pT3a N0 M(N/A)
29359	3	37	Male	Other/Not Hispanic or Latino	clear cell papillary RCC	G2	pT3NXM(N/A)
29370	4	74	Female	White/Not Hispanic or Latino	clear cell RCC	G3	pT3aNxM(N/A)
29721	5	70	Female	White/Not Hispanic or Latino	clear cell RCC	G2	pT3apNXpM(N/A)
29446	6	59	Male	White/Not Hispanic or Latino	Chromophobe RCC	N/A	pT3aNxM(N/A)

29712	7	82	Male	White/Not Hispanic or Latino	clear cell RCC	G2	pT3apNXpM(N/A)
29722	8	67	Male	White/Not Hispanic or Latino	clear cell RCC	G2	pT3aN0M(N/A)
29821	9	43	Female	White/Not Hispanic or Latino	clear cell RCC	G2	pT1a NX M(N/A)
29858	10	66	Male	White/Not Hispanic or Latino	clear cell RCC	G4	pT3a NX M(N/A)
29996	11	34	Female	Hispanic or Latino	clear cell RCC	G2	pT1b NX M(N/A)
30000	12	53	Male	White/Not Hispanic or Latino	clear cell RCC	G2	pT1a NX M(N/A)
29651	13	70	Male	White/Not Hispanic or Latino	clear cell RCC	G3	pT3a NX M1
29665	14	60	Male	White/Not Hispanic or Latino	clear cell RCC	G3	pT1b NX M(N/A)
24774	15	62	Male	White/Not Hispanic or Latino	invasive high grade urothelial carcinoma	Low Grade	pT4 N1 M(N/A)
28281	16	57	Male	White/Not Hispanic or Latino	clear cell RCC	G2	pT2bpN0pM(N/A)
28369	17	70	Male	White/Not Hispanic or Latino	clear cell RCC	G2	pT3a NX M(/N/A)
29623	18	70	Male	White/Not Hispanic or Latino	Papillary RCC	G4	pT3aNXM(N/A)
28382	19	82	Male	White/Not Hispanic or Latino	clear cell RCC	G2	pT3aNxM(N/A)
28383	20	57	Male	White/Not Hispanic or Latino	Papillary RCC	G3	pT3aNxM(N/A)
28912	21	43	Male	White/Not Hispanic or Latino	Hemorrhagic Cyst w/ benign epithelial lining	N/A	N/A
24862	22	68	Male	Hispanic or Latino	Papillary RCC	G1	pT1bNxM(N/A)
28406	23	62	Male	Hispanic or Latino	clear cell RCC	G2	pT1aNxM(N/A)
24875	24	56	Female	White/Not Hispanic or Latino	clear cell RCC	G2	pT3aNxM(N/A)

28445	25	70	Male	White/Not Hispanic or Latino	clear cell RCC	G2	pT1bNxM(N/A)
28434	26	64	Male	White/Not Hispanic or Latino	Oncocytoma	N/A	N/A
24941	27	63	Male	White/Not Hispanic or Latino	Papillary RCC	G3	pT3Nx
24951	28	52	Male	White/Not Hispanic or Latino	clear cell RCC	G1	pT1aNx
28484	29	69	Male	White/Not Hispanic or Latino	clear cell RCC	G4	pT3a N0 M(N/A)
28486	30	44	Female	White/Not Hispanic or Latino	clear cell RCC	G2	pT1apNxpM(N/A)
28544	31	62	Male	White/Not Hispanic or Latino	Papillary RCC	G2	pT3aNxM(N/A)
28564	32	40	Female	White/Not Hispanic or Latino	clear cell RCC	G2	pT1bNxM(N/A)
28609	33	88	Female	White/Not Hispanic or Latino	clear cell RCC	G2	pT1aNxM(N/A)
28614	34	59	Male	White/Not Hispanic or Latino	clear cell RCC	G2	pT3bN1M(N/A)
28624	35	61	Female	Black or African American	Papillary RCC	G2	pT2aN0M(N/A)
28651	36	47	Male	White/Not Hispanic or Latino	RCC, unclassified	G2	mpT1bNxM(N/A)
28573	37	50	Male	White/Not Hispanic or Latino	clear cell RCC	G3	pT3aNxM(N/A)
30919	38	44	Female	White/Not Hispanic or Latino	clear cell RCC	G2	pT1a NX M(N/A)
30924	39	61	Male	White/Not Hispanic or Latino	clear cell RCC	G1	pT1a NX M(N/A)
33197	40	46	Male	White/Not Hispanic or Latino	clear cell RCC	G2	pT1aNxM(N/A)
33249	41	61	Male	White/Not Hispanic or Latino	clear cell RCC	G3	pT1a NX M(N/A)
33260	42	72	Female	White/Not Hispanic or Latino	clear cell RCC	G4	pT3a N1 (6/6) M1

33261	43	58	Male	Hispanic or Latino	clear cell RCC	G3	pT3a NX M(N/A)
30998	44	62	Male	White/Not Hispanic or Latino	clear cell RCC	G2	pT3apNxM(N/A)
31028	45	71	Male	White/Not Hispanic or Latino	clear cell RCC	G4	pT3a N0 M1
31032	46	65	Female	White/Not Hispanic or Latino	clear cell RCC	G3	pT1aNxM(N/A)
33287	47	64	Male	White/Not Hispanic or Latino	Chromophobe RCC	N/A	pT1bNxM(N/A)
31076	48	80	Male	White/Not Hispanic or Latino	Papillary RCC	G1	pT2aNx
31110	49	58	Male	White/Not Hispanic or Latino	clear cell RCC	G3	pT1aNxM(N/A)
33324	50	59	Male	Hispanic or Latino	clear cell RCC	G2	pT1bNx
31145	51	56	Female	White/Not Hispanic or Latino	clear cell RCC	G3	pT2a NX M(N/A)
33277	52	55	Male	White/Not Hispanic or Latino	Clear Cell RCC	G2	pT1b NX M(N/A)
33696	PRCC 1	61	Male	White/Not Hispanic or Latino	Clear Cell RCC	G2	pT2a NX M(N/A)
33710	53	57	Female	White/Not Hispanic or Latino	Clear Cell RCC	G2	pT1a NX M(N/A)
33750	54	58	Male	White/Not Hispanic or Latino	Clear Cell RCC	G2	pT1b N0(0/6) M(N/A)
33792	56	60	Male	White/Not Hispanic or Latino	Clear Cell RCC	G2	pT3b N0(0/10) M1
33821	*57	44	Female	White/Not Hispanic or Latino	Clear Cell RCC	G2	pT3a NX M(N/A)
33836	58	69	Female	White/Not Hispanic or Latino	Clear Cell RCC	G3	pT3a NX M(N/A)
33851	59	46	Female	White/Not Hispanic or Latino	Chromophobe RCC	G3	pT3a NX M(N/A)
33885	60	62	Female	White/Not Hispanic or Latino	Clear Cell RCC	G2	pT1b N0(0/9) M(N/A)
33906	61	24	Male	White/Not Hispanic or Latino	Clear Cell RCC	G2	pT1b N0(0/2) M(N/A)

33915	*62	48	Male	White/Not Hispanic or Latino	Clear Cell RCC	G4	pT3a N1(15/17) M1
33956	63	74	Female	White/Not Hispanic or Latino	Papillary RCC	G2	pT2b NX M(N/A)
33962	*64	79	Male	White/Not Hispanic or Latino	Clear Cell RCC	G2	pT3a NX M(N/A)
35707	65	84	Male	White/Not Hispanic or Latino	Papillary RCC	G3	pT2a NX M(N/A)
35712	*66	58	Female	White/Not Hispanic or Latino	Clear Cell RCC	G2	pT1a NX M(N/A)
32147	67	75	Male	White/Not Hispanic or Latino	Clear Cell RCC	G2	pT1b NX M(N/A)
35769	*68	64	Male	White/Not Hispanic or Latino	Clear Cell RCC	G4	pT3a NX M(N/A)
39288	*69	53	Male	White/Not Hispanic or Latino	Clear Cell RCC	G4	pT3a NX M(N/A)
35862	70	53	Female	White/Not Hispanic or Latino	Clear Cell RCC	G2	pT1a NX M(N/A)
35887	71	85	Male	White/Not Hispanic or Latino	Clear Cell RCC	G4	pT3aNxM(N/A)
35891	72	62	Male	Asian	clear cell papillary RCC	G1	pT1a
35934	74	49	Male	White/Not Hispanic or Latino	Metastatic Clear Cell RCC	Unavailable	Unavailable
35955	75	69	Male	White/Not Hispanic or Latino	Clear Cell RCC	G2	pT1b NX M(N/A)

Table 2. Summary of RCC Patient and sample characteristics. The KUMC Biospecimen Repository Core Facility (BRCF) identification number, RCC sample number designation for this study, age of patient, gender, race/ethnicity, histologic subtype, grade and stage of all the samples used in this study.

Successful TIL generation was considered to be a cell culture which required splitting at least 4 times (1 well of a 24 well plate to an upright 175 cm^2 flask) using the panning protocol or 3 times (2 wells of a 24 well plate to an upright 175 cm^2) using the PreREP or

FTD + beads protocols in the 14-day time frame (see **Chapter 5: Materials and Methods** for additional detail). Average TIL yield was 23.6 x 10^7 (range = 5.5 x 10^7 – 4.8 x 10^8) using the panning protocol, 6.6 x 10^7 (range = 4.6 x 10^6 – 2.5 x 10^8) using the PreREP protocol and 18.1 x 10^7 (range = 4.5 x 10^7 – 3.7 x 10^8) using the FTD + beads protocol (**Figure 4A**). Using the described criteria for successful TIL generation, of the 6 samples used for comparing the protocols 6/6 panning, 3/6 PreREP, and 6/6 FTD + beads were successful; however, there were enough viable cells in the three failed PreREP cultures to perform immunophenotyping and functional assays – which was the rationale for using a minimum of 4 x 10^6 total cells to initiate each culture. An average of 93.2%, 82.6%, and

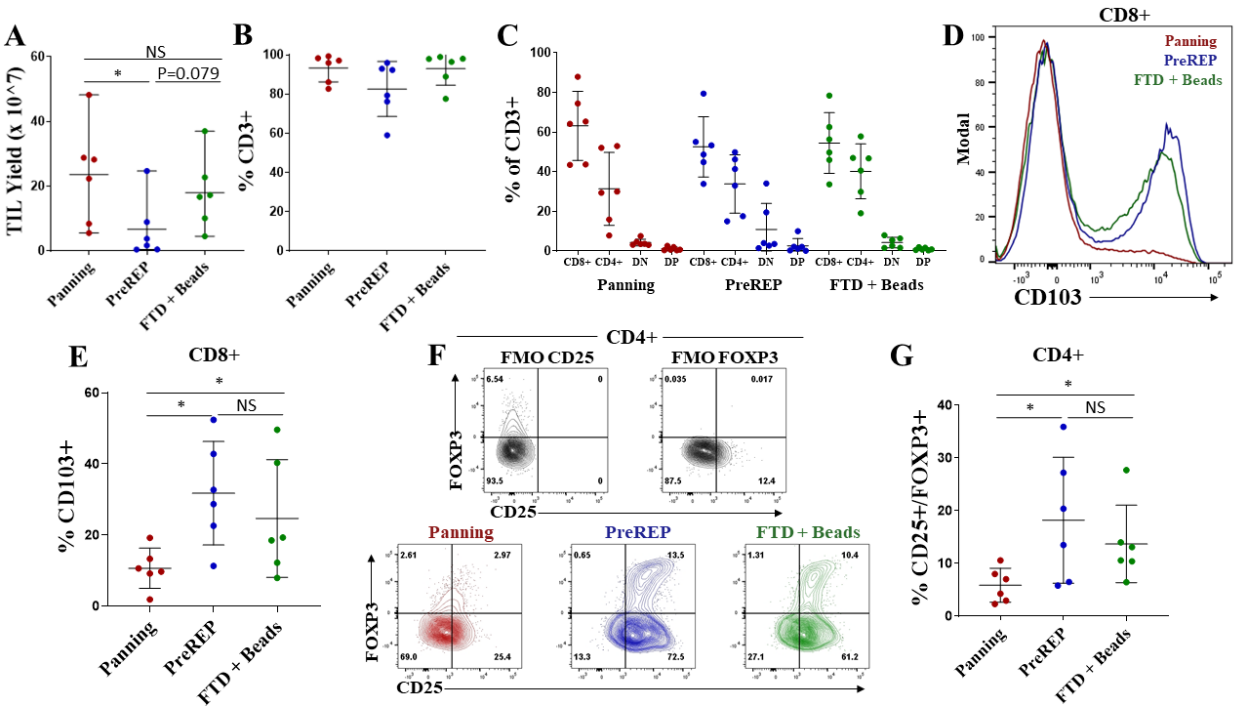

Figure 4. TILs generated by panning have an optimal phenotype for adoptive transfer. (**A**) TIL yields from 6 clear cell RCC samples using the Panning, PreREP, and FTD + beads protocols to expand autologous TILs. (**B**) Percentage of $CD3^+$ cells in the final TIL products. (**C**) Frequencies of $CD8^+$, $CD4^+$, DN, and DP T-cells in the final TIL products. (**D**) Representative CD103 staining of $CD3^+/CD8^+$ T-cells in the final TIL products. (**E**) Frequency of $CD103^+/CD8^+$ T-cells in the final TIL products. (**F**) Representative T_{reg} staining and fluorescence minus one (FMO) control. **G**) Frequencies of $CD25^+/FOXP3^+$ T-cells within the CD4+ subset in the final TIL products.

93.0% of cells were $CD3^+$ after expansion using the panning, PreREP and FTD + beads protocols, respectively (**Figure 4B**) and there were no statistically significant differences in the percentage of $CD4^+$ or $CD8^+$ T-cells generated by each protocol (**Figure 4C**). However, TILs expanded from two donors via PreREP had greater than 20% double-negative (DN) T-cells which parallels Markel et al's report (2009) using the PreREP protocol for generating TILs from RCC (84), but the biological significance of these post-expansion DN TILs is largely unknown.

Significantly fewer $CD103^+/CD8^+$ T-cells were observed when TILs were expanded by panning relative to both other protocols with an average of 10.6%, 31.8%, and 24.6% of $CD8^+$ T-cells expressing CD103 in the TIL products expanded by panning, PreREP, and FTD + beads, respectively (**Figure 4D, E**). CD103 is a marker of tissue-resident memory T-cells (T_{RM}) and binds to E-cadherin, playing a role in retaining these T-cells in epithelial tissues (150, 151). Although T_{RM}-cells may play an important role in the immune response to tumors derived from the epithelium, we believe they are not optimal for adoptive transfer because they are not known to recirculate (152) and therefore are unlikely to contribute to systemic responses after adoptive transfer. It is also known that T_{RM} cells can be generated by less differentiated T-cell subsets and therefore creating a TIL product enriched with these more desirable memory subsets is our aim and further described in **Chapter 4**. Another T-cell subset that we believe is not optimal for adoptive transfer is regulatory T-cells (T_{regs}), which are known to suppress anti-tumor effector functions. We show that panning produces a significantly smaller proportion of presumptive T_{regs} (T_{regs} = $CD4^+/CD25^+/FOXP3^+$) with an average of 5.9%, 18.2%, and

13.7% of $CD4^+$ T-cells expressing CD25 and FOXP3 after expansion by panning, PreREP, and FTD + beads, respectively (**Figure 4F, G**). The high levels of presumptive T_{regs} produced by both other protocols may be a result of simultaneous activation and PD-1/PD-L1 signaling that occurs as a result of leaving adherent cells in the culture. This combination of stimulatory and inhibitory signaling has been implicated in T_{reg} induction (153). There were no statistically significant differences in the expression of common markers used to determine the differentiation state of T-cells such as CD28, CD27, KLRG1, CD62L, or IL-7Ra as a result of expansion method; however, a slight (average 2.1% vs 3.8%), but statistically significant increase in CCR7 expression was observed when TILs were expanded by FTD + beads relative to panning (**Figure 5**). This is believed to be an anomaly, without biological significance, and is a result of using our predetermined statistical measure, the ratio-paired t test. When the same data is analyzed using a conventional paired t test, statistical significance is not reached. Although there is no clear difference in expression when evaluating each of these markers individually, when we evaluate co-expression of all of these markers

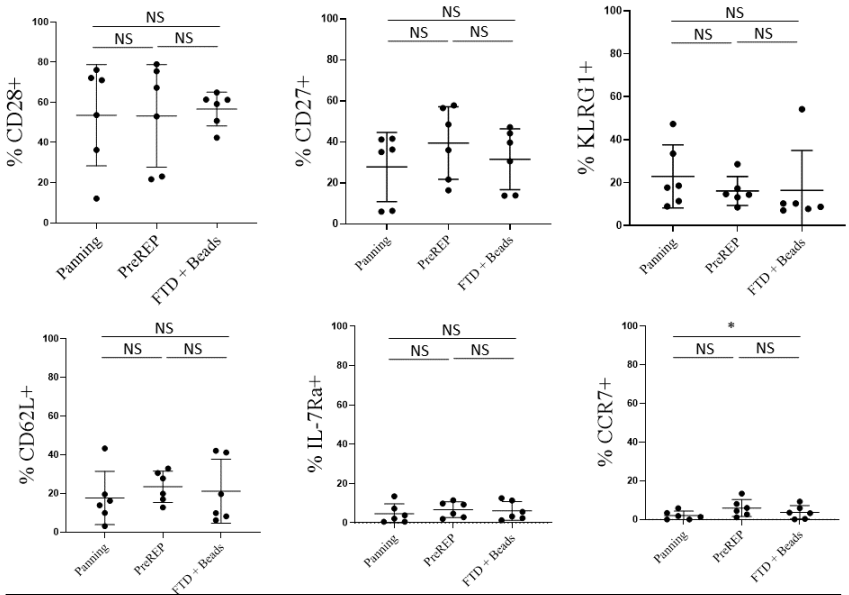

Figure 5. TIL expansion protocol does not affect the expression of proteins associated with T-cell differentiation states. Percent expression of CD28, CD27, KLRG1, CD62L, IL-7Ra, and CCR7 on the T-cells in the final TIL product.

simultaneously using t-distributed stochastic neighbor embedding (tSNE), we see differential clustering indicating that the different TIL expansion protocols do preferentially expand unique T-cell subsets which are not appreciated by single-variable analysis (**Figure 6**).

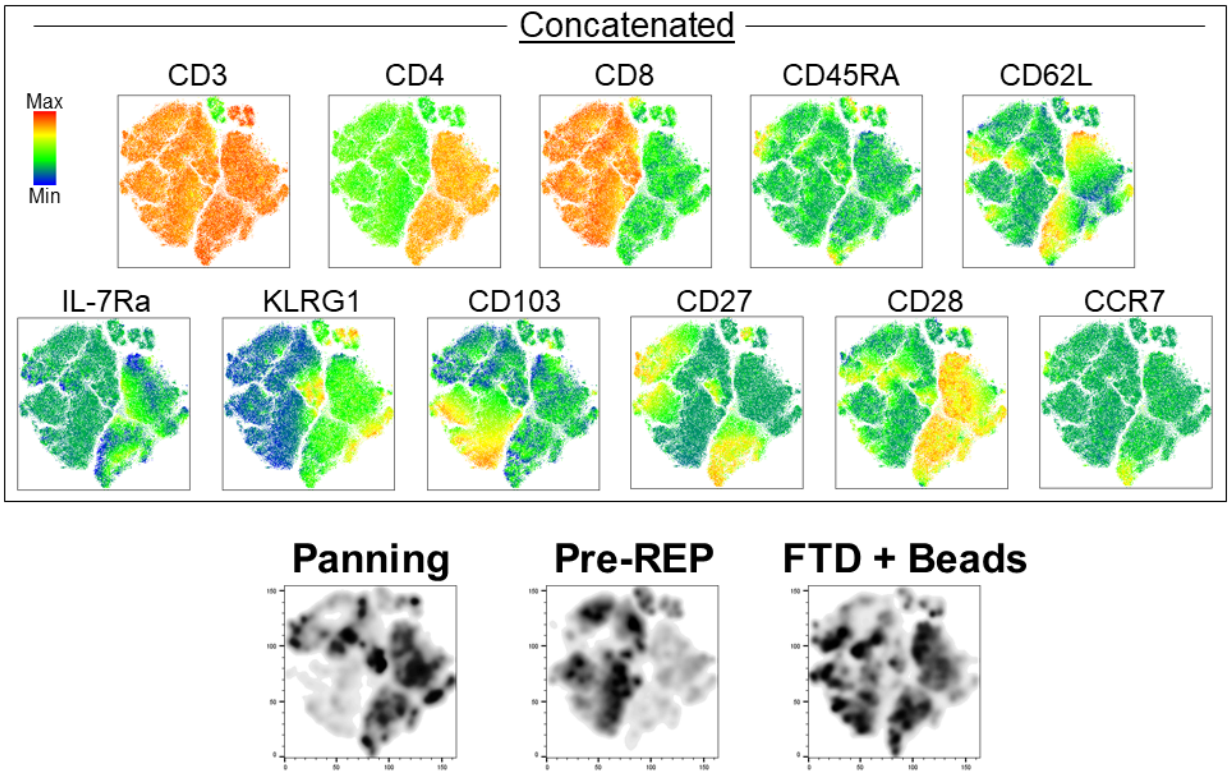

Figure 6. tSNE reveals differential T-cell expansion because of TIL production protocol. Representative tSNE plots of autologous TIL expanded by each protocol. Heat maps of the concatenated files shows relative expression of each indicated marker and density plots show where TIL expanded by each method cluster.

There is strong evidence that co-expression of multiple inhibitory immune checkpoints correlates with a state of decreased function and “exhaustion” (154, 155), therefore we also characterized the presence and relative abundance of immune checkpoint molecules on TILs following expansion using each of the three protocols. We report that the panning method, compared to the previously reported PreREP, and FTD + beads protocols,

generates significantly fewer PD-1+ T-cells (an average of 7.2%, 31.2%, and 15.4%, respectively) (**Figure 7A, B**). We show that on average over 75% of RCC TILs expanded in all conditions express TIM-3 (**Figure 7A, C**) with no significant differences in the percentage of TIM-3^{+} T-cells between methods. However, the percentage of PD-1^{+}/TIM-3^{+} double-positive T-cells is also significantly lower in the TIL products expanded by panning relative to PreREP and FTD + beads with an average of 6.0%, 23.0%, and 12.9% of T-cells expressing both PD-1 and TIM-3, respectively (**Figure 7A, D**). These PD-1+/TIM-3+ T-cells are known to be severely dysfunctional, terminally differentiated and have even been shown to produce the suppressive cytokine IL-10, which makes them

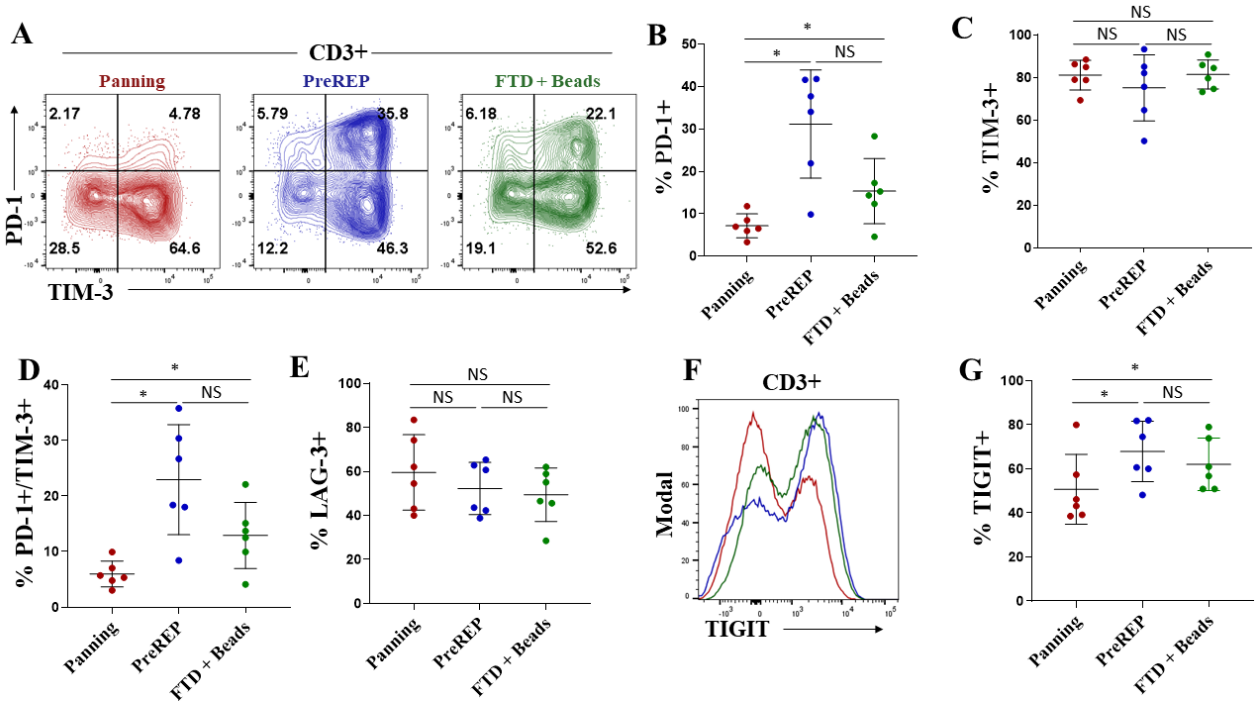

Figure 7. TILs generated by panning have reduced co-expression of immune checkpoints. (**A**) Representative TIM-3 vs PD-1 staining of autologous TIL products. (**B**) Frequency of PD-1^{+} T-cells in the final TIL products. (**C**) Frequency of TIM-3^{+} T-cells in the final TIL products. (**D**) Frequency of PD-1^{+}/TIM-3^{+} double-positive T-cells in the final TIL products. (**E**) Frequency of LAG-3^{+} T-cells in the final TIL products. (**F**) Representative TIGIT staining of autologous TIL products. (**G**) Frequency of TIGIT^{+} T-cells in the final TIL products.

suboptimal for adoptive transfer (156). We did not observe a significant difference in the percentage of T-cells expressing the LAG-3 immune checkpoint (**Figure 7E**); however, we also see a significant decrease in TIGIT^{+} T-cells when panning is used, as compared to PreREP and FTD + beads, with an average of 50.8%, 67.9%, and 62.1% of T-cells expressing TIGIT, respectively (**Figure 7F, G**). Taken together, our results demonstrate a decrease in co-expression of inhibitory immune checkpoints when TILs are expanded by panning which may indicate a decreased relative state of exhaustion making them superior for adoptive transfer.

3.4 Bead-based expansion generates TIL products with increased clonal diversity

TILs are known to respond to a variety of tumor specific neoantigens created by somatic mutations within protein coding genes which are transcribed, translated, degraded and ultimately presented as mutated peptide fragments on major histocompatibility complexes (MHC). TILs recognize these mutated peptide fragments/MHC complexes through their unique T-cell receptors (TCRs). The most diverse region of the TCR is the complementarity determining region 3 (CDR3) on the beta chain and it is statistically improbable that two different T-cell clones share the same TCRB CDR3 sequence; therefore, this region can be used to identify unique T-cell clones.

We preformed TCRB CDR3 sequencing on autologous TILs expanded by panning, PreREP, and FTD + beads from three donors. Donor 68 was selected for further studies because it was the outlier in which TIL yields were nearly identical using all three methods (22.4×10^7, 24.7×10^7, and 22.8×10^7, respectively) and donors 57 and 62 were selected

because TILs from these samples fit the trends in yield, phenotype, and function which we are reporting. We found that TILs expanded using pan-CD3 stimulation via anti-CD3/CD28 beads (panning and FTD + beads) results in a TIL product with a greater absolute number of T-cell clones (**Figure 8A**). An average of 13,822, 4,279, and 11,381 clones were detected in the TIL products expanded by panning, PreREP and FTD + beads, respectively based on productive TCRB CDR3 DNA sequences which result in a unique amino acid sequence (*i.e.,* unique but synonymous DNA sequences were

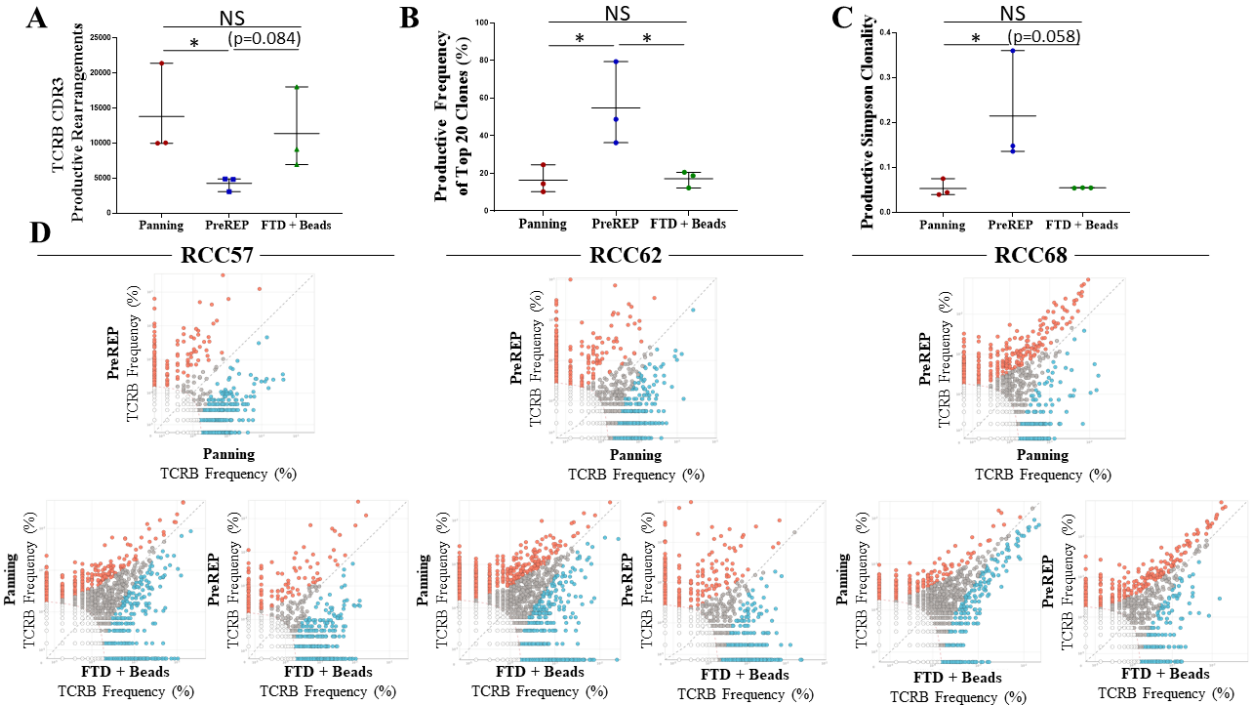

Figure 8. Bead-based TIL expansion generates TIL products with increased clonal diversity. We noted that dominant clones are identical and were expanded by all methods. (**A**) Absolute number of productive TCRB CDR3 rearrangements detected in the TIL products expanded by each method. (**B**) The combined productive frequency of the top 20 clones expanded by each method. (**C**) The productive Simpson clonality metric for the TIL products expanded by each method. (**D**) Comparison of clonal frequency for each specimen and method: clear dots represent clones which were too infrequent to be analyzed (each dot may represent multiple clones), grey dots represent clones which were not significantly enriched due to expansion method, blue dots represent clones which were significantly enriched by the method on the x-axis and red dots represent clones which were significantly enriched by the method on the y-axis.

considered identical clones). The top 20 most abundant clones detected in the TIL products expanded by the three methods accounted for an average of 16.5%, 54.8% and 17.2% of the total TCR repertoires, respectively (**Figure 8B**). In agreement with these trends the productive Simpson clonality was greatest in the TIL products expanded by PreREP (**Figure 8C**). Finally, we show that although the overall clonal diversity within the TIL products differed, the most abundant clones expanded by each method tend to be identical (**Figure 8D**). This is exemplified by TILs expanded from donor 68 in which gross TIL yields were nearly identical and the frequency of the most abundant clones were also highly comparable.

TILs generated by panning are tumor reactive

A potential concern when expanding TILs using immediate pan-CD3 stimulation via anti-CD3/CD28 beads is that the increased clonal diversity of the TILs may be the result of expanding bystander T-cells which are not specific for tumor antigens. This could create a dilute TIL product relative to the PreREP protocol. However, on the contrary the increased clonal diversity could be attributed to tumor reactive T-cell clones which are eliminated because of the suppressive signaling that occurs when leaving adherent cells

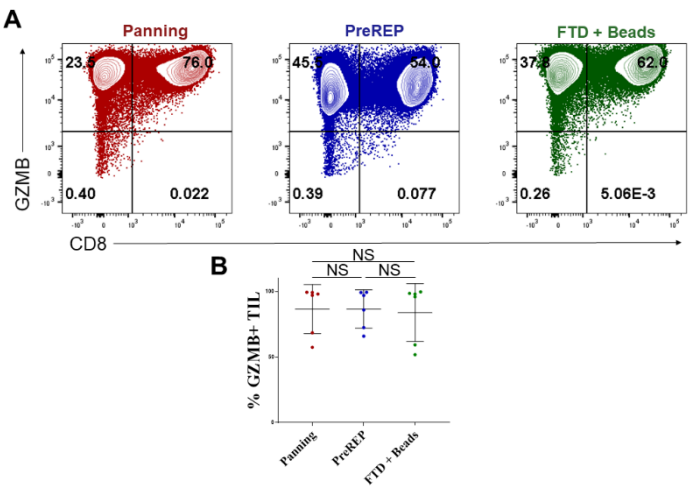

Figure 9. Uniform GZMB expression in post-expansion TIL. (A) Representative CD8 vs GZMB staining of autologous TIL expanded by the indicated method. (B) Summary of the percentage of GZMB$^+$ TIL from each sample.

in the TIL culture. First, we confirmed that a on average over 80% of TILs expanded by all methods express the effector molecule granzyme B (GZMB) which is known to be stored in preformed granules within T-cells allowing for rapid release and cytotoxic potential upon antigen recognition (**Figure 9A, B**). Surprisingly, there was not a significant difference in the proportion of TILs which degranulated ($CD107a^+$) after co-culture with autologous tumor cells as a result of the expansion method. Both a $CD8^+$ and $CD8^-$

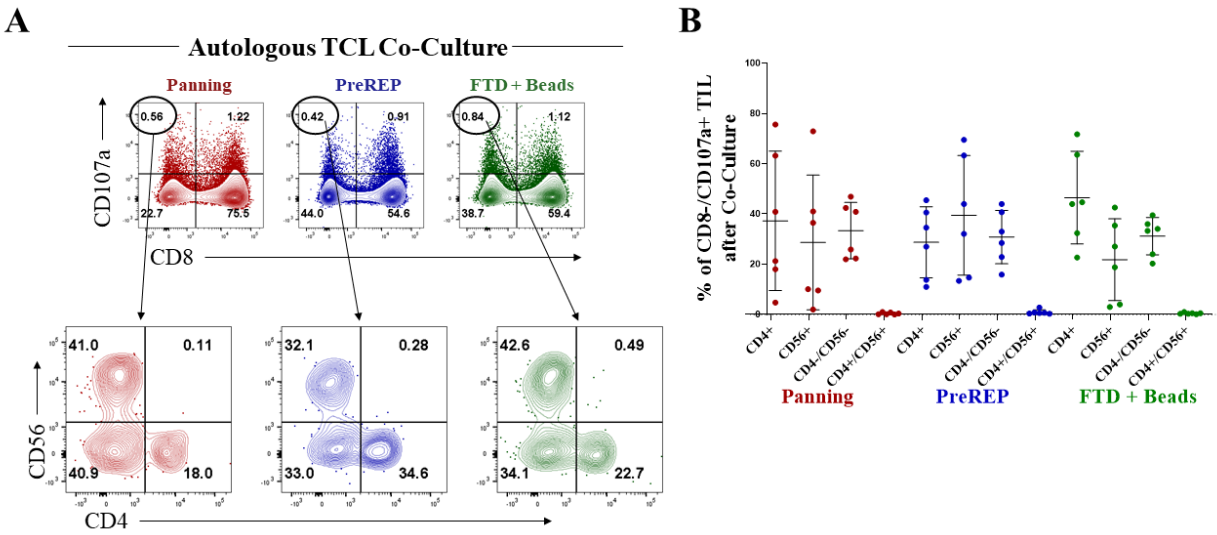

Figure 10. Degranulation of $CD8^+$ and $CD8^-$ TIL in response to autologous tumor cells. (A) Representative plots of CD8- TIL degranulation in response to autologous tumor cells. (B) Summary of the $CD8^-$ TIL response from all samples.

response was observed and the CD8- response consisted of $CD3^+/CD4^+$ T-cells, $CD3^+/CD56^+$ presumptive NKT-cells as well as $CD3^+/CD4^-/CD8^-/CD56^-$ T-cells and there were no significant differences in $CD8^-$ responses observed as a result of expansion method (**Figure 10A, B**). The average percentage of total T-cells degranulating in response to autologous tumor cells was greatest using the PreREP protocol with a mean of 2.2%, 3.8%, and 1.9% of TILs expanded by panning, PreREP, and FTD + beads transiently expressing CD107a at their cell surface (**Figure 11A, B**). Of note, there were as many as 3.2% of TILs degranulating in the unstimulated condition after PreREP

expansion and up to 1.8% using the FTD + beads protocols. This observation may indicate tumor cells and/or antigen are still in the TIL cultures at the 14-day mark using these protocols. There was also no significant difference in the percentage of TILs which produced IFNɣ in response to autologous tumor cells with an average of 1.5%, 2.0%, and 1.0% of TILs producing this effector molecule after expansion by panning, PreREP, and FTD + beads respectively. A similar phenomenon of IFNγ production in the unstimulated populations, which were not subjected to panning, was noted (**Figure 11C, D**). Interestingly, in response to autologous tumor cells, TILs generated by all protocols were rarely polyfunctional (*i.e.,* simultaneously degranulated and produced IFNɣ) (**Figure 11E**). As shown, only ~16.5% (0.89/5.39) of the TILs which responded in co-culture with autologous tumor cells produced IFNγ and degranulated, even though of the cells capable of degranulating and/or producing IFNγ (OKT3 positive control) ~40.8% (17.3/42.4) were polyfunctional. This could be a result of bystander TILs, which are only activated in the positive control, having increased levels of polyfunctionality or it may be that the tumor cells are suppressing a polyfunctional response by an unknown mechanism. These results parallel the report by Markel and colleagues who showed that non-pooled PreREP RCC TIL cultures displayed either lytic activity or IFNɣ secretion, but not both (84). The average percentage of tumor reactive T-cells generated – defined as CD107a+ and/or IFNγ+ when co-cultured with autologous tumor cells – was greatest using the PreREP protocol (**Figure 11F**). An average of 3.4%, 5.3%, and 2.8% of TIL were tumor reactive in the final TIL products expanded by panning, PreREP and FTD + beads, respectively. However, when we multiplied the percentage of tumor reactive TIL (**Figure 11F**) by the absolute number of TILs generated in each condition from each sample (**Figure 4A**), we

observed an average of 8.0 x 10^6, 2.7 x 10^6, and 4.6 x 10^6 total tumor reactive TILs generated by panning, PreREP and FTD + beads, respectively (**Figure 11G**). These results indicate that although a greater percentage of bystander TIL are potentially being generated when anti-CD3/CD28 beads are added to the initial TIL culture, the combination of adherent cell depletion and bead-based TIL stimulation generates an increased total number of RCC reactive TIL in a 14-day time frame.

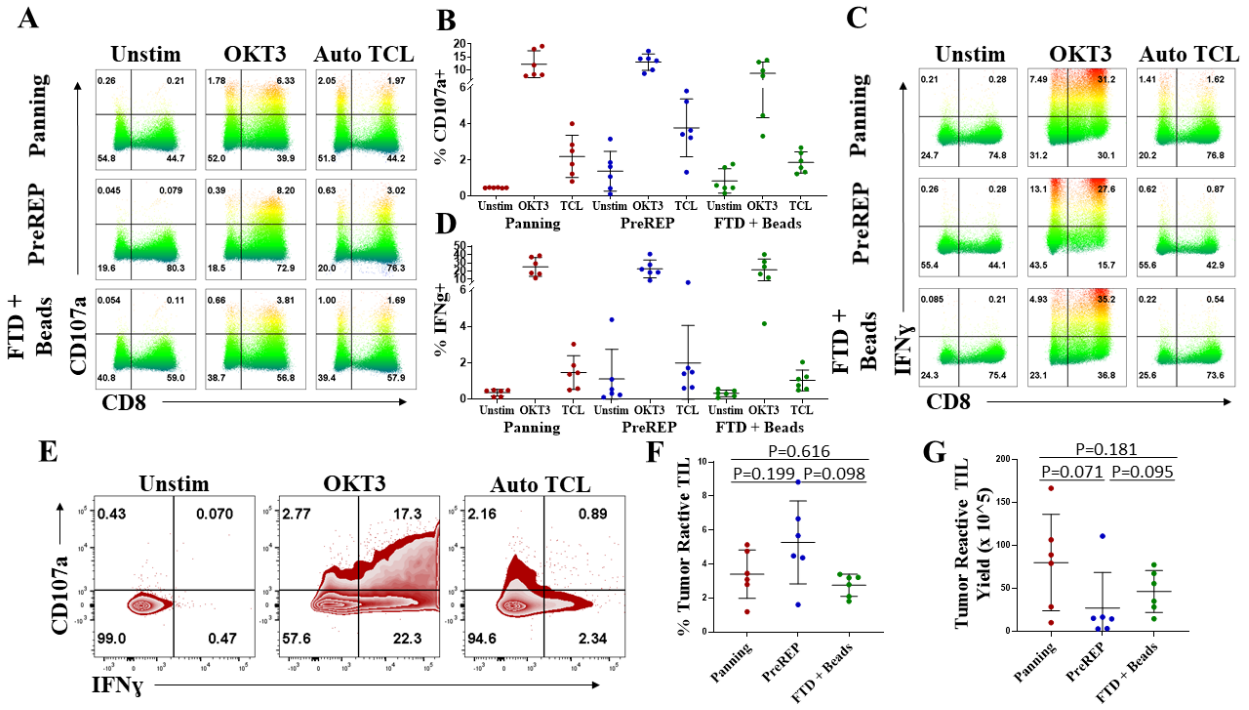

Figure 11. TILs generated by panning are tumor reactive. (**A**) Degranulation ($CD107a^+$) of autologous TIL products left unstimulated, OKT3 stimulated or in response to the autologous tumor cell line (auto TCL). (**B**) Frequency of degranulation of the final TIL products. (**C**) IFNγ expression by autologous TILs in the indicated conditions. (**D**) Frequency of IFNγ expression within the final TIL products. (**E**) Co-staining IFNγ vs CD107a of Panning TIL in response to autologous tumor cells. (**F**) Percentage of T-cells which degranulated and/or produced IFNγ in response to autologous tumor cells (Tumor Reactive TIL) in the final TIL products. (**G**) Tumor reactive TIL yield - calculated by multiplying the percentage of tumor reactive TIL by the total TIL yield for each condition and sample.

3.5 Discussion

Consistent generation of TIL cultures from RCC has been historically problematic which has hindered the development of this potentially curative cell therapy for patients with kidney cancer (12). Here we demonstrate that a novel protocol for TIL expansion allows for the consistent production of tumor reactive TIL from ccRCC as well as the consistent establishment of autologous adherent tumor cell cultures from patient samples. This creates an *in vitro* model for studying TIL therapy and also allows for evaluating the complex interplay between autologous tumor cells and T-cells in an *in vitro* setting which may mimic the tumor microenvironment (TME) (**Figure 12**) (157).

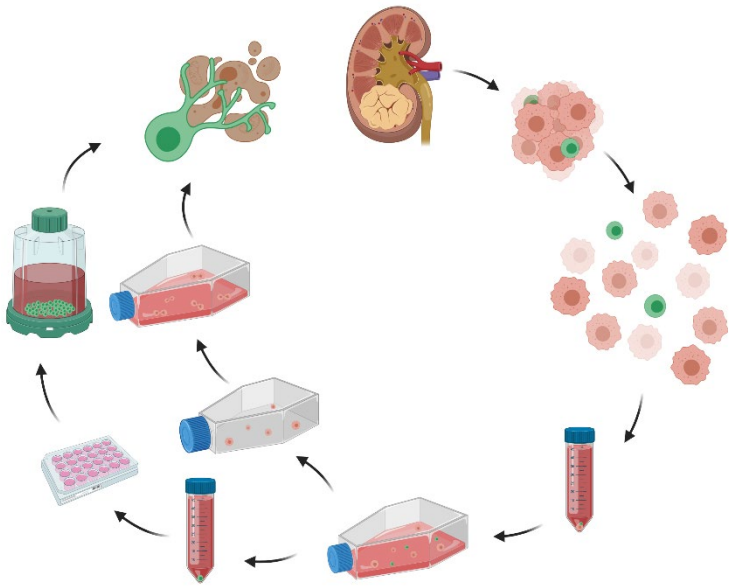

Figure 12. An *in vitro* model for evaluating autologous T-cell and tumor cell interactions in ccRCC. Representative image depicting the process of creating autologous TIL and tumor cell lines using the adherent cell depletion method by Braun et al. This image was created with BioRender.com.

Critically, the panning approach advances the field of T-cell therapy for RCC by demonstrating that the phenotype of the resulting TIL product is superior for adoptive transfer relative to autologous TILs produced by other protocols. Mechanistically, we hypothesize these phenotypic differences are a result of expanding TILs in the absence of immunosuppressive tumor cells. An activated T-cell within a whole FTD secretes inflammatory molecules (*e.g.,* IFNγ) and as a result adherent tumor cells in culture actively upregulate PD-L1 which is known

to suppress TIL activation. Simultaneously, secretion of galectin-9 by tumor cells may teather TIM-3 to the supramolecular activation cluster on T-cells (146). The significance of galectin-9/TIM-3 interaction alone has been somewhat controversial; however, this interaction has been shown to lead to the phosphorylation of tyrosine 265 on the cytoplasmic tail of TIM-3 and most evidence points to this interaction playing a role in suppressing type 1 T-cell responses (146, 158-161). Other ligands of TIM-3 which have been shown to modulate function which can be restored with TIM-3 blockade are phosphatidylserine (PS), carcinoembryonic antigen cell adhesion molecule 1 (CEACAM1), and high mobility group box 1 (HMGB1) and these ligands have binding clefts separate from galectin-9's on the TIM-3 receptor (160, 162). Therefore, if the activated T-cell does manage to degranulate and lyse an adherent tumor cell during TIL expansion, the flipping of PS to the outermembrane of tumor cell derived apoptotic bodies may deliver this second immunosuppressive signal via the galectin-9 primed TIM-3 receptor. We believe this combination of activating and inhibitory signals is responsible for inducing a regulatory and exhausted phenotype which can be minimized by ACD prior to TIL expansion.

The proposed panning method also likely reduces TIL exposure to the CD103 ligand, E-cadherin, which is expressed by adherent epithelial cells. We hypothesize that decreased ligand exposure is the mechanisms which leads to a TIL product with fewer CD103+ tissue-resident memory T-cells. Although T_{RM}-cells have been implicated in anti-tumor responses (163), we believe they are not ideal for adoptive transfer because durable systemic responses will likely require tumor reactive T-cells with a memory phenotype

which allows them to recirculate. Therefore, the phenotypic differences that result from expanding RCC TILs after adherent cell depletion are optimal for adoptive transfer.

We show that the proposed panning method produces a greater absolute number of tumor reactive T-cells on average, as determined by *in vitro* co-culture with autologous tumor cells. However, we believe it is likely that both the percent and absolute number of tumor reactive T-cells are being underestimated using this method. Indeed, the NGS data (*i.e.,* >98% allele frequency for a given mutation) suggests that short-term *in vitro* propagation of the adherent tumor cells leads to clonal populations. However, it does not represent the more heterogeneous tumor cell populations that exist *in vivo*. Therefore, there may be tumor reactive TILs expanded by all methods that are not appreciated in these assays because a clonal tumor cell population was used as the target.

Finally, it has been suggested that there is an inverse correlation between *in vitro* culture time and the efficacy of the TIL product; however, it has also been demonstrated that there is a direct correlation between the absolute number of TILs infused and response rates. Balancing these two opposing curves is an overarching challenge in the field of TIL therapy. We are proposing the panning protocol as a single-phase, modified rapid expansion protocol to generate a TIL product in an unprecedented 14-day time frame. The absolute TIL yields reported here are a result of starting with only a fraction of the tumor digests which were generated using discard tissue after surgical pathology processed the samples. In the clinical trial setting, a larger portion of tissue would likely be obtained for TIL generation and the entire sample could be used to generate a TIL

product via panning which would drastically scale up TIL yields in the same time frame. TIL counts of 10^{10} to 10^{11} are the usual target yields prior to cell infusion using the two-phase PreREP/REP protocol; however, cell manufacturing can take up to 6 to 8 weeks to achieve these counts using this method. A two-week TIL product would be of great interest to patients dealing with the mental and physical stresses associated with waiting for TIL production as well as clinicians monitoring disease progression during this same time frame; therefore, we propose further evaluation of this single-phase protocol to expand TILs with a firm 14-day timeline from surgery to infusion of the cell product.

These studies demonstrate the consistent and rapid generation of tumor reactive TILs from clear cell RCC is possible. The stigma from the 1990's that TIL therapy is not feasible for RCC should be disregarded and renewed efforts at translating this potentially promising therapy into the clinics for patients with advanced ccRCC is warranted.

Chapter 4: Induction of a Memory T-cell Phenotype During ccRCC TIL Expansion

Now that it has been demonstrated that the rapid and consistent *in vitro* production of TILs from ccRCC is feasible, we aimed to further enhance potency of the TIL products created using the ACD method by attempting to induce a long lived central and/or stem cell-like memory phenotype. Although effector and effector-memory T-cells are the subsets which have the greatest ability to directly lyse cancer cells, they have limited proliferative potential upon repeat antigen encounter. Therefore, these cells have a lower level of absolute anti-tumor efficacy relative to their less differentiated central and stem-cell like memory counterparts which are able to persist, proliferate and produce a pool of effectors upon repeat antigen encounter after adoptive transfer (15). As shown in the previous chapter, the TIL expansion protocol did not have a significant impact on memory phenotypes other than the T_{RM} subset. This observation is likely due to all methods relying on IL-2 mediated expansion which inevitably leads to differentiation. There have been several proposed methods for inducing the more desirable memory phenotypes including lineage reprogramming via forced expression of transcription factors through genetic modification, using different combinations co-receptor and cytokine stimulation and the pharmacologic modification of T-cell signaling while using conventional methods of stimulation (164). In these studies, we pursued the latter with the rationale that it would be feasible to rapidly translate the findings into the clinic.

4.1 Inhibition of AKT induces a memory-like $CD8^+$ T-cell phenotype while expanding RCC TILs, but negatively affects proliferation

First, we pursued targeting the AKT signaling pathway which has been shown to induce a desirable memory phenotype while expanding melanoma TILs with the

PreREP/REP protocol without impacting TIL proliferation (165). We evaluated peripheral blood T-cell expansion using healthy donor samples in the presence of increasing concentrations of an AKT inhibitor via a CFSE dye dilution assay in order to reveal a general concentration range which ideally would not impact TIL proliferation. We used the same AKT inhibitor (AKTi VIII – Calbiochem) which was used in the melanoma TIL study and found that short term T-cell proliferation was unaffected by up to 8 μM of this drug (**Figure 13**). This result was encouraging because the melanoma study reported a consistent dose as low as 1 μM, induced the desirable phenotype, therefore we believed we had a large window (between 1-8 μM) to hopefully obtain similar results from RCC.

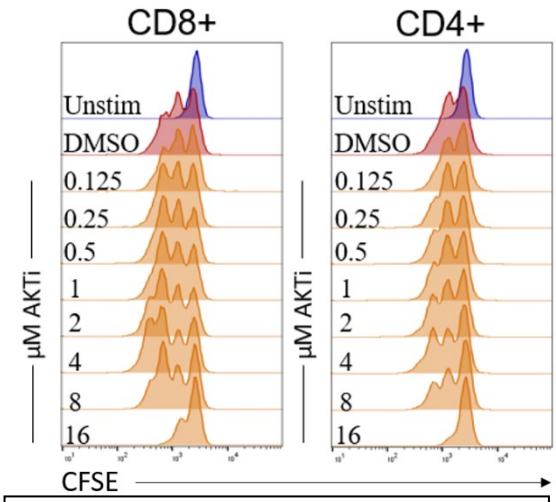

Figure 13. Impact of AKTi on healthy donor T-cell proliferation. Healthy donor T-cells labeled with CFSE and stimulated identically to TIL cultures, evaluated at 72 hours for dye dilution in the indicated concentration of AKTi.

Using our adherent cell depletion protocol to expand TIL from RCC we began using the same 1 μM dose of AKTi which was used in the melanoma study and compared autologous TIL expansion to expansion without the inhibitor (evaluating autologous TIL expansion with numerous parameters [multiple concentrations] is not consistently feasible because of the limited tissue which is obtained for research purposes). We found that after 14 days of expansion with AKTi, $CD8^+$ RCC TILs consistently expressed higher levels of the lymph-node home molecule CD62L which is associated with a central-

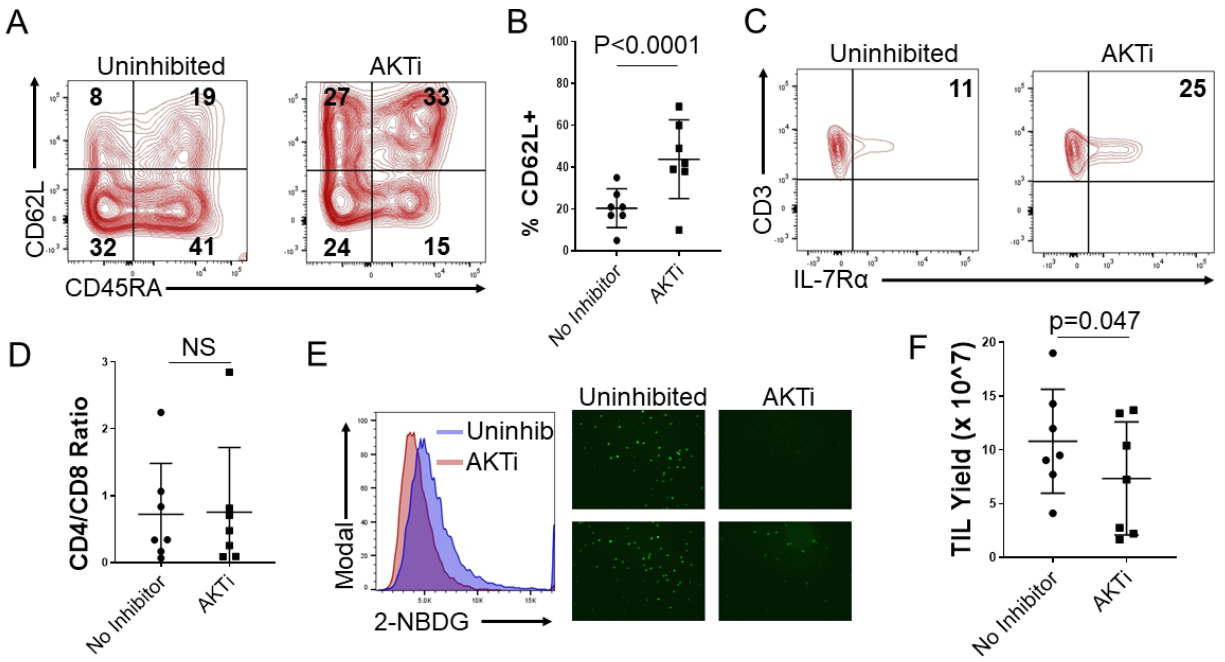

Figure 14. AKT inhibition induces a memory-like phenotype while expanding RCC TILs, but negatively affects proliferation. (A) Representative CD45RA vs CD62L staining of autologous $CD8^+$ RCC TILs expanded with and without AKT inhibition. (B) Percentage of $CD8^+$ TILs which express CD62L from seven separate patients. (B) IL-7Rα vs CD3 staining of RCC TIL expanded with and without AKT inhibition. (D) CD4/CD8 ratio of RCC TIL expanded with and without AKTi from seven RCC samples. (E) 2-NBDG uptake assay evaluated by flow cytometry and fluorescent microscopy (two representative field of view for each condition). (F) TIL yields after 14 days of expansion with and without AKTi.

memory ($CD45RA^-/CD62L^+$) and stem cell-like memory/naïve ($CD45RA^+/CD62L^+$) phenotype (**Figure 14A, B**). We also found higher levels of IL-7 receptor alpha (IL-7Rα) expression on T-cells expanded with AKTi (**Figure 14C**) and as described in **Chapter 2**, IL-7 is associated with memory T-cell homeostasis. The CD4/CD8 ratio of the T-cells in the final TIL product was not affected by AKTi (**Figure 14D**). Another indication that a desirable memory phenotype is induced by AKTi is that glucose uptake is altered. Effector T-cells are known to utilize more glucose to generate energy, while memory T-cells preferentially perform oxidative phosphorylation and fatty acid metabolism to generate ATP (166). In agreement with this report, TILs following treatment with a AKTi had lower

levels of 2-NBDG uptake, which is a fluorescent glucose analog (**Figure 14E**). Critically however, in contrast to the report by Crompton et al. (165), TIL expansion was decreased when the AKTi was used (**Figure 14F**).

The decreased proliferation observed when using an AKTi was discouraging. It should be noted that although the range in **Figure 14F** appears broad and overlapping, when evaluating each of the seven paired, autologous TIL expansions, the absolute yield was decreased in 7/7 using the AKT inhibitor. This observation led to the re-evaluation of whether or not AKTi should be further explored using different drugs in the same class.

We identified four additional AKT inhibitors (afuresertib, MK-2206, perifosine and triciribine) which had been explored in the clinical setting for various indications and

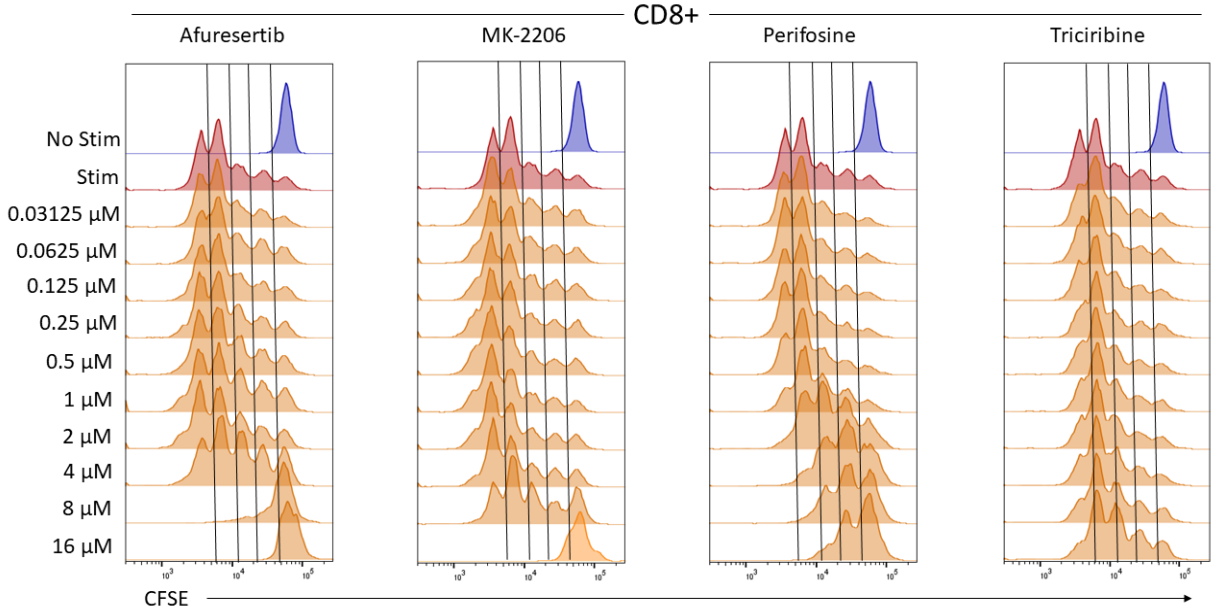

Figure 15. Limited effects on short-term T-cell proliferation using low dose clinical grade AKT inhibitors. 96-hour CFSE dye dilution assay using healthy donor peripheral blood T-cells unstimulated or stimulated identically to TIL cultures in the presence of the indicated drug and concentration.

decided to evaluate whether a similar induction of memory characteristics could be achieved without impacting proliferation by using one of these different drugs in the same class. Again, we screened the new drugs for their effect on proliferation using healthy donor peripheral blood T-cells and a CFSE dye dilution assay (**Figure 15**). Using the short-term proliferation data, we identified concentration ranges for each drug which we hoped would induce a desirable memory phenotype without altering proliferation during prolonged T-cell expansion. We moved forward with the screening, again using healthy donor peripheral blood T-cells so that we would be able to compare many culture conditions and hopefully identify a candidate to move forward with for subsequent TIL expansions. During prolonged 14-day expansions we noted a disappointing trend, the

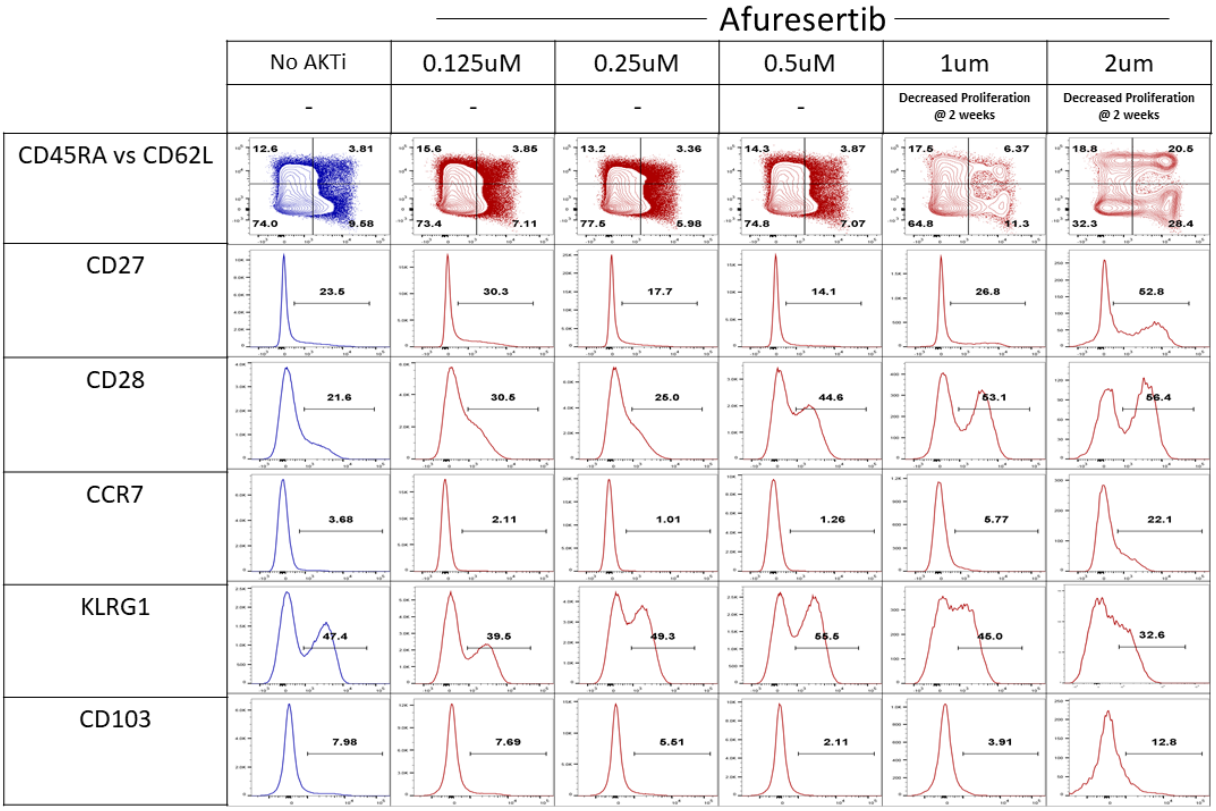

Figure 16. Effects of afuresertib on T-cell proliferation. Healthy donor T-cells expanded in the presence of the indicated concentration of afuresertib and evaluated by flow cytometry. Grossly reduced T-cell proliferation was noted via light microscopy.

concentrations of these various AKT inhibitors which induced a desirable phenotype consistently decreased proliferation. We evaluated the expression of CD45RA vs CD62L to split T_{scm}/T_n ($CD45RA^+/CD62L^+$), T_{cm} ($CD45RA^-/CD62L^+$), T_{em} ($CD45RA^-/CD62L^+$) and $T_{eff/emra}$ ($CD45RA^+/CD62L^-$) T-cells. We also stained for CD27 and CD28 expression which are co-stimulatory receptors and both tend to be expressed on less differentiated T-cells and CCR7 expression which is a chemokine receptor playing a role in lymph node homing and the generally expressed by naïve, central-memory and stem cell-like memory T-cells. The final parameters in this screening panel were KLRG1, which is an inhibitory receptor expressed by differentiated T-cells, and CD103, which is expressed by tissue-resident memory T-cells. Therefore, the expression of both molecules would be viewed

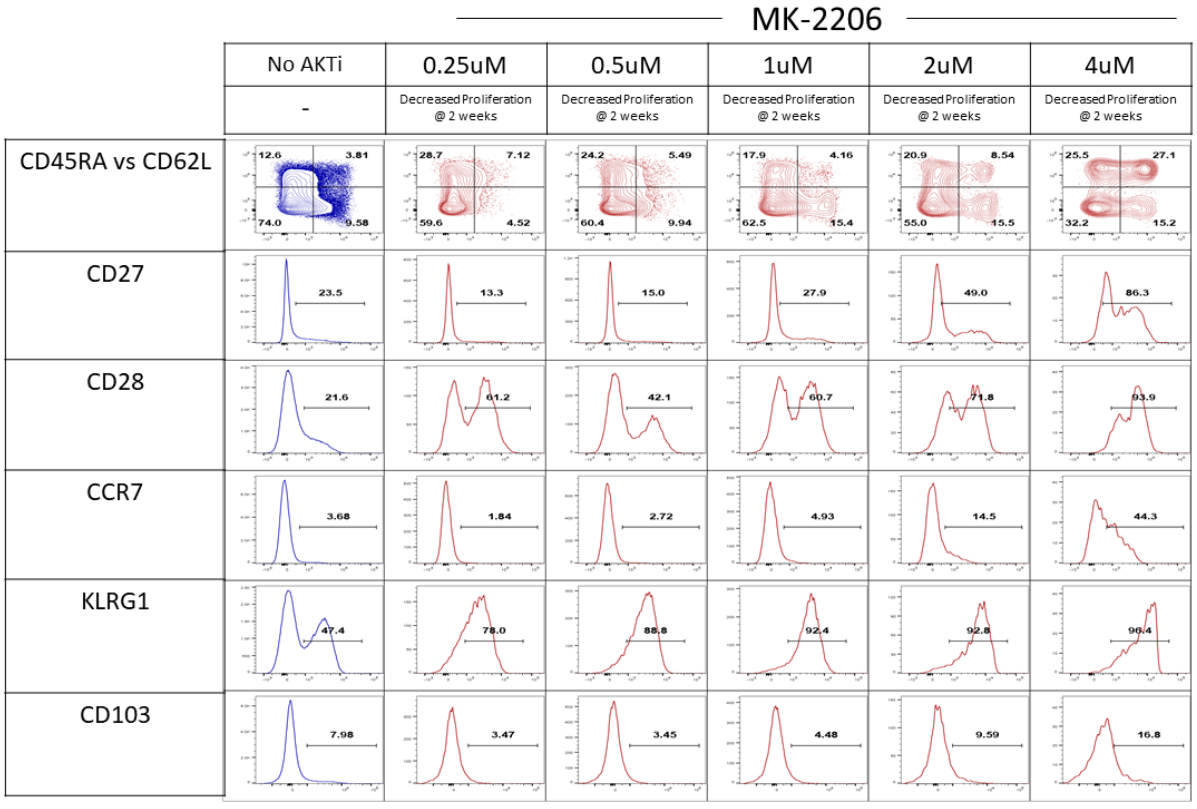

Figure 17. Effects of MK-2206 on T-cell proliferation. Healthy donor T-cells expanded in the presence of the indicated concentration of MK-2206 and evaluated by flow cytometry. Grossly reduced T-cell proliferation was noted via light microscopy.

as non-desirable. Increased CD62L expression was noted at concentrations at and above 1 μM when screening the drug afuresertib; however, decreased proliferation was also noted at these concentrations (**Figure 16**). All concentrations of MK-2206 which were screened negatively affected T-cell proliferation; however, increased CD62L expression and co-stimulatory receptor expression was observed (**Figure 17**). Initially, we were intrigued to determine if an even lower concentration could induce this phenotype without altering proliferation. However, the

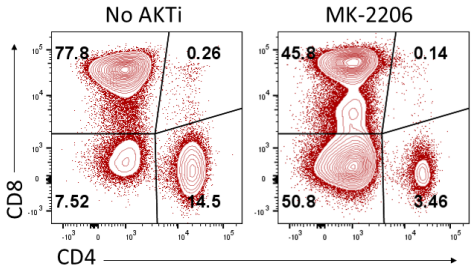

Figure 18. MK-2206 induces double-negative T-cells. CD4 vs CD8 staining of healthy donor T-cells expanded in the presence of MK-2206 for 14 days.

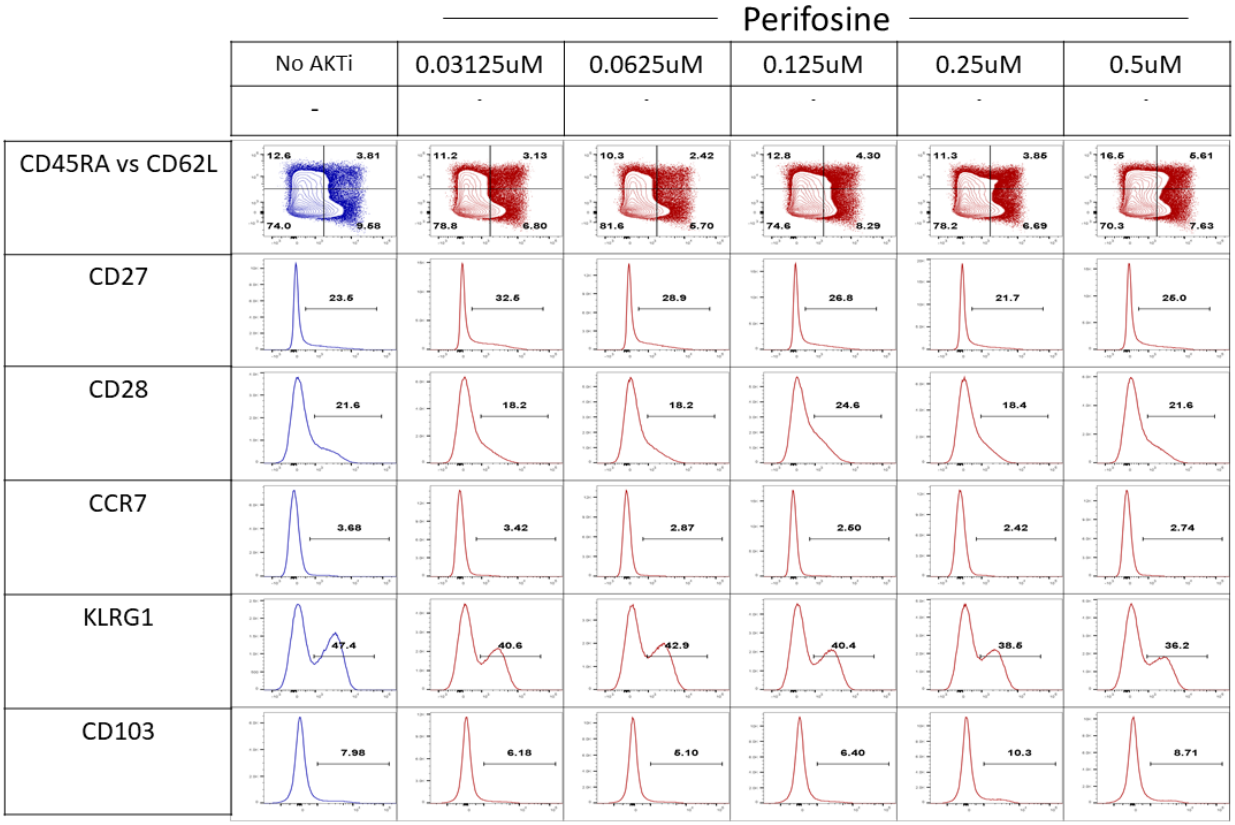

Figure 19. Effects of perifosine on T-cell proliferation. Healthy donor T-cells expanded in the presence of the indicated concentration of perifosine and evaluated by flow cytometry. Grossly reduced T-cell proliferation was noted via light microscopy.

unexpected and rather bizarre finding of increased KLRG1 expression as well as observing that over 50% of the $CD3^+$ cells expanded in the presence of this drug were CD4/CD8 double-negative, led us to stop pursuing this AKT inhibitor (**Figures 17 & 18**). Concentrations of up to 0.5 μM of perifosine were used during the 14-day expansion screening and this range did not appear to have any obvious effect on T-cell phenotypes nor T-cell expansion (**Figure 19**). Of note, concentrations of this drug at and above 1μM began to have adverse effects on T-cell proliferation during the short-term CFSE dye dilution assay (**Figure 15**). All concentrations of the fourth AKT inhibitor, triciribine, also had a negative impact on proliferation, but we observed an increased CD62L, co-

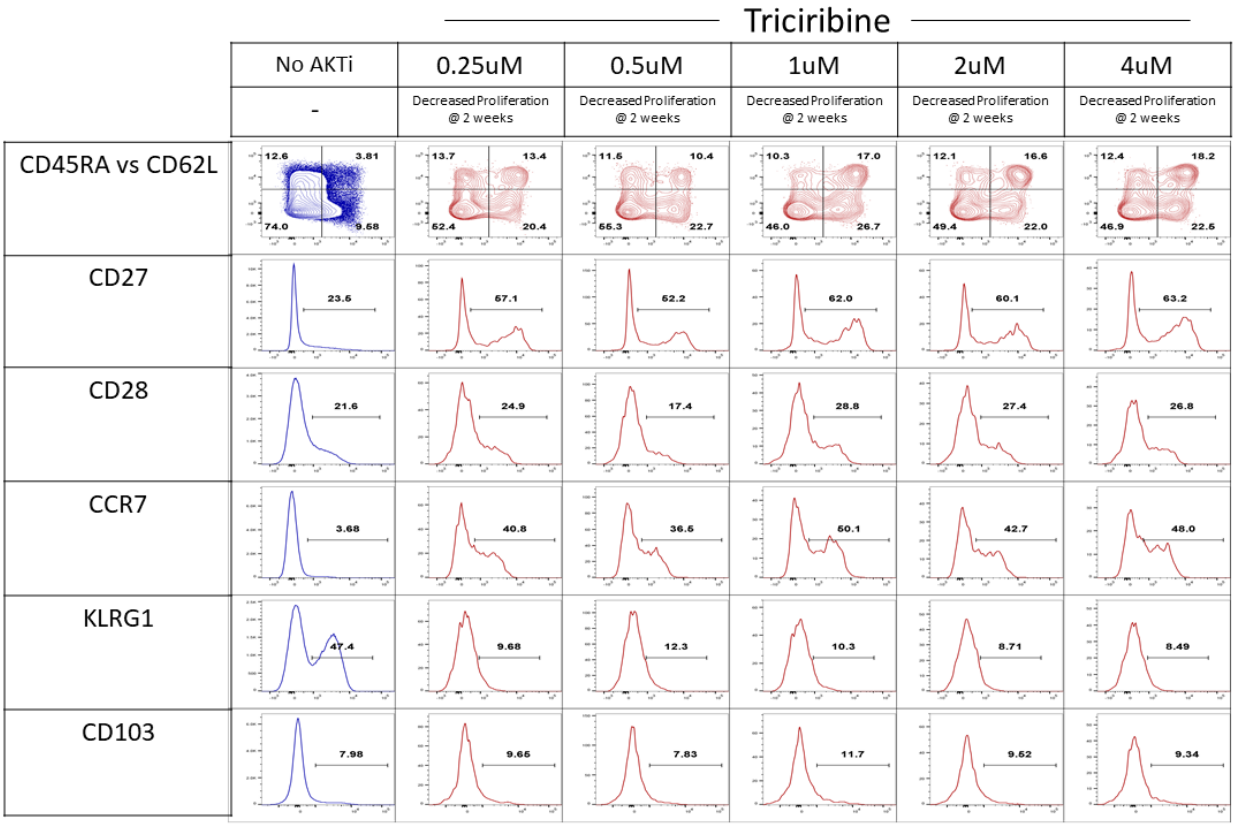

Figure 20. Effects of triciribine on T-cell proliferation. Healthy donor T-cells expanded in the presence of the indicated concentration of triciribine and evaluated by flow cytometry. Grossly reduced T-cell proliferation was noted via light microscopy.

stimulatory receptor expression, and CCR7 expression without an impact on KLRG1 or the CD4/CD8 ratio or double negatives (**Figure 20**). Therefore, we moved forward and explored the effects of this drug when expanding TILs at half of the lowest concentration used to screen the healthy donor T-cells (*i.e.,* 125 nM) from a single RCC sample. We found that this concentration reduced TIL proliferation (3.11 x 10^8 TILs obtained with no inhibitor and 1.46 x 10^8 TILs obtained with 125 nM triciribine) but did not lead to an increase in CD62L expression. Therefore, we began to re-evaluate whether AKT inhibition was the best approach to induce a memory T-cell phenotype during RCC TIL expansion.

Early during the study of AKT inhibitors, we performed a reverse phase protein array (RPPA) in order to obtain a better understanding of the larger changes in signaling and

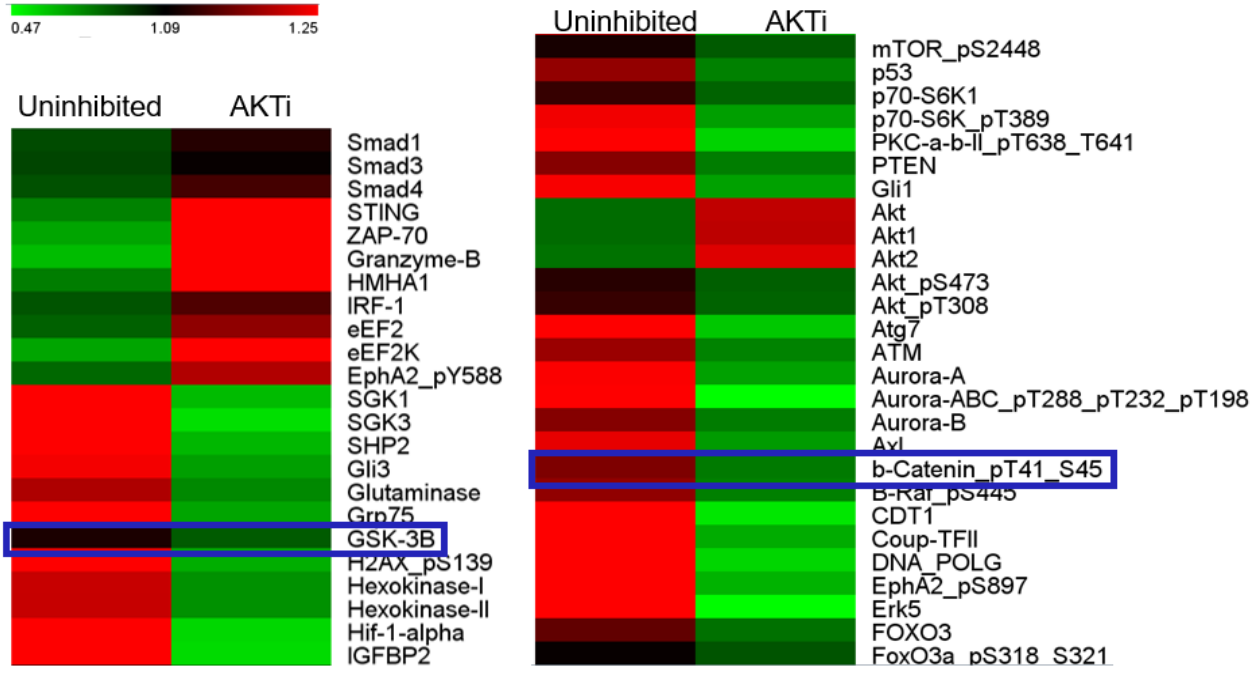

Figure 21. Reverse phase protein array (RPPA) reveals GSK-3B down regulation in the setting of AKTi. Selected results from an RPPA array performed on protein isolated from autologous RCC TILs expanded with and without AKT inhibitor VIII.

protein expression that result from treatment with AKTi VIII (**Figure 21**). These results confirmed that phosphorylation of AKT was reduced when TILs were expanded in the presence of this drug and that interestingly total AKT was increased. There were numerous intriguing hits within this data set that could be associated with T-cell function, metabolism and memory phenotypes and a notable result which stood out was the decreased expression of glycogen synthase kinase 3 beta (GSK-3B) and corresponding decrease in the phosphorylation of β-catenin (blue boxes). GSK-3B inhibition has been reported to arrest effector differentiation and promote $CD8^+$ T-cell memory (167); however, it has also been suggested that this only prevents the differentiation of T-cells and it does not revert CD45RA-negative T_{eff}/T_{em} (which is the phenotype of a vast majority of pre-expansion $CD8^+$ T-cells [**Figure 1D, E**]) to a less differentiated phenotype (168). Since, these studies were not performed on TILs, we decided to evaluate the effects of the GSK-3B inhibitor (TWS119) on TIL expansion using our adherent cell depletion method (**Chapter 3**) (83).

4.2 Inhibition of GSK-3B induces a memory-like CD8+ T-cell phenotype, without altering the proliferation of RCC TILs

Considering the failure of a short-term proliferation assay using healthy donor T-cells to predict a desired concentration of the AKT inhibitors which would not alter TIL expansion; we decided to screen the GSK-3B inhibitor (GSK-3Bi), TWS119, using a narrow range of drug concentrations (0.5 to 2 μM) using small scale autologous TIL cultures. We found a sharp drop off of absolute yield of TILs during a 14-day expansion at concentrations above 1 μM (**Figure 22**). Therefore, we conducted TIL expansion studies using media containing 750 nM TWS119 to reduce the chance of technical error which could potentially lead to a sharp drop off in proliferation.

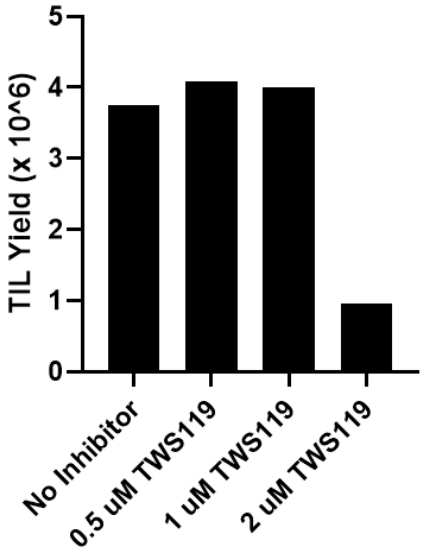

Figure 22. Impact of GSK-3B inhibition on TIL proliferation. Absolute TIL yields obtained from autologous TIL cultures expanded in the indicated concentration of TWS119.

Using these conditions to expand TILs from three independent ccRCC samples we found that the average TIL yield was not significantly affected (**Figure 23A**). Nearly all cells in the post-expansion TIL products were T-cells ($CD3^+$) both with and without GSK-3Bi (**Figure 23B**) and percentage of $CD4^+$, $CD8^+$, double-negative, and double-positive T-cells was not significantly affected by TWS119 (**Figure 23C**). Remarkably, we saw a significant increase in CD62L expression within the $CD8^+$ T-cell subset, which was strikingly similar to the results obtained with the AKT inhibitor (**Figure 23D, E**). The major

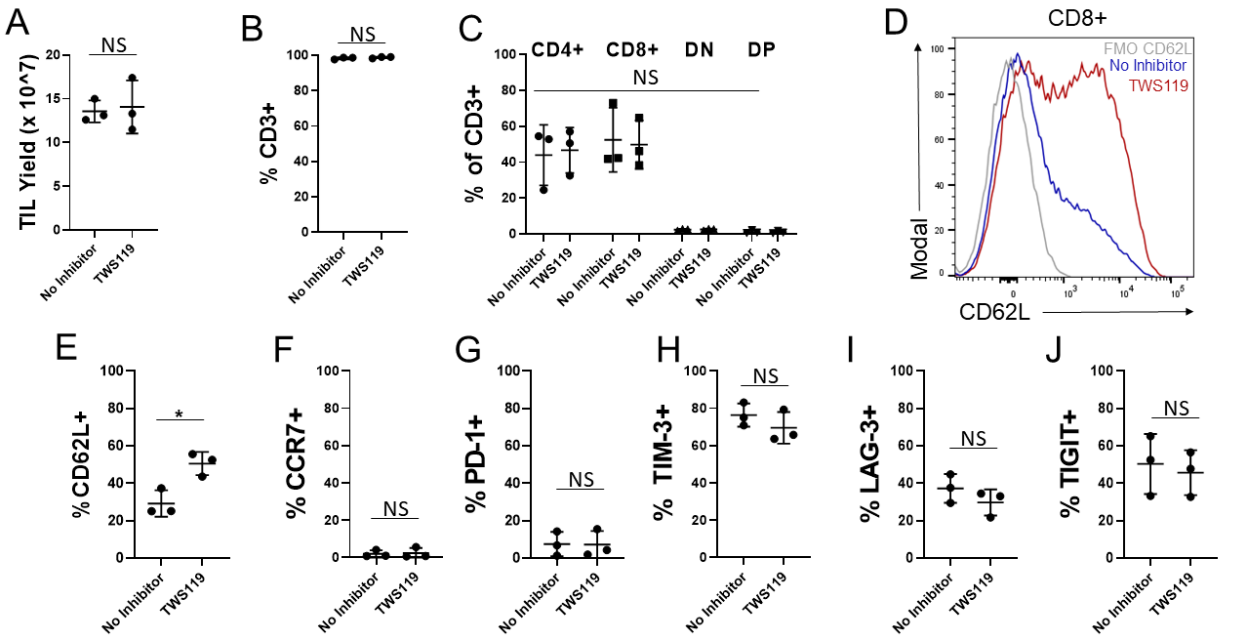

Figure 23. GSK-3B inhibition induces a CD8⁺/CD62L⁺/CCR7⁻ phenotype without altering RCC TIL proliferation. (A) Absolute TIL yield from 3 samples expanded with and without TWS119. (B) Percent CD3⁺ T-cells in the final TIL products. (C) Percent CD4⁺, CD8⁺, double-negative (DN) and double-positive (DP) T-cells in the final TIL products. (D) Representative plot showing CD62L expression on autologous TIL expanded with and without TWS119. Grey = fluorescence minus one (FMO) CD62L control, blue = no inhibitor, red = TWS119. (E) Percent of CD8⁺ T-cells expressing CD62L in the final TIL products. (F) Percent of CD8⁺ TIL expressing CCR7 in the final TIL products. (G) Percent of CD8⁺ TIL expressing PD-1 in the final TIL products. (H) Percent of CD8⁺ TIL expressing TIM-3 in the final TIL products. (I) Percent of CD8⁺ TIL expressing LAG-3 in the final TIL products. (J) Percent of CD8⁺ TIL expressing TIGIT in the final TIL products.

difference being continuous treatment with TWS119 did not negatively affect TIL proliferation. Interestingly, CCR7 expression was virtually absent on the CD8⁺ T-cells expanded both with and without the GSK-3B inhibitor (**Figure 23F**). Bona-fide central and stem cell-like memory T-cells are commonly thought to co-express CD62L and CCR7 and it is common for only one of these parameters to be evaluated when phenotyping T-cell subsets. There is limited research which has evaluated the function or reported the presence of the CD8⁺/CD62L⁺/CCR7⁻ T-cells which are being created at large numbers

as a result of expanding RCC TILs with constant exposure to low levels of the GSK-3Bi. For this reason, we refer to these cells using the broad term “memory-like” CD8$^+$ T-cells. Finally, no significant difference was observed in the expression of the inhibitory immune checkpoints PD-1, TIM-3, LAG-3 or TIGIT within this cohort (**Figure 23G-J**).

Observing a lack of effect on TIL proliferation when using the GSK-3Bi and a similar induction of CD62L on CD8$^+$ T-cells as compared to when the AKT inhibitor was used was an intriguing preliminary result. However, we were concerned about the effect of modulating this signaling pathway on the CD4$^+$ T-cell subset and potentially inducing suppressive cells (169). Therefore, we stained for regulatory T-cells within the autologous TIL products created with and without GSK3Bi. Although statistical significance was not reached in our study of 3 patient samples (p=0.115) using our predetermined statistical measure, the average percent of CD4$^+$ T-cells co-expressing CD25/FOXP3 was actually decreased when TILs were expanded with TWS119. Further, each pair autologous TIL cultures had a relative decrease of this non-desirable T-cell population (**Figure 24**).

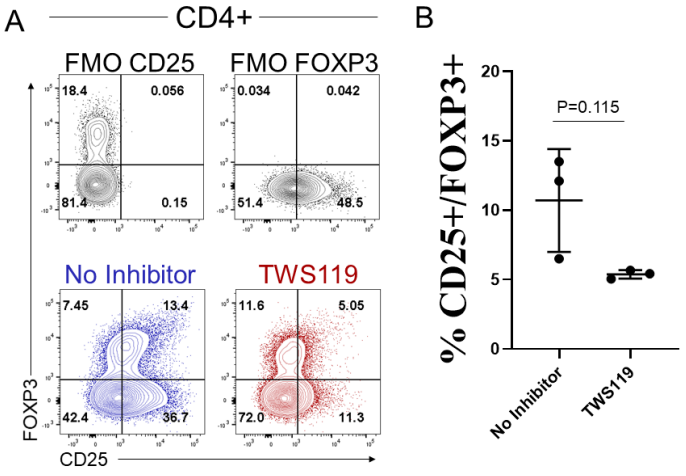

Figure 24. Decreased average CD4$^+$/CD25$^+$/FOXP3$^+$ yields when expanding RCC TIL with TWS110. (A) Representative CD25 vs FOXP3 staining of autologous TIL expanded with and without TWS119. (B) Percent of CD4$^+$ T-cells expressing CD25 and FOXP3 from the three samples.

Next, we aimed to determine if the CD62L expressing $CD8^+$ T-cells which were induced by TWS119 treatment expressed the pioneer transcription factor T-cell factor 1 (TCF1, also known as transcription factor 7 (TCF7)) which has been shown to be involved in chromatin remodeling and stem-cell like features within T-cells (170-173). We found that TCF1 was expressed at significantly higher levels within the post-expansion $CD8^+/CD62L^+$ TILs relative to $CD8^+/CD62L^-$ TILs (**Figure 25A, B**). This was the case

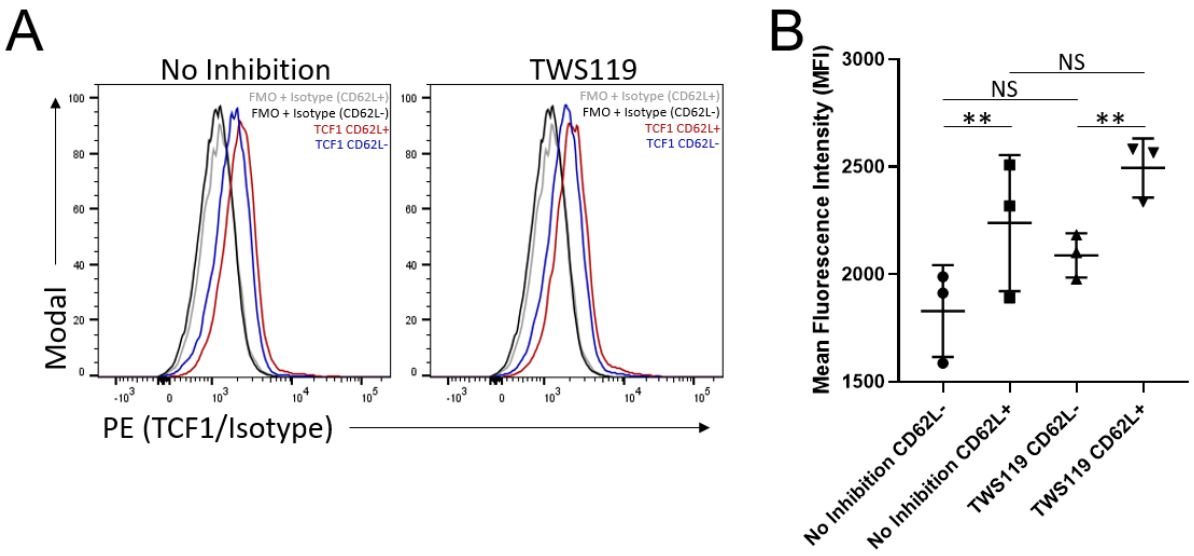

Figure 25. Increased TCF1 expression within post-expansion $CD8^+/CD62L^+$ TILs. (A) Representative histograms showing TCF1 expression within $CD8^+/CD62L^+$ T-cells (red histogram) relative to $CD8^+/CD62L^-$ T-cells (blue histogram) when autologous TILs were expanded with and without TWS119. (Grey histogram represents the fluorescence minus one (FMO) control with prior gating on $CD62L^+$ cells and the black histograms represents the FMO control with prior gating on CD62L- cells. (B) Summary of TCF1 mean fluorescence intensity (MFI).

when the TILs were expanded with or without TWS119 and although the average mean fluorescence intensity (MFI) was higher in the $CD62L^+$ subset expanded with the TWS119, there was not a statistically significant increase in TCF1 expression between $CD62L^+$ TILs expanded with the inhibitor relative to without. Nevertheless, the absolute number of $CD8^+/CD62L^+$ cells was greater when TILs were expanded with TWS119; so, there is an increase in overall TCF1 expression within the TIL products expanded in the

presence of GSK-3Bi and this is potentially contributing to stem-cell like features within these T-cells.

Finally, we aimed to determine which pre-expansion TIL subsets were giving rise to these $CD8^+/CD62L^+/CCR7^-$ T-cells which were preferentially expanded using a GSK-3Bi since it had been previously reported that TWS119 can arrest effector differentiation but cannot cause a reversion to a less differentiated state (168). After performing adherent cell depletion on a large ccRCC fresh tumor digest, we sorted populations of T_{emra}/T_{eff} cells ($CD3^+/CD62L^-/CCR7^-/CD45RA^+$), T_{em} cells ($CD3^+/CD62L^-/CCR7^-/CD45RA^-$) and $T_{cm}/T_{scm}/T_n$ cells ($CD3^+/CD62L^+$ and/or $CCR7^+/CD45RA^{+/-}$) (**Figure 26A**). This sorting schema was designed to have the highest degree of purity within the T_{emra}/T_{eff} and T_{em} populations since these were the primary experimental subsets which were not expected to contribute to the post-expansion $CD62L^+$ population (168). After sorting, we expanded bulk TILs along with each sorted subpopulation in parallel both with and without 750 nM TWS119. As we had previously observed within the bulk TIL population (red), there was an increase in CD62L expression when TILs were expanded with continuous exposure to low dose TWS119. As expected, we also saw increased CD62L expression within the $T_{cm}/T_{scm}/T_n$ cells (orange) which were sorted and expanded with the TWS119 relative to without and this parallels the report that GSK-3Bi can arrest differentiation. We did not observe appreciable CD62L expression within the T_{emra}/T_{eff} cells (blue) which were sorted and expanded with or without TWS119, but interestingly a vast majority of these cells became CD45RA-negative. Intriguingly though, the T_{em} subset (green) which was sorted and expanded did give rise to a $CD62L^+$ subset and there was increased $CD8^+$ T-cells

expressing CD62L when expanded with TWS119 relative to without, 48.5% and 24.1%, respectively (**Figure 26B**). This finding contradicts previous reports and indicates that GSK-3B inhibition may be reverting effector-memory TILs to a less differentiated phenotype.

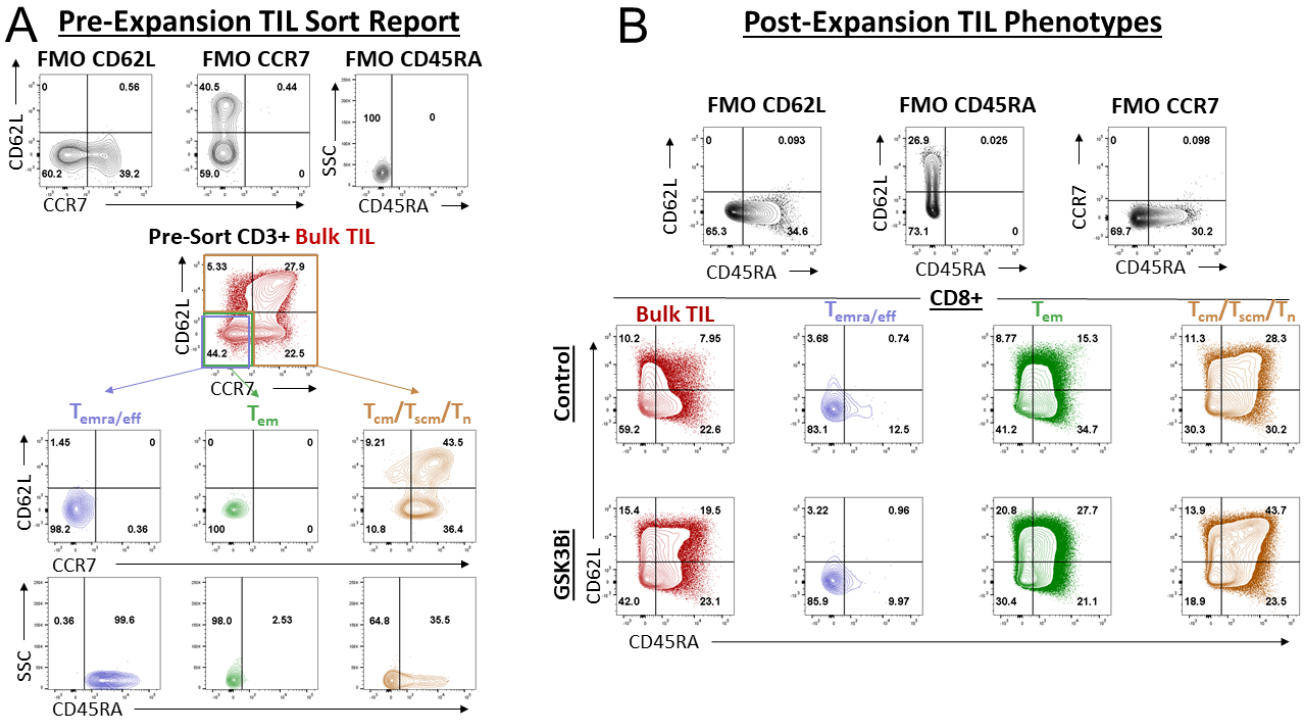

Figure 26. GSK-3Bi induces expression of CD62L in CD8⁺ T_{em} cells. (A) Pre-expansion ccRCC TIL sort report showing isolation of T_{emra}/T_{eff}, T_{em}, and $T_{cm}/T_{scm}/T_n$ cells. (B) Post-expansion phenotypes of each subset expanded with TWS119 and without (control).

Discussion

This report demonstrates that chemical inhibition of GSK-3B during *in vitro* ccRCC TIL expansion has the potential to create a potent T-cell product enriched with a memory-like phenotype and we hypothesize that this cell therapy will show efficacy in the clinic. In contrast to reports expanding T-cells from melanoma using the “young TIL approach”

(165), we show that AKT inhibition is not an ideal method to induce a memory-like phenotype because of the overall decrease in TIL yields. This biological limitation is important given that the absolute number of T-cells infused during ACT has been shown to be directly correlated with response rates (72, 174). TWS119 has been shown to arrest effector differentiation of T-cells already expressing a minimally differentiated phenotype, however it has been suggested that reversion to a less differentiated state is not achieved by targeting this pathway (167, 168). We show for the first time that $CD8^+$ T_{em} TILs can be induced to become $CD62L^+/CCR7^-$ via GSK-3B inhibition and these $CD62L^+$ cells express higher levels of the pioneer transcription factor associated with T-cell stemness, TCF1, relative to their $CD62L^-$ counterparts. These findings have the potential to impact the clinical value of TIL therapy for ccRCC and pose an intriguing basic science inquiry into how these memory-like $CD8^+/CD62L^+/CCR7^-$ cells function *in vivo*. The combination of a novel protocol for the rapid and consistent generation of TIL products and the ability to induce a desirable memory-like phenotype has renewed hopes that personalized T-cell based therapies for ccRCC can be successfully translated into the clinic and improve outcomes for patients with aggressive disease.

Chapter 5: Materials and Methods

5.1 Patients and samples

Deidentified clinical samples were provided from the Biospecimen Repository Core Facility (BRCF) at the University of Kansas Medical Center (KUMC) along with relevant clinical information. Tissue specimens were obtained from patients enrolled under the repository's institutional review board approved protocol (HSC no: 5929) and following the US Common Rule. Tissue from patients who underwent radical or partial nephrectomy within the University of Kansas Health System for suspected RCC was obtained between August 2017 and January 2020. **Table 2** provides clinical information on each of these patient samples. Tissues were delivered from the operating room to surgical pathology where the BRCF staff obtained a portion of the discarded tissues, deidentified the samples, and immediately transported the specimens at room temperature in RPMI-1640 to the basic research laboratory for TIL and tumor cell line (TCL) generation.

5.2 Creation of fresh tumor digests (FTDs)

Using aseptic techniques in a laminar flow hood, fibrotic, necrotic, and normal adjacent tissues were grossly dissected from viable tumor. Viable tumor was mechanically and enzymatically digested in a cocktail containing RPMI-1640 (without serum), 1 mg/mL type IV collagenase (Sigma), 100 units/mL deoxyribonuclease I (MP Bio), 1× penicillin, streptomycin, and amphotericin B (Antibiotic-Antimycotic; Gibco). Viable tumor and digestion cocktail were added to a Miltenyi C Tube and disrupted using a gentleMACS Dissociator followed by a 30 min incubation at 37°C with gentle rocking; mechanical disruption and 30 min incubations were continued until a slurry was obtained (approximately 1–1.5 hours). The slurry was passed through a 100 μm cell strainer,

pelleted, subjected to ammonium chloride–potassium (ACK)-mediated RBC lysis (BioLegend) and washed in phosphate-buffered saline (PBS). This FTD was either used immediately for culture or cryopreserved for future use. Digests of normal adjacent kidney tissue were performed on selected samples using the same protocol.

5.3 Generation of TIL and TCL cultures by panning, PreREP, and FTD+ beads

Panning protocol:

Total viable cells of 4 to 6×10^6 from an FTD were plated in a BioLite 175 cm^2 vented flask (Thermo Fisher Scientific) and incubated overnight at 37°C and 5% CO_2 in T-cell media consisting of RPMI-1640 with 2.05 mM L-glutamine, 10% fetal bovine serum (FBS), 25 mM HEPES (Gibco), 1 mM sodium pyruvate (HyClone), 1× non-essential amino acids (HyClone), and 1× penicillin/streptomycin (HyClone). Non-adherent cells were then pooled by washing five to eight times with PBS until no non-adherent cells were observed in the flask. The non-adherent cells were pelleted and resuspended in 2 mL of fresh T-cell media and transferred to a single well of a 24-well plate. 6,000 IU/mL of IL-2 (teceleukin) and 4×10^5 anti-CD3/anti-CD28 Dynabeads (Thermo Fisher Scientific) were then added. TILs were split three times (1 well to 8 wells of a 24-well plate) by resuspending the T cells and transferring 1 mL into a fresh well and then adding 1 mL of fresh media (FM) to each well. Splitting of TILs occurred when clusters of expanding T cells were grossly visible in the well. Eight wells of TILs were then pooled and transferred to an upright 175 cm^2 flask with 50 mL of media (16 mL of TILs + 34 mL FM). 50 mL of additional media was added 24–48 hours later and subsequent 1:1 splitting to multiple upright T175 flasks occurred when a carpet of expanding T cells was grossly visible in

the flask. Media was never removed from the TIL culture using the panning protocol because splitting was always indicated before media acidified and 6000 IU/mL of IL-2 was maintained by bolus addition after each splitting. Beads were removed at the completion of TIL expansion (day 14). Adherent cells were grown in parallel in DMEM (Dulbecco's Modified Eagle Medium) with high glucose (HyClone) supplemented with 10% FBS, 1× penicillin/streptomycin (HyClone), and 1× Insulin-Transferrin-Selenium (Gibco) to establish TCLs.

PreREP protocol:

Total viable cells of 4–6×10^6 of an FTD were plated in 2 wells of a 24-well plate (2–3×10^6/well) with 2 mL of T-cell media per well and 6,000 IU/mL of IL-2. Splitting occurred as described in the panning protocol; however, half of the media was regularly required to be removed (slowly pipetting from the top of the well) and replaced with FM and IL-2 before splitting was indicated. 6,000 IU/mL of IL-2 was maintained by bolus addition after each splitting or media replacement.

FTD+ beads protocol:

Total viable cells of 4–6×10^6 of an FTD were plated in 2 wells of a 24-well plate (2–3×10^6/well) with 2 mL of T-cell media per well, 4×10^5 anti-CD3/anti-CD28 Dynabeads and 6,000 IU/mL of IL-2. Splitting occurred as described in the panning protocol; however, half of the media was regularly required to be removed (slowly pipetting from the top of the well) and replaced with FM and IL-2 before splitting was indicated. 6,000 IU/mL of IL-2 was maintained by bolus addition after each splitting or media replacement. Beads were

removed at the completion TIL expansion (day 14). All cell counts in this study were performed using a Muse Cell Analyzer (MilliporeSigma) and the Muse Cell Count and Viability kit.

5.4 Immunohistochemistry, immunocytochemistry, and histology

Prior to digestion, a portion of the RCC sample and normal adjacent tissue were fixed in 10% neutral buffered formalin at room temperature for 48 hours. Tissues were then dehydrated in 70% ethanol for 24 hours. The samples were then embedded in paraffin and processed by the KUMC BRCF staff using a Tissue-Tek Processor (Sakura). Microtomy was performed on a Leica RM2255 Microtome (Leica Biosystems). Automated staining for pan-cytokeratin and the paired box 8 protein (PAX-8) was performed using an intelliPATH instrument (Biocare). Immunocytochemistry was performed using the same protocol with cell pellets of the primary TCLs established from the tumor sample. Images were acquired using MetaMorph Microscopy Image Analysis Software (Molecular Devices) on a Nikon Eclipse 80i Microscope.

5.6 Flow cytometry

Flow cytometry was performed using a BD LSR II in the KUMC Flow Cytometry Core Laboratory. Cell surface staining was performed in 2% FBS in PBS, and BD Horizon Brilliant Stain Buffer (BD Biosciences) was added when multiple BV dyes were used in the same panel. Cells were subsequently washed in protein-free PBS and stained for viability using Ghost Dye 780 (Tonbo). Cells were resuspended in 2% FBS in PBS for analysis. Transcription factor staining was performed using the True Nuclear

Transcription Factor Buffer Set (BioLegend), and cytokine staining was performed using the eBioscience IC Fixation Buffer and Permeabilization Buffer (Invitrogen). Analyses were performed using FlowJo (V.10.6.1, V.10.6.2, and V10.7.1; FlowJo). Analyses included debris exclusion (Forward Scatter-Area vs Side Scatter-Area (FSC-A vs SSC-A)), single events (Forward Scatter-Area vs Forward Scatter-Height (FSC-A vs FSC-H)), and live cell gates before examining other parameters (**Figure 27**).

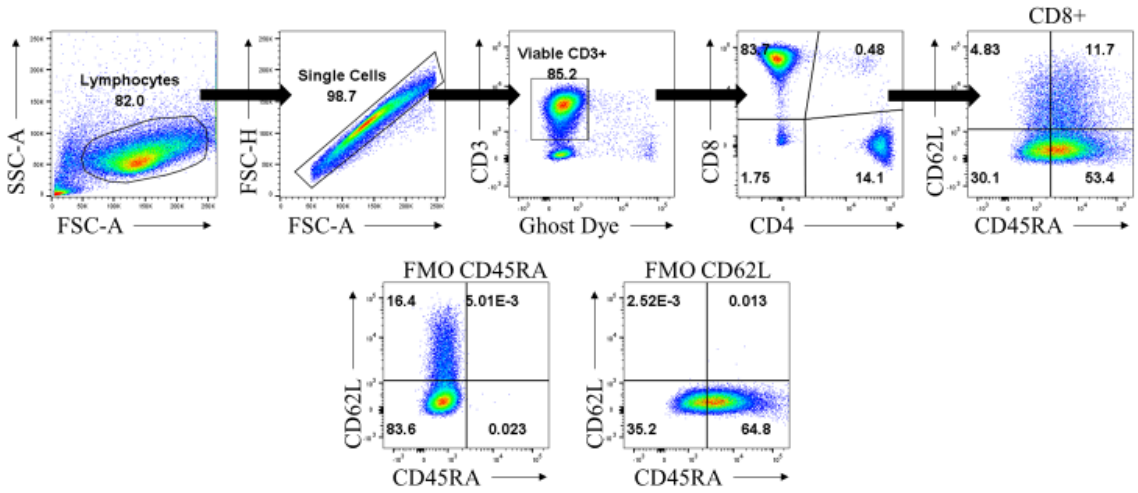

Figure 27. Representative flow cytometry gating scheme. Representative plots showing a gating scheme and controls using FlowJo.

5.7 Lymphocyte function assay

Expanded TILs rested overnight in the absence of CD3/CD28 stimulation and/or cytokines were either left unstimulated, stimulated with 10 µg/mL of OKT3 or added to autologous tumor cells in T-cell media at an effector:target ratio of 5:1 (5×10^5 TIL:1×10^5 tumor cells). The cells were cultured in the presence of 0.7 µL/mL monensin (BD GolgiStop) and anti-CD107a-BV421 in a final volume of 100 µL/condition at 37°C and 5% CO_2 for 4 hours after being briefly centrifuged to promote immediate effector/target

contact. Cells were then stained with the remainder of the panel using the indicated antibodies, viability dye, and fix/perm buffer set.

5.8 Next-generation sequencing (NGS) of primary RCC cell lines and parent tissue

DNA was extracted from primary TCLs which were established from three consecutive RCC samples using the QIAmp DNA Mini Kit. DNA was quantified using a Tecan NanoQuant Plate on a Tecan Infinite M200 Pro and then underwent a multiplex PCR reaction targeting exons of 275 solid tumor-related genes using a commercially available kit (Qiagen). The prepared libraries were then subjected to NGS on a NextSeq 500 instrument (Illumina) to generate fastQ files (text-based format for storing nucleotide sequences). The reads were mapped to the Homo_sapiens_sequence hg19 reference using QIAGEN Biomedical Genomics Workbench pipeline. Metrics for reported variants such as depth of coverage, variant allele frequency, and average quality cut-offs were evaluated individually for pathogenic and likely pathogenic hits compared with uncertain significance variants. The Variant Call Format files were generated and loaded into QIAGEN Clinical Insight (QCI-I) to assess individual calls for pathogenicity and quality control parameters.

5.9 TCRB CDR3 sequencing

DNA was extracted from TILs expanded in each condition from three specimens using the QIAmp DNA Mini Kit. Samples were provided to Adaptive Biotechnologies for TCRB CDR3 sequencing. Adaptive Biotechnologies performed quality checks and data

normalization using their established pipeline and uploaded the data for analysis using the ImmunoSEQ Analyzer 3.0 platform.

5.10 Statistical analysis

Statistical significance was considered a p-value less than 0.05 determined by using a ratio paired t-test on Graph Pad Prism 8.2.1.

Chapter 6: Future Directions

My primary career aim is to translate novel T-cell based therapies into the clinic for patients with cancer. A tremendous amount of pre-clinical and regulatory work remains prior to this therapy coming to fruition. From a basic science standpoint, comprehensive phenotyping, and functional analysis of GSK-3β inhibition induced memory-like T-cells remains to be elucidated. There is ongoing work evaluating broader changes in protein expression within control and GSK-3βi TIL via a reverse phase protein array and *in vivo* murine models are being developed to help expand the myriad of preclinical studies needed to begin to bridge discovery with improved outcomes for patients with cancer (**Figure 28**). Specifically, we will be evaluating tumor regression, T-cell persistence and T-cell localization using these *in vivo* models. As discussed in **Chapter 2** there is rationale

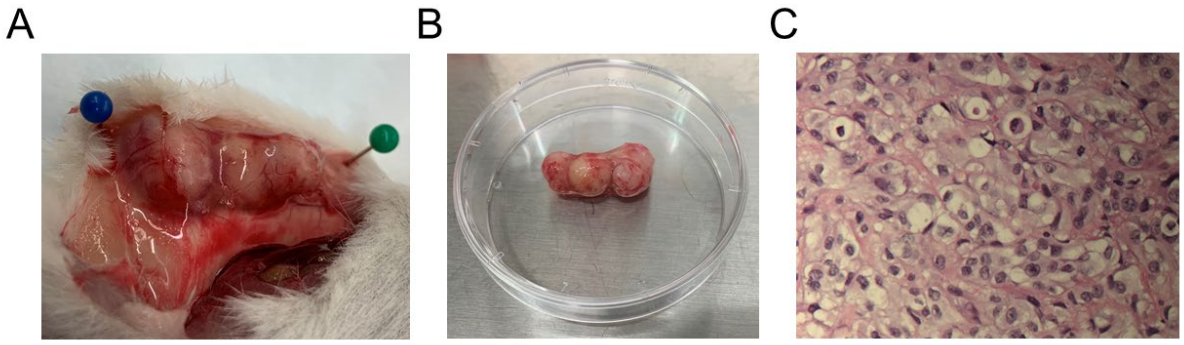

Figure 28. Establishment of a ccRCC xenograft model. (A) Photograph of subcutaneous tumor growth established from a grade 4/pT3aN1M1 ccRCC patient sample. (B) Photograph of the excised tumor xenograft. (C) Hematoxylin and eosin staining of the first passage xenograft.

for combining immune checkpoint inhibition with TIL therapy and as a result studies evaluating the impact of clinically relevant checkpoint inhibitors on *ex vivo* expanded TILs are also being conducted.

Large financial investments will be necessary to transition our novel pre-clinical TIL manufacturing methods into current good manufacturing practices (cGMP) compliant

platform which is essential for future use in humans. As a result, future funding opportunities from the National Institutes of Health (NIH) and Department of Defense (DoD) will be rigorously pursued. Collaborations with the biopharmaceutical industry will be essential as well as establishing a timeline for an investigational new drug (IND) application consisting of a novel type 351 human somatic cell product with the food and drug administration (FDA).

This endeavor will be laborious; however, it is one for which I am ready to embark. Margaret Mead once said, “Never doubt that a small group of thoughtful, committed citizens can change the world; indeed, it’s the only thing that ever has.” In response I say, “Why can’t we be the small group that changes outcomes for patients with advanced cancer.”

References

1. Coley WB. The treatment of malignant tumors by repeated inoculations of erysipelas. With a report of ten original cases. 1893. Clinical orthopaedics and related research. 1991(262):3-11. Epub 1991/01/01. PubMed PMID: 1984929.

2. Burnet M. Cancer; a biological approach. I. The processes of control. Br Med J. 1957;1(5022):779-86. Epub 1957/04/06. doi: 10.1136/bmj.1.5022.779. PubMed PMID: 13404306; PMCID: PMC1973174.

3. Burnet FM. The concept of immunological surveillance. Prog Exp Tumor Res. 1970;13:1-27. Epub 1970/01/01. doi: 10.1159/000386035. PubMed PMID: 4921480.

4. Cellular and Humoral Aspects of the Hypersensitive States: A Symposium at the New York Academy of Medicine. Journal of the American Medical Association. 1959;170(7):883-. doi: 10.1001/jama.1959.03010070123025.

5. Rosenberg SA, Yannelli JR, Yang JC, Topalian SL, Schwartzentruber DJ, Weber JS, Parkinson DR, Seipp CA, Einhorn JH, White DE. Treatment of patients with metastatic melanoma with autologous tumor-infiltrating lymphocytes and interleukin 2. J Natl Cancer Inst. 1994;86(15):1159-66. Epub 1994/08/03. doi: 10.1093/jnci/86.15.1159. PubMed PMID: 8028037.

6. Fyfe G, Fisher RI, Rosenberg SA, Sznol M, Parkinson DR, Louie AC. Results of treatment of 255 patients with metastatic renal cell carcinoma who received high-dose recombinant interleukin-2 therapy. J Clin Oncol. 1995;13(3):688-96. Epub 1995/03/01. doi: 10.1200/JCO.1995.13.3.688. PubMed PMID: 7884429.

7. Klapper JA, Downey SG, Smith FO, Yang JC, Hughes MS, Kammula US, Sherry RM, Royal RE, Steinberg SM, Rosenberg S. High-dose interleukin-2 for the treatment of metastatic renal cell carcinoma : a retrospective analysis of response and survival in patients treated in the surgery branch at the National Cancer Institute between 1986 and 2006. Cancer. 2008;113(2):293-301. Epub 2008/05/07. doi: 10.1002/cncr.23552. PubMed PMID: 18457330; PMCID: PMC3486432.

8. Negrier S, Escudier B, Lasset C, Douillard JY, Savary J, Chevreau C, Ravaud A, Mercatello A, Peny J, Mousseau M, Philip T, Tursz T. Recombinant human interleukin-2, recombinant human interferon alfa-2a, or both in metastatic renal-cell carcinoma. Groupe Francais d'Immunotherapie. N Engl J Med. 1998;338(18):1272-8. Epub 1998/05/01. doi: 10.1056/NEJM199804303381805. PubMed PMID: 9562581.

9. Interferon-alpha and survival in metastatic renal carcinoma: early results of a randomised controlled trial. Medical Research Council Renal Cancer Collaborators. Lancet. 1999;353(9146):14-7. Epub 1999/02/19. PubMed PMID: 10023944.

10. Powles T, Albiges L, Staehler M, Bensalah K, Dabestani S, Giles RH, Hofmann F, Hora M, Kuczyk MA, Lam TB, Marconi L, Merseburger AS, Fernandez-Pello S, Tahbaz R, Volpe A, Ljungberg B, Bex A. Updated European Association of Urology Guidelines Recommendations for the Treatment of First-line Metastatic Clear Cell Renal Cancer. Eur Urol. 2017. Epub 2017/12/11. doi: 10.1016/j.eururo.2017.11.016. PubMed PMID: 29223605.

11. Atkins MB, Clark JI, Quinn DI. Immune checkpoint inhibitors in advanced renal cell carcinoma: experience to date and future directions. Ann Oncol. 2017;28(7):1484-94. Epub 2017/04/07. doi: 10.1093/annonc/mdx151. PubMed PMID: 28383639.

12. Figlin RA, Thompson JA, Bukowski RM, Vogelzang NJ, Novick AC, Lange P, Steinberg GD, Belldegrun AS. Multicenter, randomized, phase III trial of CD8(+) tumor-infiltrating lymphocytes in combination with recombinant interleukin-2 in metastatic renal cell carcinoma. J Clin Oncol. 1999;17(8):2521-9. Epub 1999/11/24. doi: 10.1200/JCO.1999.17.8.2521. PubMed PMID: 10561318.

13. Andersen R, Westergaard MCW, Kjeldsen JW, Muller A, Pedersen NW, Hadrup SR, Met O, Seliger B, Kromann-Andersen B, Hasselager T, Donia M, Svane IM. T-cell Responses in the Microenvironment of Primary Renal Cell Carcinoma-Implications for Adoptive Cell Therapy. Cancer Immunol Res. 2018;6(2):222-35. Epub 2018/01/06. doi: 10.1158/2326-6066.CIR-17-0467. PubMed PMID: 29301752.

14. Baldan V, Griffiths R, Hawkins RE, Gilham DE. Efficient and reproducible generation of tumour-infiltrating lymphocytes for renal cell carcinoma. Br J Cancer. 2015;112(9):1510-8. Epub 2015/04/14. doi: 10.1038/bjc.2015.96. PubMed PMID: 25867267; PMCID: PMC4453687.

15. Restifo NP, Dudley ME, Rosenberg SA. Adoptive immunotherapy for cancer: harnessing the T cell response. Nat Rev Immunol. 2012;12(4):269-81. Epub 2012/03/23. doi: 10.1038/nri3191. PubMed PMID: 22437939; PMCID: PMC6292222.

16. Klebanoff CA, Gattinoni L, Restifo NP. CD8+ T-cell memory in tumor immunology and immunotherapy. Immunol Rev. 2006;211:214-24. Epub 2006/07/11. doi: 10.1111/j.0105-2896.2006.00391.x. PubMed PMID: 16824130; PMCID: PMC1501075.

17. Gattinoni L, Powell DJ, Jr., Rosenberg SA, Restifo NP. Adoptive immunotherapy for cancer: building on success. Nat Rev Immunol. 2006;6(5):383-93. Epub 2006/04/20. doi: 10.1038/nri1842. PubMed PMID: 16622476; PMCID: PMC1473162.

18. Busch DH, Frassle SP, Sommermeyer D, Buchholz VR, Riddell SR. Role of memory T cell subsets for adoptive immunotherapy. Semin Immunol. 2016;28(1):28-34. Epub 2016/03/16. doi: 10.1016/j.smim.2016.02.001. PubMed PMID: 26976826; PMCID: PMC5027130.

19. Gattinoni L, Speiser DE, Lichterfeld M, Bonini C. T memory stem cells in health and disease. Nat Med. 2017;23(1):18-27. Epub 2017/01/07. doi: 10.1038/nm.4241. PubMed PMID: 28060797; PMCID: PMC6354775.

20. Gattinoni L. Memory T cells officially join the stem cell club. Immunity. 2014;41(1):7-9. Epub 2014/07/19. doi: 10.1016/j.immuni.2014.07.003. PubMed PMID: 25035947; PMCID: PMC6377559.

21. Graef P, Buchholz VR, Stemberger C, Flossdorf M, Henkel L, Schiemann M, Drexler I, Hofer T, Riddell SR, Busch DH. Serial transfer of single-cell-derived immunocompetence reveals stemness of CD8(+) central memory T cells. Immunity. 2014;41(1):116-26. Epub 2014/07/19. doi: 10.1016/j.immuni.2014.05.018. PubMed PMID: 25035956.

22. Takaoka A, Hayakawa S, Yanai H, Stoiber D, Negishi H, Kikuchi H, Sasaki S, Imai K, Shibue T, Honda K, Taniguchi T. Integration of interferon-alpha/beta signalling to p53 responses in tumour suppression and antiviral defence. Nature. 2003;424(6948):516-23. Epub 2003/07/23. doi: 10.1038/nature01850. PubMed PMID: 12872134.

23. Heise R, Amann PM, Ensslen S, Marquardt Y, Czaja K, Joussen S, Beer D, Abele R, Plewnia G, Tampe R, Merk HF, Hermanns HM, Baron JM. Interferon Alpha Signalling and Its Relevance for the Upregulatory Effect of Transporter Proteins Associated with Antigen Processing (TAP) in Patients with Malignant Melanoma. PLoS One. 2016;11(1):e0146325. Epub 2016/01/07. doi: 10.1371/journal.pone.0146325. PubMed PMID: 26735690; PMCID: PMC4703378.

24. Raval A, Puri N, Rath PC, Saxena RK. Cytokine regulation of expression of class I MHC antigens. Exp Mol Med. 1998;30(1):1-13. Epub 1999/01/05. doi: 10.1038/emm.1998.1. PubMed PMID: 9873816.

25. Paquette RL, Hsu NC, Kiertscher SM, Park AN, Tran L, Roth MD, Glaspy JA. Interferon-alpha and granulocyte-macrophage colony-stimulating factor differentiate peripheral blood monocytes into potent antigen-presenting cells. J Leukoc Biol. 1998;64(3):358-67. Epub 1998/09/17. doi: 10.1002/jlb.64.3.358. PubMed PMID: 9738663.

26. Kasimir S, Brom J, Konig W. Effect of interferon-alpha on neutrophil functions. Immunology. 1991;74(2):271-8. Epub 1991/10/01. PubMed PMID: 1660854; PMCID: PMC1384604.

27. Ivashkiv LB, Donlin LT. Regulation of type I interferon responses. Nat Rev Immunol. 2014;14(1):36-49. Epub 2013/12/24. doi: 10.1038/nri3581. PubMed PMID: 24362405; PMCID: PMC4084561.

28. Muller L, Aigner P, Stoiber D. Type I Interferons and Natural Killer Cell Regulation in Cancer. Front Immunol. 2017;8:304. Epub 2017/04/15. doi: 10.3389/fimmu.2017.00304. PubMed PMID: 28408907; PMCID: PMC5374157.

29. Hervas-Stubbs S, Perez-Gracia JL, Rouzaut A, Sanmamed MF, Le Bon A, Melero I. Direct effects of type I interferons on cells of the immune system. Clin Cancer Res. 2011;17(9):2619-27. Epub 2011/03/05. doi: 10.1158/1078-0432.CCR-10-1114. PubMed PMID: 21372217.

30. Morgan DA, Ruscetti FW, Gallo R. Selective in vitro growth of T lymphocytes from normal human bone marrows. Science. 1976;193(4257):1007-8. Epub 1976/09/10. doi: 10.1126/science.181845. PubMed PMID: 181845.

31. Ruscetti FW, Morgan DA, Gallo RC. Functional and morphologic characterization of human T cells continuously grown in vitro. J Immunol. 1977;119(1):131-8. Epub 1977/07/01. PubMed PMID: 141483.

32. Liao W, Lin JX, Leonard WJ. IL-2 family cytokines: new insights into the complex roles of IL-2 as a broad regulator of T helper cell differentiation. Curr Opin Immunol. 2011;23(5):598-604. Epub 2011/09/06. doi: 10.1016/j.coi.2011.08.003. PubMed PMID: 21889323; PMCID: PMC3405730.

33. Tahvildari M, Dana R. Low-Dose IL-2 Therapy in Transplantation, Autoimmunity, and Inflammatory Diseases. J Immunol. 2019;203(11):2749-55. Epub 2019/11/20. doi: 10.4049/jimmunol.1900733. PubMed PMID: 31740549; PMCID: PMC6986328.

34. Matsuoka K, Koreth J, Kim HT, Bascug G, McDonough S, Kawano Y, Murase K, Cutler C, Ho VT, Alyea EP, Armand P, Blazar BR, Antin JH, Soiffer RJ, Ritz J. Low-dose interleukin-2 therapy restores regulatory T cell homeostasis in patients with chronic graft-versus-host disease. Sci Transl Med. 2013;5(179):179ra43. Epub 2013/04/05. doi: 10.1126/scitranslmed.3005265. PubMed PMID: 23552371; PMCID: PMC3686517.

35. Whangbo JS, Kim HT, Nikiforow S, Koreth J, Alho AC, Falahee B, Kim S, Dusenbury K, Fields MJ, Reynolds CG, Alyea EP, 3rd, Armand P, Cutler CS, Ho VT, Antin JH, Soiffer RJ, Ritz J. Functional analysis of clinical response to low-dose IL-2 in patients with refractory chronic graft-versus-host disease. Blood Adv. 2019;3(7):984-94. Epub 2019/04/03. doi: 10.1182/bloodadvances.2018027474. PubMed PMID: 30936059; PMCID: PMC6457229.

36. Pulliam SR, Uzhachenko RV, Adunyah SE, Shanker A. Common gamma chain cytokines in combinatorial immune strategies against cancer. Immunol Lett. 2016;169:61-72. Epub 2015/11/26. doi: 10.1016/j.imlet.2015.11.007. PubMed PMID: 26597610; PMCID: PMC4710466.

37. Bhatia SK, Tygrett LT, Grabstein KH, Waldschmidt TJ. The effect of in vivo IL-7 deprivation on T cell maturation. J Exp Med. 1995;181(4):1399-409. Epub 1995/04/01. doi: 10.1084/jem.181.4.1399. PubMed PMID: 7699326; PMCID: PMC2191957.

38. Tan JT, Dudl E, LeRoy E, Murray R, Sprent J, Weinberg KI, Surh CD. IL-7 is critical for homeostatic proliferation and survival of naive T cells. Proc Natl Acad Sci U S A. 2001;98(15):8732-7. Epub 2001/07/12. doi: 10.1073/pnas.161126098. PubMed PMID: 11447288; PMCID: PMC37504.

39. Richer MJ, Pewe LL, Hancox LS, Hartwig SM, Varga SM, Harty JT. Inflammatory IL-15 is required for optimal memory T cell responses. J Clin Invest. 2015;125(9):3477-90. Epub 2015/08/05. doi: 10.1172/JCI81261. PubMed PMID: 26241055; PMCID: PMC4588296.

40. Xia J, Liu W, Hu B, Tian Z, Yang Y. IL-15 promotes regulatory T cell function and protects against diabetes development in NK-depleted NOD mice. Clin Immunol. 2010;134(2):130-9. Epub 2009/10/31. doi: 10.1016/j.clim.2009.09.011. PubMed PMID: 19875339.

41. Imamichi H, Sereti I, Lane HC. IL-15 acts as a potent inducer of CD4(+)CD25(hi) cells expressing FOXP3. Eur J Immunol. 2008;38(6):1621-30. Epub 2008/05/22. doi: 10.1002/eji.200737607. PubMed PMID: 18493981; PMCID: PMC2684826.

42. Gleisner MA, Pereda C, Tittarelli A, Navarrete M, Fuentes C, Avalos I, Tempio F, Araya JP, Becker MI, Gonzalez FE, Lopez MN, Salazar-Onfray F. A heat-shocked melanoma cell lysate vaccine enhances tumor infiltration by prototypic effector T cells inhibiting tumor growth. J Immunother Cancer. 2020;8(2). Epub 2020/07/22. doi: 10.1136/jitc-2020-000999. PubMed PMID: 32690772; PMCID: PMC7373330.

43. D'Alise AM, Leoni G, Cotugno G, Troise F, Langone F, Fichera I, De Lucia M, Avalle L, Vitale R, Leuzzi A, Bignone V, Di Matteo E, Tucci FG, Poli V, Lahm A, Catanese MT, Folgori A, Colloca S, Nicosia A, Scarselli E. Adenoviral vaccine targeting multiple neoantigens as strategy to eradicate large tumors combined with checkpoint blockade. Nat Commun. 2019;10(1):2688. Epub 2019/06/21. doi: 10.1038/s41467-019-10594-2. PubMed PMID: 31217437; PMCID: PMC6584502.

44. Cheever MA, Higano CS. PROVENGE (Sipuleucel-T) in prostate cancer: the first FDA-approved therapeutic cancer vaccine. Clin Cancer Res. 2011;17(11):3520-6. Epub 2011/04/08. doi: 10.1158/1078-0432.CCR-10-3126. PubMed PMID: 21471425.

45. Liau LM, Ashkan K, Tran DD, Campian JL, Trusheim JE, Cobbs CS, Heth JA, Salacz M, Taylor S, D'Andre SD, Iwamoto FM, Dropcho EJ, Moshel YA, Walter KA, Pillainayagam CP, Aiken R, Chaudhary R, Goldlust SA, Bota DA, Duic P, Grewal J, Elinzano H, Toms SA, Lillehei KO, Mikkelsen T, Walbert T, Abram SR, Brenner AJ, Brem S, Ewend MG, Khagi S, Portnow J, Kim LJ, Loudon WG, Thompson RC, Avigan DE, Fink KL, Geoffroy FJ, Lindhorst S, Lutzky J, Sloan AE, Schackert G, Krex D, Meisel HJ, Wu J,

Davis RP, Duma C, Etame AB, Mathieu D, Kesari S, Piccioni D, Westphal M, Baskin DS, New PZ, Lacroix M, May SA, Pluard TJ, Tse V, Green RM, Villano JL, Pearlman M, Petrecca K, Schulder M, Taylor LP, Maida AE, Prins RM, Cloughesy TF, Mulholland P, Bosch ML. First results on survival from a large Phase 3 clinical trial of an autologous dendritic cell vaccine in newly diagnosed glioblastoma. J Transl Med. 2018;16(1):142. Epub 2018/05/31. doi: 10.1186/s12967-018-1507-6. PubMed PMID: 29843811; PMCID: PMC5975654.

46. Morse MA, Clay TM, Colling K, Hobeika A, Grabstein K, Cheever MA, Lyerly HK. HER2 dendritic cell vaccines. Clin Breast Cancer. 2003;3 Suppl 4:S164-72. Epub 2003/03/07. doi: 10.3816/cbc.2003.s.007. PubMed PMID: 12620155.

47. Alvarez-Dominguez C, Calderon-Gonzalez R, Teran-Navarro H, Salcines-Cuevas D, Garcia-Castano A, Freire J, Gomez-Roman J, Rivera F. Dendritic cell therapy in melanoma. Ann Transl Med. 2017;5(19):386. Epub 2017/11/09. doi: 10.21037/atm.2017.06.13. PubMed PMID: 29114544; PMCID: PMC5653516.

48. Lau SP, van Montfoort N, Kinderman P, Lukkes M, Klaase L, van Nimwegen M, van Gulijk M, Dumas J, Mustafa DAM, Lievense SLA, Groeneveldt C, Stadhouders R, Li Y, Stubbs A, Marijt KA, Vroman H, van der Burg SH, Aerts J, van Hall T, Dammeijer F, van Eijck CHJ. Dendritic cell vaccination and CD40-agonist combination therapy licenses T cell-dependent antitumor immunity in a pancreatic carcinoma murine model. J Immunother Cancer. 2020;8(2). Epub 2020/07/22. doi: 10.1136/jitc-2020-000772. PubMed PMID: 32690771; PMCID: PMC7373331.

49. Berntsen A, Trepiakas R, Wenandy L, Geertsen PF, thor Straten P, Andersen MH, Pedersen AE, Claesson MH, Lorentzen T, Johansen JS, Svane IM. Therapeutic dendritic cell vaccination of patients with metastatic renal cell carcinoma: a clinical phase 1/2 trial. J Immunother. 2008;31(8):771-80. Epub 2008/09/10. doi: 10.1097/CJI.0b013e3181833818. PubMed PMID: 18779742.

50. Lam H, McNeil LK, Starobinets H, DeVault VL, Cohen RB, Twardowski P, Johnson ML, Gillison ML, Stein MN, Vaishampayan UN, DeCillis AP, Foti JJ, Vemulapalli V, Tjon E, Ferber K, DeOliveira DB, Broom W, Agnihotri P, Jaffee EM, Wong KK, Drake CG, Carroll PM, Davis TA, Flechtner JB. An Empirical Antigen Selection Method Identifies Neoantigens That Either Elicit Broad Antitumor T-cell Responses or Drive Tumor Growth. Cancer Discov. 2021. Epub 2021/01/29. doi: 10.1158/2159-8290.CD-20-0377. PubMed PMID: 33504579.

51. Overman MJ, Lonardi S, Wong KYM, Lenz HJ, Gelsomino F, Aglietta M, Morse MA, Van Cutsem E, McDermott R, Hill A, Sawyer MB, Hendlisz A, Neyns B, Svrcek M, Moss RA, Ledeine JM, Cao ZA, Kamble S, Kopetz S, Andre T. Durable Clinical Benefit With Nivolumab Plus Ipilimumab in DNA Mismatch Repair-Deficient/Microsatellite Instability-High Metastatic Colorectal Cancer. J Clin Oncol. 2018;36(8):773-9. Epub 2018/01/23. doi: 10.1200/JCO.2017.76.9901. PubMed PMID: 29355075.

52. Vaddepally RK, Kharel P, Pandey R, Garje R, Chandra AB. Review of Indications of FDA-Approved Immune Checkpoint Inhibitors per NCCN Guidelines with the Level of Evidence. Cancers (Basel). 2020;12(3). Epub 2020/04/05. doi: 10.3390/cancers12030738. PubMed PMID: 32245016; PMCID: PMC7140028.

53. Pons-Tostivint E, Latouche A, Vaflard P, Ricci F, Loirat D, Hescot S, Sablin M-P, Rouzier R, Kamal M, Morel C, Lecerf C, Servois V, Paoletti X, Tourneau CL. Comparative Analysis of Durable Responses on Immune Checkpoint Inhibitors Versus Other Systemic Therapies: A Pooled Analysis of Phase III Trials. JCO Precision Oncology. 2019(3):1-10. doi: 10.1200/po.18.00114.

54. Hunig T. The storm has cleared: lessons from the CD28 superagonist TGN1412 trial. Nat Rev Immunol. 2012;12(5):317-8. Epub 2012/04/11. doi: 10.1038/nri3192. PubMed PMID: 22487653.

55. Segal NH, He AR, Doi T, Levy R, Bhatia S, Pishvaian MJ, Cesari R, Chen Y, Davis CB, Huang B, Thall AD, Gopal AK. Phase I Study of Single-Agent Utomilumab (PF-05082566), a 4-1BB/CD137 Agonist, in Patients with Advanced Cancer. Clin Cancer Res. 2018;24(8):1816-23. Epub 2018/03/20. doi: 10.1158/1078-0432.CCR-17-1922. PubMed PMID: 29549159.

56. Glisson BS, Leidner RS, Ferris RL, Powderly J, Rizvi NA, Keam B, Schneider R, Goel S, Ohr JP, Burton J, Zheng Y, Eck S, Gribbin M, Streicher K, Townsley DM, Patel SP. Safety and Clinical Activity of MEDI0562, a Humanized OX40 Agonist Monoclonal Antibody, in Adult Patients with Advanced Solid Tumors. Clin Cancer Res. 2020;26(20):5358-67. Epub 2020/08/21. doi: 10.1158/1078-0432.CCR-19-3070. PubMed PMID: 32816951.

57. Tran B, Carvajal RD, Marabelle A, Patel SP, LoRusso PM, Rasmussen E, Juan G, Upreti VV, Beers C, Ngarmchamnanrith G, Schoffski P. Dose escalation results from a first-in-human, phase 1 study of glucocorticoid-induced TNF receptor-related protein agonist AMG 228 in patients with advanced solid tumors. J Immunother Cancer. 2018;6(1):93. Epub 2018/09/27. doi: 10.1186/s40425-018-0407-x. PubMed PMID: 30253804; PMCID: PMC6156919.

58. Zak KM, Grudnik P, Magiera K, Domling A, Dubin G, Holak TA. Structural Biology of the Immune Checkpoint Receptor PD-1 and Its Ligands PD-L1/PD-L2. Structure. 2017;25(8):1163-74. Epub 2017/08/03. doi: 10.1016/j.str.2017.06.011. PubMed PMID: 28768162.

59. De Sousa Linhares A, Battin C, Jutz S, Leitner J, Hafner C, Tobias J, Wiedermann U, Kundi M, Zlabinger GJ, Grabmeier-Pfistershammer K, Steinberger P. Therapeutic PD-L1 antibodies are more effective than PD-1 antibodies in blocking PD-1/PD-L1 signaling. Sci Rep. 2019;9(1):11472. Epub 2019/08/09. doi: 10.1038/s41598-019-47910-1. PubMed PMID: 31391510; PMCID: PMC6685986.

60. El Osta B, Hu F, Sadek R, Chintalapally R, Tang SC. A meta-analysis of immune-related adverse events (irAE) of immune checkpoint inhibitors (ICI) from cancer clinical trials. Annals of Oncology. 2016;27:vi369. doi: 10.1093/annonc/mdw378.31.

61. Haslam A, Prasad V. Estimation of the Percentage of US Patients With Cancer Who Are Eligible for and Respond to Checkpoint Inhibitor Immunotherapy Drugs. JAMA Netw Open. 2019;2(5):e192535. Epub 2019/05/06. doi: 10.1001/jamanetworkopen.2019.2535. PubMed PMID: 31050774; PMCID: PMC6503493.

62. Mullinax JE, Hall M, Prabhakaran S, Weber J, Khushalani N, Eroglu Z, Brohl AS, Markowitz J, Royster E, Richards A, Stark V, Zager JS, Kelley L, Cox C, Sondak VK, Mule JJ, Pilon-Thomas S, Sarnaik AA. Combination of Ipilimumab and Adoptive Cell Therapy with Tumor-Infiltrating Lymphocytes for Patients with Metastatic Melanoma. Front Oncol. 2018;8:44. Epub 2018/03/20. doi: 10.3389/fonc.2018.00044. PubMed PMID: 29552542; PMCID: PMC5840208.

63. Bjoern J, Lyngaa R, Andersen R, Holmich LR, Hadrup SR, Donia M, Svane IM. Influence of ipilimumab on expanded tumour derived T cells from patients with metastatic melanoma. Oncotarget. 2017;8(16):27062-74. Epub 2017/04/21. doi: 10.18632/oncotarget.16003. PubMed PMID: 28423678; PMCID: PMC5432318.

64. Jin J, Sabatino M, Somerville R, Wilson JR, Dudley ME, Stroncek DF, Rosenberg SA. Simplified method of the growth of human tumor infiltrating lymphocytes in gas-permeable flasks to numbers needed for patient treatment. J Immunother. 2012;35(3):283-92. Epub 2012/03/17. doi: 10.1097/CJI.0b013e31824e801f. PubMed PMID: 22421946; PMCID: PMC3315105.

65. Dudley ME, Gross CA, Langhan MM, Garcia MR, Sherry RM, Yang JC, Phan GQ, Kammula US, Hughes MS, Citrin DE, Restifo NP, Wunderlich JR, Prieto PA, Hong JJ, Langan RC, Zlott DA, Morton KE, White DE, Laurencot CM, Rosenberg SA. CD8+ enriched "young" tumor infiltrating lymphocytes can mediate regression of metastatic melanoma. Clin Cancer Res. 2010;16(24):6122-31. Epub 2010/07/30. doi: 10.1158/1078-0432.CCR-10-1297. PubMed PMID: 20668005; PMCID: PMC2978753.

66. Tran KQ, Zhou J, Durflinger KH, Langhan MM, Shelton TE, Wunderlich JR, Robbins PF, Rosenberg SA, Dudley ME. Minimally cultured tumor-infiltrating lymphocytes display optimal characteristics for adoptive cell therapy. J Immunother. 2008;31(8):742-51. Epub 2008/09/10. doi: 10.1097/CJI.0b013e31818403d5. PubMed PMID: 18779745; PMCID: PMC2614999.

67. Donia M, Junker N, Ellebaek E, Andersen MH, Straten PT, Svane IM. Characterization and comparison of 'standard' and 'young' tumour-infiltrating lymphocytes for adoptive cell therapy at a Danish translational research institution. Scand J Immunol. 2012;75(2):157-67. Epub 2011/10/01. doi: 10.1111/j.1365-3083.2011.02640.x. PubMed PMID: 21955245.

68. Dudley ME, Wunderlich JR, Yang JC, Sherry RM, Topalian SL, Restifo NP, Royal RE, Kammula U, White DE, Mavroukakis SA, Rogers LJ, Gracia GJ, Jones SA, Mangiameli DP, Pelletier MM, Gea-Banacloche J, Robinson MR, Berman DM, Filie AC, Abati A, Rosenberg SA. Adoptive cell transfer therapy following non-myeloablative but lymphodepleting chemotherapy for the treatment of patients with refractory metastatic melanoma. J Clin Oncol. 2005;23(10):2346-57. Epub 2005/04/01. doi: 10.1200/JCO.2005.00.240. PubMed PMID: 15800326; PMCID: PMC1475951.

69. Antony PA, Piccirillo CA, Akpinarli A, Finkelstein SE, Speiss PJ, Surman DR, Palmer DC, Chan CC, Klebanoff CA, Overwijk WW, Rosenberg SA, Restifo NP. CD8+ T cell immunity against a tumor/self-antigen is augmented by CD4+ T helper cells and hindered by naturally occurring T regulatory cells. J Immunol. 2005;174(5):2591-601. Epub 2005/02/25. doi: 10.4049/jimmunol.174.5.2591. PubMed PMID: 15728465; PMCID: PMC1403291.

70. Gattinoni L, Finkelstein SE, Klebanoff CA, Antony PA, Palmer DC, Spiess PJ, Hwang LN, Yu Z, Wrzesinski C, Heimann DM, Surh CD, Rosenberg SA, Restifo NP. Removal of homeostatic cytokine sinks by lymphodepletion enhances the efficacy of adoptively transferred tumor-specific CD8+ T cells. J Exp Med. 2005;202(7):907-12. Epub 2005/10/06. doi: 10.1084/jem.20050732. PubMed PMID: 16203864; PMCID: PMC1397916.

71. Rohaan MW, van den Berg JH, Kvistborg P, Haanen J. Adoptive transfer of tumor-infiltrating lymphocytes in melanoma: a viable treatment option. J Immunother Cancer. 2018;6(1):102. Epub 2018/10/05. doi: 10.1186/s40425-018-0391-1. PubMed PMID: 30285902; PMCID: PMC6171186.

72. Andersen R, Donia M, Ellebaek E, Borch TH, Kongsted P, Iversen TZ, Holmich LR, Hendel HW, Met O, Andersen MH, Thor Straten P, Svane IM. Long-Lasting Complete Responses in Patients with Metastatic Melanoma after Adoptive Cell Therapy with Tumor-Infiltrating Lymphocytes and an Attenuated IL2 Regimen. Clin Cancer Res. 2016;22(15):3734-45. Epub 2016/03/24. doi: 10.1158/1078-0432.CCR-15-1879. PubMed PMID: 27006492.

73. Khammari A, Knol AC, Nguyen JM, Bossard C, Denis MG, Pandolfino MC, Quereux G, Bercegeay S, Dreno B. Adoptive TIL transfer in the adjuvant setting for melanoma: long-term patient survival. J Immunol Res. 2014;2014:186212. Epub 2014/04/18. doi: 10.1155/2014/186212. PubMed PMID: 24741578; PMCID: PMC3987883.

74. Larkin J, Chiarion-Sileni V, Gonzalez R, Grob JJ, Rutkowski P, Lao CD, Cowey CL, Schadendorf D, Wagstaff J, Dummer R, Ferrucci PF, Smylie M, Hogg D, Hill A, Marquez-Rodas I, Haanen J, Guidoboni M, Maio M, Schoffski P, Carlino MS, Lebbe C, McArthur G, Ascierto PA, Daniels GA, Long GV, Bastholt L, Rizzo JI, Balogh A, Moshyk A, Hodi FS, Wolchok JD. Five-Year Survival with Combined Nivolumab and Ipilimumab

in Advanced Melanoma. N Engl J Med. 2019;381(16):1535-46. Epub 2019/09/29. doi: 10.1056/NEJMoa1910836. PubMed PMID: 31562797.

75. Rosenberg SA, Yang JC, Sherry RM, Kammula US, Hughes MS, Phan GQ, Citrin DE, Restifo NP, Robbins PF, Wunderlich JR, Morton KE, Laurencot CM, Steinberg SM, White DE, Dudley ME. Durable complete responses in heavily pretreated patients with metastatic melanoma using T-cell transfer immunotherapy. Clin Cancer Res. 2011;17(13):4550-7. Epub 2011/04/19. doi: 10.1158/1078-0432.CCR-11-0116. PubMed PMID: 21498393; PMCID: PMC3131487.

76. Stevanovic S, Helman SR, Wunderlich JR, Langhan MM, Doran SL, Kwong MLM, Somerville RPT, Klebanoff CA, Kammula US, Sherry RM, Yang JC, Rosenberg SA, Hinrichs CS. A Phase II Study of Tumor-infiltrating Lymphocyte Therapy for Human Papillomavirus-associated Epithelial Cancers. Clin Cancer Res. 2019;25(5):1486-93. Epub 2018/12/07. doi: 10.1158/1078-0432.CCR-18-2722. PubMed PMID: 30518633; PMCID: PMC6397671.

77. Andersen R, Donia M, Westergaard MC, Pedersen M, Hansen M, Svane IM. Tumor infiltrating lymphocyte therapy for ovarian cancer and renal cell carcinoma. Hum Vaccin Immunother. 2015;11(12):2790-5. Epub 2015/08/27. doi: 10.1080/21645515.2015.1075106. PubMed PMID: 26308285; PMCID: PMC5054777.

78. Zacharakis N, Chinnasamy H, Black M, Xu H, Lu YC, Zheng Z, Pasetto A, Langhan M, Shelton T, Prickett T, Gartner J, Jia L, Trebska-McGowan K, Somerville RP, Robbins PF, Rosenberg SA, Goff SL, Feldman SA. Immune recognition of somatic mutations leading to complete durable regression in metastatic breast cancer. Nat Med. 2018;24(6):724-30. Epub 2018/06/06. doi: 10.1038/s41591-018-0040-8. PubMed PMID: 29867227; PMCID: PMC6348479.

79. Jiang SS, Tang Y, Zhang YJ, Weng DS, Zhou ZG, Pan K, Pan QZ, Wang QJ, Liu Q, He J, Zhao JJ, Li J, Chen MS, Chang AE, Li Q, Xia JC. A phase I clinical trial utilizing autologous tumor-infiltrating lymphocytes in patients with primary hepatocellular carcinoma. Oncotarget. 2015;6(38):41339-49. Epub 2015/10/31. doi: 10.18632/oncotarget.5463. PubMed PMID: 26515587; PMCID: PMC4747409.

80. Tran E, Robbins PF, Lu YC, Prickett TD, Gartner JJ, Jia L, Pasetto A, Zheng Z, Ray S, Groh EM, Kriley IR, Rosenberg SA. T-Cell Transfer Therapy Targeting Mutant KRAS in Cancer. N Engl J Med. 2016;375(23):2255-62. Epub 2016/12/14. doi: 10.1056/NEJMoa1609279. PubMed PMID: 27959684; PMCID: PMC5178827.

81. Belldegrun A, Muul LM, Rosenberg SA. Interleukin 2 expanded tumor-infiltrating lymphocytes in human renal cell cancer: isolation, characterization, and antitumor activity. Cancer Res. 1988;48(1):206-14. Epub 1988/01/01. PubMed PMID: 3257161.

82. Figlin RA, Pierce WC, Kaboo R, Tso CL, Moldawer N, Gitlitz B, deKernion J, Belldegrun A. Treatment of metastatic renal cell carcinoma with nephrectomy, interleukin-

2 and cytokine-primed or CD8(+) selected tumor infiltrating lymphocytes from primary tumor. J Urol. 1997;158(3 Pt 1):740-5. Epub 1997/09/01. doi: 10.1097/00005392-199709000-00012. PubMed PMID: 9258071.

83. Braun MW, Abdelhakim H, Li M, Hyter S, Pessetto Z, Koestler DC, Pathak HB, Dunavin N, Godwin AK. Adherent cell depletion promotes the expansion of renal cell carcinoma infiltrating T cells with optimal characteristics for adoptive transfer. J Immunother Cancer. 2020;8(2). Epub 2020/10/11. doi: 10.1136/jitc-2020-000706. PubMed PMID: 33037114; PMCID: PMC7549459.

84. Markel G, Cohen-Sinai T, Besser MJ, Oved K, Itzhaki O, Seidman R, Fridman E, Treves AJ, Keisari Y, Dotan Z, Ramon J, Schachter J. Preclinical evaluation of adoptive cell therapy for patients with metastatic renal cell carcinoma. Anticancer Res. 2009;29(1):145-54. Epub 2009/04/01. PubMed PMID: 19331144.

85. June CH, Sadelain M. Chimeric Antigen Receptor Therapy. N Engl J Med. 2018;379(1):64-73. Epub 2018/07/05. doi: 10.1056/NEJMra1706169. PubMed PMID: 29972754; PMCID: PMC7433347.

86. Mullard A. FDA approves fourth CAR-T cell therapy. Nat Rev Drug Discov. 2021. Epub 2021/02/13. doi: 10.1038/d41573-021-00031-9. PubMed PMID: 33574586.

87. Misbah SA, Weeratunga P. Immunoglobulin replacement and quality of life after CAR T-cell therapy. Lancet Oncol. 2020;21(1):e6. Epub 2020/01/08. doi: 10.1016/S1470-2045(19)30782-X. PubMed PMID: 31908309.

88. Hill JA, Giralt S, Torgerson TR, Lazarus HM. CAR-T - and a side order of IgG, to go? - Immunoglobulin replacement in patients receiving CAR-T cell therapy. Blood Rev. 2019;38:100596. Epub 2019/08/17. doi: 10.1016/j.blre.2019.100596. PubMed PMID: 31416717; PMCID: PMC6810871.

89. Maude SL, Laetsch TW, Buechner J, Rives S, Boyer M, Bittencourt H, Bader P, Verneris MR, Stefanski HE, Myers GD, Qayed M, De Moerloose B, Hiramatsu H, Schlis K, Davis KL, Martin PL, Nemecek ER, Yanik GA, Peters C, Baruchel A, Boissel N, Mechinaud F, Balduzzi A, Krueger J, June CH, Levine BL, Wood P, Taran T, Leung M, Mueller KT, Zhang Y, Sen K, Lebwohl D, Pulsipher MA, Grupp SA. Tisagenlecleucel in Children and Young Adults with B-Cell Lymphoblastic Leukemia. N Engl J Med. 2018;378(5):439-48. Epub 2018/02/01. doi: 10.1056/NEJMoa1709866. PubMed PMID: 29385370; PMCID: PMC5996391.

90. Schuster SJ, Bishop MR, Tam CS, Waller EK, Borchmann P, McGuirk JP, Jager U, Jaglowski S, Andreadis C, Westin JR, Fleury I, Bachanova V, Foley SR, Ho PJ, Mielke S, Magenau JM, Holte H, Pantano S, Pacaud LB, Awasthi R, Chu J, Anak O, Salles G, Maziarz RT, Investigators J. Tisagenlecleucel in Adult Relapsed or Refractory Diffuse Large B-Cell Lymphoma. N Engl J Med. 2019;380(1):45-56. Epub 2018/12/07. doi: 10.1056/NEJMoa1804980. PubMed PMID: 30501490.

91. Wang M, Munoz J, Goy A, Locke FL, Jacobson CA, Hill BT, Timmerman JM, Holmes H, Jaglowski S, Flinn IW, McSweeney PA, Miklos DB, Pagel JM, Kersten MJ, Milpied N, Fung H, Topp MS, Houot R, Beitinjaneh A, Peng W, Zheng L, Rossi JM, Jain RK, Rao AV, Reagan PM. KTE-X19 CAR T-Cell Therapy in Relapsed or Refractory Mantle-Cell Lymphoma. N Engl J Med. 2020;382(14):1331-42. Epub 2020/04/04. doi: 10.1056/NEJMoa1914347. PubMed PMID: 32242358; PMCID: PMC7731441.

92. Chong EA, Ruella M, Schuster SJ, Lymphoma Program Investigators at the University of P. Five-Year Outcomes for Refractory B-Cell Lymphomas with CAR T-Cell Therapy. N Engl J Med. 2021;384(7):673-4. Epub 2021/02/18. doi: 10.1056/NEJMc2030164. PubMed PMID: 33596362.

93. Neelapu SS, Locke FL, Bartlett NL, Lekakis LJ, Miklos DB, Jacobson CA, Braunschweig I, Oluwole OO, Siddiqi T, Lin Y, Timmerman JM, Stiff PJ, Friedberg JW, Flinn IW, Goy A, Hill BT, Smith MR, Deol A, Farooq U, McSweeney P, Munoz J, Avivi I, Castro JE, Westin JR, Chavez JC, Ghobadi A, Komanduri KV, Levy R, Jacobsen ED, Witzig TE, Reagan P, Bot A, Rossi J, Navale L, Jiang Y, Aycock J, Elias M, Chang D, Wiezorek J, Go WY. Axicabtagene Ciloleucel CAR T-Cell Therapy in Refractory Large B-Cell Lymphoma. N Engl J Med. 2017;377(26):2531-44. Epub 2017/12/12. doi: 10.1056/NEJMoa1707447. PubMed PMID: 29226797; PMCID: PMC5882485.

94. Pan J, Tan Y, Deng B, Tong C, Hua L, Ling Z, Song W, Xu J, Duan J, Wang Z, Guo H, Yu X, Chang AH, Zheng Q, Feng X. Frequent occurrence of CD19-negative relapse after CD19 CAR T and consolidation therapy in 14 TP53-mutated r/r B-ALL children. Leukemia. 2020;34(12):3382-7. Epub 2020/04/30. doi: 10.1038/s41375-020-0831-z. PubMed PMID: 32346068.

95. Gardner R, Wu D, Cherian S, Fang M, Hanafi LA, Finney O, Smithers H, Jensen MC, Riddell SR, Maloney DG, Turtle CJ. Acquisition of a CD19-negative myeloid phenotype allows immune escape of MLL-rearranged B-ALL from CD19 CAR-T-cell therapy. Blood. 2016;127(20):2406-10. Epub 2016/02/26. doi: 10.1182/blood-2015-08-665547. PubMed PMID: 26907630; PMCID: PMC4874221.

96. Zah E, Lin MY, Silva-Benedict A, Jensen MC, Chen YY. T Cells Expressing CD19/CD20 Bispecific Chimeric Antigen Receptors Prevent Antigen Escape by Malignant B Cells. Cancer Immunol Res. 2016;4(6):498-508. Epub 2016/04/10. doi: 10.1158/2326-6066.CIR-15-0231. PubMed PMID: 27059623; PMCID: PMC4933590.

97. Shah NN, Johnson BD, Schneider D, Zhu F, Szabo A, Keever-Taylor CA, Krueger W, Worden AA, Kadan MJ, Yim S, Cunningham A, Hamadani M, Fenske TS, Dropulic B, Orentas R, Hari P. Bispecific anti-CD20, anti-CD19 CAR T cells for relapsed B cell malignancies: a phase 1 dose escalation and expansion trial. Nat Med. 2020;26(10):1569-75. Epub 2020/10/07. doi: 10.1038/s41591-020-1081-3. PubMed PMID: 33020647.

98. He X, Feng Z, Ma J, Ling S, Cao Y, Gurung B, Wu Y, Katona BW, O'Dwyer KP, Siegel DL, June CH, Hua X. Bispecific and split CAR T cells targeting CD13 and TIM3 eradicate acute myeloid leukemia. Blood. 2020;135(10):713-23. Epub 2020/01/18. doi: 10.1182/blood.2019002779. PubMed PMID: 31951650; PMCID: PMC7059518.

99. Zah E, Nam E, Bhuvan V, Tran U, Ji BY, Gosliner SB, Wang X, Brown CE, Chen YY. Systematically optimized BCMA/CS1 bispecific CAR-T cells robustly control heterogeneous multiple myeloma. Nat Commun. 2020;11(1):2283. Epub 2020/05/10. doi: 10.1038/s41467-020-16160-5. PubMed PMID: 32385241; PMCID: PMC7210316.

100. Reinhard K, Rengstl B, Oehm P, Michel K, Billmeier A, Hayduk N, Klein O, Kuna K, Ouchan Y, Woll S, Christ E, Weber D, Suchan M, Bukur T, Birtel M, Jahndel V, Mroz K, Hobohm K, Kranz L, Diken M, Kuhlcke K, Tureci O, Sahin U. An RNA vaccine drives expansion and efficacy of claudin-CAR-T cells against solid tumors. Science. 2020;367(6476):446-53. Epub 2020/01/04. doi: 10.1126/science.aay5967. PubMed PMID: 31896660.

101. Majzner RG, Rietberg SP, Sotillo E, Dong R, Vachharajani VT, Labanieh L, Myklebust JH, Kadapakkam M, Weber EW, Tousley AM, Richards RM, Heitzeneder S, Nguyen SM, Wiebking V, Theruvath J, Lynn RC, Xu P, Dunn AR, Vale RD, Mackall CL. Tuning the Antigen Density Requirement for CAR T-cell Activity. Cancer Discov. 2020;10(5):702-23. Epub 2020/03/21. doi: 10.1158/2159-8290.CD-19-0945. PubMed PMID: 32193224.

102. Caruso HG, Hurton LV, Najjar A, Rushworth D, Ang S, Olivares S, Mi T, Switzer K, Singh H, Huls H, Lee DA, Heimberger AB, Champlin RE, Cooper LJ. Tuning Sensitivity of CAR to EGFR Density Limits Recognition of Normal Tissue While Maintaining Potent Antitumor Activity. Cancer Res. 2015;75(17):3505-18. Epub 2015/09/04. doi: 10.1158/0008-5472.CAN-15-0139. PubMed PMID: 26330164; PMCID: PMC4624228.

103. Liu X, Jiang S, Fang C, Yang S, Olalere D, Pequignot EC, Cogdill AP, Li N, Ramones M, Granda B, Zhou L, Loew A, Young RM, June CH, Zhao Y. Affinity-Tuned ErbB2 or EGFR Chimeric Antigen Receptor T Cells Exhibit an Increased Therapeutic Index against Tumors in Mice. Cancer Res. 2015;75(17):3596-607. Epub 2015/09/04. doi: 10.1158/0008-5472.CAN-15-0159. PubMed PMID: 26330166; PMCID: PMC4560113.

104. Maus MV, June CH. Making Better Chimeric Antigen Receptors for Adoptive T-cell Therapy. Clin Cancer Res. 2016;22(8):1875-84. Epub 2016/04/17. doi: 10.1158/1078-0432.CCR-15-1433. PubMed PMID: 27084741; PMCID: PMC4843171.

105. Zhang J, Wang L. The Emerging World of TCR-T Cell Trials Against Cancer: A Systematic Review. Technol Cancer Res Treat. 2019;18:1533033819831068. Epub 2019/02/26. doi: 10.1177/1533033819831068. PubMed PMID: 30798772; PMCID: PMC6391541.

106. Schultz-Thater E, Noppen C, Gudat F, Durmuller U, Zajac P, Kocher T, Heberer M, Spagnoli GC. NY-ESO-1 tumour associated antigen is a cytoplasmic protein detectable by specific monoclonal antibodies in cell lines and clinical specimens. Br J Cancer. 2000;83(2):204-8. Epub 2000/07/20. doi: 10.1054/bjoc.2000.1251. PubMed PMID: 10901371; PMCID: PMC2363487.

107. Robbins PF, Kassim SH, Tran TL, Crystal JS, Morgan RA, Feldman SA, Yang JC, Dudley ME, Wunderlich JR, Sherry RM, Kammula US, Hughes MS, Restifo NP, Raffeld M, Lee CC, Li YF, El-Gamil M, Rosenberg SA. A pilot trial using lymphocytes genetically engineered with an NY-ESO-1-reactive T-cell receptor: long-term follow-up and correlates with response. Clin Cancer Res. 2015;21(5):1019-27. Epub 2014/12/30. doi: 10.1158/1078-0432.CCR-14-2708. PubMed PMID: 25538264; PMCID: PMC4361810.

108. Stadtmauer EA, Faitg TH, Lowther DE, Badros AZ, Chagin K, Dengel K, Iyengar M, Melchiori L, Navenot JM, Norry E, Trivedi T, Wang R, Binder GK, Amado R, Rapoport AP. Long-term safety and activity of NY-ESO-1 SPEAR T cells after autologous stem cell transplant for myeloma. Blood Adv. 2019;3(13):2022-34. Epub 2019/07/11. doi: 10.1182/bloodadvances.2019000194. PubMed PMID: 31289029; PMCID: PMC6616263.

109. Xia Y, Tian X, Wang J, Qiao D, Liu X, Xiao L, Liang W, Ban D, Chu J, Yu J, Wang R, Tian G, Wang M. Treatment of metastatic non-small cell lung cancer with NY-ESO-1 specific TCR engineered-T cells in a phase I clinical trial: A case report. Oncol Lett. 2018;16(6):6998-7007. Epub 2018/12/14. doi: 10.3892/ol.2018.9534. PubMed PMID: 30546433; PMCID: PMC6256329.

110. Ellis JM, Henson V, Slack R, Ng J, Hartzman RJ, Katovich Hurley C. Frequencies of HLA-A2 alleles in five U.S. population groups. Predominance Of A*02011 and identification of HLA-A*0231. Hum Immunol. 2000;61(3):334-40. Epub 2000/02/26. doi: 10.1016/s0198-8859(99)00155-x. PubMed PMID: 10689125.

111. Lu YC, Yao X, Crystal JS, Li YF, El-Gamil M, Gross C, Davis L, Dudley ME, Yang JC, Samuels Y, Rosenberg SA, Robbins PF. Efficient identification of mutated cancer antigens recognized by T cells associated with durable tumor regressions. Clin Cancer Res. 2014;20(13):3401-10. Epub 2014/07/06. doi: 10.1158/1078-0432.CCR-14-0433. PubMed PMID: 24987109; PMCID: PMC4083471.

112. Prickett TD, Crystal JS, Cohen CJ, Pasetto A, Parkhurst MR, Gartner JJ, Yao X, Wang R, Gros A, Li YF, El-Gamil M, Trebska-McGowan K, Rosenberg SA, Robbins PF. Durable Complete Response from Metastatic Melanoma after Transfer of Autologous T Cells Recognizing 10 Mutated Tumor Antigens. Cancer Immunol Res. 2016;4(8):669-78. Epub 2016/06/18. doi: 10.1158/2326-6066.CIR-15-0215. PubMed PMID: 27312342; PMCID: PMC4970903.

113. Parkhurst M, Gros A, Pasetto A, Prickett T, Crystal JS, Robbins P, Rosenberg SA. Isolation of T-Cell Receptors Specifically Reactive with Mutated Tumor-Associated Antigens from Tumor-Infiltrating Lymphocytes Based on CD137 Expression. Clin Cancer

Res. 2017;23(10):2491-505. Epub 2016/11/09. doi: 10.1158/1078-0432.CCR-16-2680. PubMed PMID: 27827318; PMCID: PMC6453117.

114. Malekzadeh P, Pasetto A, Robbins PF, Parkhurst MR, Paria BC, Jia L, Gartner JJ, Hill V, Yu Z, Restifo NP, Sachs A, Tran E, Lo W, Somerville RP, Rosenberg SA, Deniger DC. Neoantigen screening identifies broad TP53 mutant immunogenicity in patients with epithelial cancers. J Clin Invest. 2019;129(3):1109-14. Epub 2019/02/05. doi: 10.1172/JCI123791. PubMed PMID: 30714987; PMCID: PMC6391139.

115. Deniger DC, Pasetto A, Robbins PF, Gartner JJ, Prickett TD, Paria BC, Malekzadeh P, Jia L, Yossef R, Langhan MM, Wunderlich JR, Danforth DN, Somerville RPT, Rosenberg SA. T-cell Responses to TP53 "Hotspot" Mutations and Unique Neoantigens Expressed by Human Ovarian Cancers. Clin Cancer Res. 2018;24(22):5562-73. Epub 2018/06/02. doi: 10.1158/1078-0432.CCR-18-0573. PubMed PMID: 29853601; PMCID: PMC6239943.

116. Bray F, Ferlay J, Soerjomataram I, Siegel RL, Torre LA, Jemal A. Global cancer statistics 2018: GLOBOCAN estimates of incidence and mortality worldwide for 36 cancers in 185 countries. CA Cancer J Clin. 2018;68(6):394-424. Epub 2018/09/13. doi: 10.3322/caac.21492. PubMed PMID: 30207593.

117. Znaor A, Lortet-Tieulent J, Laversanne M, Jemal A, Bray F. International variations and trends in renal cell carcinoma incidence and mortality. Eur Urol. 2015;67(3):519-30. Epub 2014/12/03. doi: 10.1016/j.eururo.2014.10.002. PubMed PMID: 25449206.

118. Siegel RL, Miller KD, Jemal A. Cancer statistics, 2020. CA Cancer J Clin. 2020;70(1):7-30. Epub 2020/01/09. doi: 10.3322/caac.21590. PubMed PMID: 31912902.

119. Muglia VF, Prando A. Renal cell carcinoma: histological classification and correlation with imaging findings. Radiol Bras. 2015;48(3):166-74. Epub 2015/07/18. doi: 10.1590/0100-3984.2013.1927. PubMed PMID: 26185343; PMCID: PMC4492569.

120. Shuch B, Amin A, Armstrong AJ, Eble JN, Ficarra V, Lopez-Beltran A, Martignoni G, Rini BI, Kutikov A. Understanding pathologic variants of renal cell carcinoma: distilling therapeutic opportunities from biologic complexity. Eur Urol. 2015;67(1):85-97. Epub 2014/05/27. doi: 10.1016/j.eururo.2014.04.029. PubMed PMID: 24857407.

121. Blum KA, Gupta S, Tickoo SK, Chan TA, Russo P, Motzer RJ, Karam JA, Hakimi AA. Sarcomatoid renal cell carcinoma: biology, natural history and management. Nat Rev Urol. 2020;17(12):659-78. Epub 2020/10/15. doi: 10.1038/s41585-020-00382-9. PubMed PMID: 33051619; PMCID: PMC7551522.

122. Farrow GM, Harrison EG, Jr., Utz DC. Sarcomas and sarcomatoid and mixed malignant tumors of the kidney in adults. 3. Cancer. 1968;22(3):556-63. Epub 1968/09/01. doi: 10.1002/1097-0142(196809)22:3<556::aid-cncr2820220310>3.0.co;2-n. PubMed PMID: 4299778.

123. Delahunt B, Eble JN. Papillary renal cell carcinoma: a clinicopathologic and immunohistochemical study of 105 tumors. Mod Pathol. 1997;10(6):537-44. Epub 1997/06/01. PubMed PMID: 9195569.

124. Amin MB, Amin MB, Tamboli P, Javidan J, Stricker H, de-Peralta Venturina M, Deshpande A, Menon M. Prognostic impact of histologic subtyping of adult renal epithelial neoplasms: an experience of 405 cases. Am J Surg Pathol. 2002;26(3):281-91. Epub 2002/02/23. doi: 10.1097/00000478-200203000-00001. PubMed PMID: 11859199.

125. Peyromaure M, Misrai V, Thiounn N, Vieillefond A, Zerbib M, Flam TA, Debre B. Chromophobe renal cell carcinoma: analysis of 61 cases. Cancer. 2004;100(7):1406-10. Epub 2004/03/26. doi: 10.1002/cncr.20128. PubMed PMID: 15042674.

126. Moore LE, Nickerson ML, Brennan P, Toro JR, Jaeger E, Rinsky J, Han SS, Zaridze D, Matveev V, Janout V, Kollarova H, Bencko V, Navratilova M, Szeszenia-Dabrowska N, Mates D, Schmidt LS, Lenz P, Karami S, Linehan WM, Merino M, Chanock S, Boffetta P, Chow WH, Waldman FM, Rothman N. Von Hippel-Lindau (VHL) inactivation in sporadic clear cell renal cancer: associations with germline VHL polymorphisms and etiologic risk factors. PLoS Genet. 2011;7(10):e1002312. Epub 2011/10/25. doi: 10.1371/journal.pgen.1002312. PubMed PMID: 22022277; PMCID: PMC3192834.

127. Mandriota SJ, Turner KJ, Davies DR, Murray PG, Morgan NV, Sowter HM, Wykoff CC, Maher ER, Harris AL, Ratcliffe PJ, Maxwell PH. HIF activation identifies early lesions in VHL kidneys: evidence for site-specific tumor suppressor function in the nephron. Cancer Cell. 2002;1(5):459-68. Epub 2002/07/19. doi: 10.1016/s1535-6108(02)00071-5. PubMed PMID: 12124175.

128. Ricketts CJ, De Cubas AA, Fan H, Smith CC, Lang M, Reznik E, Bowlby R, Gibb EA, Akbani R, Beroukhim R, Bottaro DP, Choueiri TK, Gibbs RA, Godwin AK, Haake S, Hakimi AA, Henske EP, Hsieh JJ, Ho TH, Kanchi RS, Krishnan B, Kwiatkowski DJ, Lui W, Merino MJ, Mills GB, Myers J, Nickerson ML, Reuter VE, Schmidt LS, Shelley CS, Shen H, Shuch B, Signoretti S, Srinivasan R, Tamboli P, Thomas G, Vincent BG, Vocke CD, Wheeler DA, Yang L, Kim WY, Robertson AG, Cancer Genome Atlas Research N, Spellman PT, Rathmell WK, Linehan WM. The Cancer Genome Atlas Comprehensive Molecular Characterization of Renal Cell Carcinoma. Cell Rep. 2018;23(1):313-26 e5. Epub 2018/04/05. doi: 10.1016/j.celrep.2018.03.075. PubMed PMID: 29617669; PMCID: PMC6075733.

129. Maxwell PH, Wiesener MS, Chang GW, Clifford SC, Vaux EC, Cockman ME, Wykoff CC, Pugh CW, Maher ER, Ratcliffe PJ. The tumour suppressor protein VHL targets hypoxia-inducible factors for oxygen-dependent proteolysis. Nature. 1999;399(6733):271-5. Epub 1999/06/03. doi: 10.1038/20459. PubMed PMID: 10353251.

130. Comerford KM, Wallace TJ, Karhausen J, Louis NA, Montalto MC, Colgan SP. Hypoxia-inducible factor-1-dependent regulation of the multidrug resistance (MDR1) gene. Cancer Res. 2002;62(12):3387-94. Epub 2002/06/18. PubMed PMID: 12067980.

131. Na X, Wu G, Ryan CK, Schoen SR, di'Santagnese PA, Messing EM. Overproduction of vascular endothelial growth factor related to von Hippel-Lindau tumor suppressor gene mutations and hypoxia-inducible factor-1 alpha expression in renal cell carcinomas. J Urol. 2003;170(2 Pt 1):588-92. Epub 2003/07/11. doi: 10.1097/01.ju.0000074870.54671.98. PubMed PMID: 12853836.

132. Escudier B. Combination Therapy as First-Line Treatment in Metastatic Renal-Cell Carcinoma. N Engl J Med. 2019;380(12):1176-8. Epub 2019/02/20. doi: 10.1056/NEJMe1900887. PubMed PMID: 30779526.

133. McDermott DF, Huseni MA, Atkins MB, Motzer RJ, Rini BI, Escudier B, Fong L, Joseph RW, Pal SK, Reeves JA, Sznol M, Hainsworth J, Rathmell WK, Stadler WM, Hutson T, Gore ME, Ravaud A, Bracarda S, Suarez C, Danielli R, Gruenwald V, Choueiri TK, Nickles D, Jhunjhunwala S, Piault-Louis E, Thobhani A, Qiu J, Chen DS, Hegde PS, Schiff C, Fine GD, Powles T. Clinical activity and molecular correlates of response to atezolizumab alone or in combination with bevacizumab versus sunitinib in renal cell carcinoma. Nat Med. 2018;24(6):749-57. Epub 2018/06/06. doi: 10.1038/s41591-018-0053-3. PubMed PMID: 29867230; PMCID: PMC6721896.

134. Braun DA, Ishii Y, Walsh AM, Van Allen EM, Wu CJ, Shukla SA, Choueiri TK. Clinical Validation of PBRM1 Alterations as a Marker of Immune Checkpoint Inhibitor Response in Renal Cell Carcinoma. JAMA Oncol. 2019. Epub 2019/09/06. doi: 10.1001/jamaoncol.2019.3158. PubMed PMID: 31486842; PMCID: PMC6735411.

135. Miao D, Margolis CA, Gao W, Voss MH, Li W, Martini DJ, Norton C, Bosse D, Wankowicz SM, Cullen D, Horak C, Wind-Rotolo M, Tracy A, Giannakis M, Hodi FS, Drake CG, Ball MW, Allaf ME, Snyder A, Hellmann MD, Ho T, Motzer RJ, Signoretti S, Kaelin WG, Jr., Choueiri TK, Van Allen EM. Genomic correlates of response to immune checkpoint therapies in clear cell renal cell carcinoma. Science. 2018;359(6377):801-6. Epub 2018/01/06. doi: 10.1126/science.aan5951. PubMed PMID: 29301960; PMCID: PMC6035749.

136. Pena-Llopis S, Vega-Rubin-de-Celis S, Liao A, Leng N, Pavia-Jimenez A, Wang S, Yamasaki T, Zhrebker L, Sivanand S, Spence P, Kinch L, Hambuch T, Jain S, Lotan Y, Margulis V, Sagalowsky AI, Summerour PB, Kabbani W, Wong SW, Grishin N, Laurent M, Xie XJ, Haudenschild CD, Ross MT, Bentley DR, Kapur P, Brugarolas J. BAP1 loss defines a new class of renal cell carcinoma. Nat Genet. 2012;44(7):751-9. Epub 2012/06/12. doi: 10.1038/ng.2323. PubMed PMID: 22683710; PMCID: PMC3788680.

137. Gudbjartsson T, Thoroddsen A, Petursdottir V, Hardarson S, Magnusson J, Einarsson GV. Effect of incidental detection for survival of patients with renal cell

carcinoma: results of population-based study of 701 patients. Urology. 2005;66(6):1186-91. Epub 2005/12/20. doi: 10.1016/j.urology.2005.07.009. PubMed PMID: 16360438.

138. Yagoda A, Petrylak D, Thompson S. Cytotoxic chemotherapy for advanced renal cell carcinoma. Urol Clin North Am. 1993;20(2):303-21. Epub 1993/05/01. PubMed PMID: 8493752.

139. Motzer RJ, Tannir NM, McDermott DF, Aren Frontera O, Melichar B, Choueiri TK, Plimack ER, Barthelemy P, Porta C, George S, Powles T, Donskov F, Neiman V, Kollmannsberger CK, Salman P, Gurney H, Hawkins R, Ravaud A, Grimm MO, Bracarda S, Barrios CH, Tomita Y, Castellano D, Rini BI, Chen AC, Mekan S, McHenry MB, Wind-Rotolo M, Doan J, Sharma P, Hammers HJ, Escudier B, CheckMate I. Nivolumab plus Ipilimumab versus Sunitinib in Advanced Renal-Cell Carcinoma. N Engl J Med. 2018;378(14):1277-90. Epub 2018/03/22. doi: 10.1056/NEJMoa1712126. PubMed PMID: 29562145; PMCID: PMC5972549.

140. Menard LC, Fischer P, Kakrecha B, Linsley PS, Wambre E, Liu MC, Rust BJ, Lee D, Penhallow B, Manjarrez Orduno N, Nadler SG. Renal Cell Carcinoma (RCC) Tumors Display Large Expansion of Double Positive (DP) CD4+CD8+ T Cells With Expression of Exhaustion Markers. Front Immunol. 2018;9:2728. Epub 2018/12/12. doi: 10.3389/fimmu.2018.02728. PubMed PMID: 30534127; PMCID: PMC6275222.

141. Desfrancois J, Moreau-Aubry A, Vignard V, Godet Y, Khammari A, Dreno B, Jotereau F, Gervois N. Double positive CD4CD8 alphabeta T cells: a new tumor-reactive population in human melanomas. PLoS One. 2010;5(1):e8437. Epub 2010/01/07. doi: 10.1371/journal.pone.0008437. PubMed PMID: 20052413; PMCID: PMC2797605.

142. Garcia-Diaz A, Shin DS, Moreno BH, Saco J, Escuin-Ordinas H, Rodriguez GA, Zaretsky JM, Sun L, Hugo W, Wang X, Parisi G, Saus CP, Torrejon DY, Graeber TG, Comin-Anduix B, Hu-Lieskovan S, Damoiseaux R, Lo RS, Ribas A. Interferon Receptor Signaling Pathways Regulating PD-L1 and PD-L2 Expression. Cell Rep. 2017;19(6):1189-201. Epub 2017/05/13. doi: 10.1016/j.celrep.2017.04.031. PubMed PMID: 28494868; PMCID: PMC6420824.

143. Mandai M, Hamanishi J, Abiko K, Matsumura N, Baba T, Konishi I. Dual Faces of IFNgamma in Cancer Progression: A Role of PD-L1 Induction in the Determination of Pro- and Antitumor Immunity. Clin Cancer Res. 2016;22(10):2329-34. Epub 2016/03/27. doi: 10.1158/1078-0432.CCR-16-0224. PubMed PMID: 27016309.

144. Fu H, Liu Y, Xu L, Liu W, Fu Q, Liu H, Zhang W, Xu J. Galectin-9 predicts postoperative recurrence and survival of patients with clear-cell renal cell carcinoma. Tumour Biol. 2015;36(8):5791-9. Epub 2015/02/27. doi: 10.1007/s13277-015-3248-y. PubMed PMID: 25716202.

145. Zhu C, Anderson AC, Schubart A, Xiong H, Imitola J, Khoury SJ, Zheng XX, Strom TB, Kuchroo VK. The Tim-3 ligand galectin-9 negatively regulates T helper type 1

immunity. Nat Immunol. 2005;6(12):1245-52. Epub 2005/11/16. doi: 10.1038/ni1271. PubMed PMID: 16286920.

146. Clayton KL, Haaland MS, Douglas-Vail MB, Mujib S, Chew GM, Ndhlovu LC, Ostrowski MA. T cell Ig and mucin domain-containing protein 3 is recruited to the immune synapse, disrupts stable synapse formation, and associates with receptor phosphatases. J Immunol. 2014;192(2):782-91. Epub 2013/12/18. doi: 10.4049/jimmunol.1302663. PubMed PMID: 24337741; PMCID: PMC4214929.

147. Imaizumi T, Kumagai M, Sasaki N, Kurotaki H, Mori F, Seki M, Nishi N, Fujimoto K, Tanji K, Shibata T, Tamo W, Matsumiya T, Yoshida H, Cui XF, Takanashi S, Hanada K, Okumura K, Yagihashi S, Wakabayashi K, Nakamura T, Hirashima M, Satoh K. Interferon-gamma stimulates the expression of galectin-9 in cultured human endothelial cells. J Leukoc Biol. 2002;72(3):486-91. Epub 2002/09/12. PubMed PMID: 12223516.

148. Popa SJ, Stewart SE, Moreau K. Unconventional secretion of annexins and galectins. Semin Cell Dev Biol. 2018;83:42-50. Epub 2018/03/05. doi: 10.1016/j.semcdb.2018.02.022. PubMed PMID: 29501720; PMCID: PMC6565930.

149. Krabbe LM, Bagrodia A, Margulis V, Wood CG. Surgical management of renal cell carcinoma. Semin Intervent Radiol. 2014;31(1):27-32. Epub 2014/03/07. doi: 10.1055/s-0033-1363840. PubMed PMID: 24596437; PMCID: PMC3930656.

150. Cepek KL, Parker CM, Madara JL, Brenner MB. Integrin alpha E beta 7 mediates adhesion of T lymphocytes to epithelial cells. J Immunol. 1993;150(8 Pt 1):3459-70. Epub 1993/04/15. PubMed PMID: 8468482.

151. Cepek KL, Shaw SK, Parker CM, Russell GJ, Morrow JS, Rimm DL, Brenner MB. Adhesion between epithelial cells and T lymphocytes mediated by E-cadherin and the alpha E beta 7 integrin. Nature. 1994;372(6502):190-3. Epub 1994/11/10. doi: 10.1038/372190a0. PubMed PMID: 7969453.

152. Jiang X, Clark RA, Liu L, Wagers AJ, Fuhlbrigge RC, Kupper TS. Skin infection generates non-migratory memory CD8+ T(RM) cells providing global skin immunity. Nature. 2012;483(7388):227-31. Epub 2012/03/06. doi: 10.1038/nature10851. PubMed PMID: 22388819; PMCID: PMC3437663.

153. Francisco LM, Salinas VH, Brown KE, Vanguri VK, Freeman GJ, Kuchroo VK, Sharpe AH. PD-L1 regulates the development, maintenance, and function of induced regulatory T cells. J Exp Med. 2009;206(13):3015-29. Epub 2009/12/17. doi: 10.1084/jem.20090847. PubMed PMID: 20008522; PMCID: PMC2806460.

154. Yi JS, Cox MA, Zajac AJ. T-cell exhaustion: characteristics, causes and conversion. Immunology. 2010;129(4):474-81. Epub 2010/03/06. doi: 10.1111/j.1365-2567.2010.03255.x. PubMed PMID: 20201977; PMCID: PMC2842494.

155. Wherry EJ, Kurachi M. Molecular and cellular insights into T cell exhaustion. Nat Rev Immunol. 2015;15(8):486-99. Epub 2015/07/25. doi: 10.1038/nri3862. PubMed PMID: 26205583; PMCID: PMC4889009.

156. Jin HT, Anderson AC, Tan WG, West EE, Ha SJ, Araki K, Freeman GJ, Kuchroo VK, Ahmed R. Cooperation of Tim-3 and PD-1 in CD8 T-cell exhaustion during chronic viral infection. Proc Natl Acad Sci U S A. 2010;107(33):14733-8. Epub 2010/08/04. doi: 10.1073/pnas.1009731107. PubMed PMID: 20679213; PMCID: PMC2930455.

157. Braun MW, Godwin AK. An in vitro Model for Evaluating Autologous T-cell and Tumor Cell Interactions in Renal Cell Carcinoma. Journal of Clinical and Cellular Immunology. 2021;12(1).

158. van de Weyer PS, Muehlfeit M, Klose C, Bonventre JV, Walz G, Kuehn EW. A highly conserved tyrosine of Tim-3 is phosphorylated upon stimulation by its ligand galectin-9. Biochem Biophys Res Commun. 2006;351(2):571-6. Epub 2006/10/31. doi: 10.1016/j.bbrc.2006.10.079. PubMed PMID: 17069754.

159. Leitner J, Rieger A, Pickl WF, Zlabinger G, Grabmeier-Pfistershammer K, Steinberger P. TIM-3 does not act as a receptor for galectin-9. PLoS Pathog. 2013;9(3):e1003253. Epub 2013/04/05. doi: 10.1371/journal.ppat.1003253. PubMed PMID: 23555261; PMCID: PMC3605152.

160. Sabatos-Peyton CA, Nevin J, Brock A, Venable JD, Tan DJ, Kassam N, Xu F, Taraszka J, Wesemann L, Pertel T, Acharya N, Klapholz M, Etminan Y, Jiang X, Huang YH, Blumberg RS, Kuchroo VK, Anderson AC. Blockade of Tim-3 binding to phosphatidylserine and CEACAM1 is a shared feature of anti-Tim-3 antibodies that have functional efficacy. Oncoimmunology. 2018;7(2):e1385690. Epub 2018/01/09. doi: 10.1080/2162402X.2017.1385690. PubMed PMID: 29308307; PMCID: PMC5749620.

161. Wolf Y, Anderson AC, Kuchroo VK. TIM3 comes of age as an inhibitory receptor. Nat Rev Immunol. 2019. Epub 2019/11/05. doi: 10.1038/s41577-019-0224-6. PubMed PMID: 31676858.

162. Anderson AC, Joller N, Kuchroo VK. Lag-3, Tim-3, and TIGIT: Co-inhibitory Receptors with Specialized Functions in Immune Regulation. Immunity. 2016;44(5):989-1004. Epub 2016/05/19. doi: 10.1016/j.immuni.2016.05.001. PubMed PMID: 27192565; PMCID: PMC4942846.

163. Corgnac S, Boutet M, Kfoury M, Naltet C, Mami-Chouaib F. The Emerging Role of CD8(+) Tissue Resident Memory T (TRM) Cells in Antitumor Immunity: A Unique Functional Contribution of the CD103 Integrin. Front Immunol. 2018;9:1904. Epub 2018/08/31. doi: 10.3389/fimmu.2018.01904. PubMed PMID: 30158938; PMCID: PMC6104123.

164. Crompton JG, Sukumar M, Restifo NP. Uncoupling T-cell expansion from effector differentiation in cell-based immunotherapy. Immunol Rev. 2014;257(1):264-76. Epub 2013/12/18. doi: 10.1111/imr.12135. PubMed PMID: 24329803; PMCID: PMC3915736.

165. Crompton JG, Sukumar M, Roychoudhuri R, Clever D, Gros A, Eil RL, Tran E, Hanada K, Yu Z, Palmer DC, Kerkar SP, Michalek RD, Upham T, Leonardi A, Acquavella N, Wang E, Marincola FM, Gattinoni L, Muranski P, Sundrud MS, Klebanoff CA, Rosenberg SA, Fearon DT, Restifo NP. Akt inhibition enhances expansion of potent tumor-specific lymphocytes with memory cell characteristics. Cancer Res. 2015;75(2):296-305. Epub 2014/11/30. doi: 10.1158/0008-5472.CAN-14-2277. PubMed PMID: 25432172; PMCID: PMC4384335.

166. van der Windt GJ, Pearce EL. Metabolic switching and fuel choice during T-cell differentiation and memory development. Immunol Rev. 2012;249(1):27-42. Epub 2012/08/15. doi: 10.1111/j.1600-065X.2012.01150.x. PubMed PMID: 22889213; PMCID: PMC3645891.

167. Gattinoni L, Zhong XS, Palmer DC, Ji Y, Hinrichs CS, Yu Z, Wrzesinski C, Boni A, Cassard L, Garvin LM, Paulos CM, Muranski P, Restifo NP. Wnt signaling arrests effector T cell differentiation and generates CD8+ memory stem cells. Nat Med. 2009;15(7):808-13. Epub 2009/06/16. doi: 10.1038/nm.1982. PubMed PMID: 19525962; PMCID: PMC2707501.

168. Muralidharan S, Hanley PJ, Liu E, Chakraborty R, Bollard C, Shpall E, Rooney C, Savoldo B, Rodgers J, Dotti G. Activation of Wnt signaling arrests effector differentiation in human peripheral and cord blood-derived T lymphocytes. J Immunol. 2011;187(10):5221-32. Epub 2011/10/21. doi: 10.4049/jimmunol.1101585. PubMed PMID: 22013128; PMCID: PMC3208052.

169. Ding Y, Shen S, Lino AC, Curotto de Lafaille MA, Lafaille JJ. Beta-catenin stabilization extends regulatory T cell survival and induces anergy in nonregulatory T cells. Nat Med. 2008;14(2):162-9. Epub 2008/02/05. doi: 10.1038/nm1707. PubMed PMID: 18246080.

170. Siddiqui I, Schaeuble K, Chennupati V, Fuertes Marraco SA, Calderon-Copete S, Pais Ferreira D, Carmona SJ, Scarpellino L, Gfeller D, Pradervand S, Luther SA, Speiser DE, Held W. Intratumoral Tcf1(+)PD-1(+)CD8(+) T Cells with Stem-like Properties Promote Tumor Control in Response to Vaccination and Checkpoint Blockade Immunotherapy. Immunity. 2019;50(1):195-211 e10. Epub 2019/01/13. doi: 10.1016/j.immuni.2018.12.021. PubMed PMID: 30635237.

171. Xing S, Li F, Zeng Z, Zhao Y, Yu S, Shan Q, Li Y, Phillips FC, Maina PK, Qi HH, Liu C, Zhu J, Pope RM, Musselman CA, Zeng C, Peng W, Xue HH. Tcf1 and Lef1 transcription factors establish CD8(+) T cell identity through intrinsic HDAC activity. Nat Immunol. 2016;17(6):695-703. Epub 2016/04/26. doi: 10.1038/ni.3456. PubMed PMID: 27111144; PMCID: PMC4873337.

172. Kratchmarov R, Magun AM, Reiner SL. TCF1 expression marks self-renewing human CD8(+) T cells. Blood Adv. 2018;2(14):1685-90. Epub 2018/07/20. doi: 10.1182/bloodadvances.2018016279. PubMed PMID: 30021780; PMCID: PMC6058237.

173. Wang Y, Hu J, Li Y, Xiao M, Wang H, Tian Q, Li Z, Tang J, Hu L, Tan Y, Zhou X, He R, Wu Y, Ye L, Yin Z, Huang Q, Xu L. The Transcription Factor TCF1 Preserves the Effector Function of Exhausted CD8 T Cells During Chronic Viral Infection. Front Immunol. 2019;10:169. Epub 2019/03/01. doi: 10.3389/fimmu.2019.00169. PubMed PMID: 30814995; PMCID: PMC6381939.

174. Besser MJ, Shapira-Frommer R, Itzhaki O, Treves AJ, Zippel DB, Levy D, Kubi A, Shoshani N, Zikich D, Ohayon Y, Ohayon D, Shalmon B, Markel G, Yerushalmi R, Apter S, Ben-Nun A, Ben-Ami E, Shimoni A, Nagler A, Schachter J. Adoptive transfer of tumor-infiltrating lymphocytes in patients with metastatic melanoma: intent-to-treat analysis and efficacy after failure to prior immunotherapies. Clin Cancer Res. 2013;19(17):4792-800. Epub 2013/05/22. doi: 10.1158/1078-0432.CCR-13-0380. PubMed PMID: 23690483.